DESIGN AND THERMO-MECHANICAL ANALYSIS OF WARM FORGING PROCESS AND DIES

A THESIS SUBMITTED TO
THE GRADUATE SCHOOL OF NATURAL AND APPLIED SCIENCES
OF
MIDDLE EAST TECHNICAL UNIVERSITY

BY

SEVGİ SARAÇ

IN PARTIAL FULFILLMENT OF THE REQUIREMENTS
FOR
THE DEGREE OF MASTER OF SCIENCE
IN
MECHANICAL ENGINEERING

SEPTEMBER 2007

Approval of the thesis:

DESIGN AND THERMO-MECHANICAL ANALYSIS OF WARM FORGING PROCESS AND DIES

Submitted by **SEVGİ SARAÇ** in partial fulfillment of the requirements for the degree of **Master of Science in Mechanical Engineering Department, Middle East Technical University** by,

Prof. Dr. Canan Özgen
Dean, Graduate School of **Natural and Applied Sciences** __________________

Prof. Dr. Kemal İder
Head of Department, **Mechanical Engineering** __________________

Prof. Dr. Mustafa İlhan Gökler
Supervisor, **Mechanical Engineering, METU** __________________

Prof. Dr. Haluk Darendeliler
Co-supervisor, **Mechanical Engineering, METU** __________________

Examining Committee Members:

Prof. Dr. Metin Akkök
Mechanical Engineering, METU __________________

Prof. Dr. Mustafa İlhan Gökler
Mechanical Engineering, METU __________________

Prof. Dr. Haluk Darendeliler
Mechanical Engineering, METU __________________

Prof. Dr. S. Kemal İder
Mechanical Engineering, METU __________________

Prof. Dr. Can Çoğun
Mechanical Engineering, Gazi University __________________

Date: __________________

I hereby declare that all information in this document has been obtained and presented in accordance with academic rules and ethical conduct. I also declare that, as required by these rules and conduct, I have fully cited and referenced all material and results that are not original to this work.

Sevgi SARAÇ

Signature:

ABSTRACT

DESIGN AND THERMO-MECHANICAL ANALYSIS OF WARM FORGING PROCESS AND DIES

SARAÇ, Sevgi

M.Sc., Department of Mechanical Engineering

Supervisor: Prof. Dr. Mustafa İlhan GÖKLER

Co-Supervisor: Prof. Dr. Haluk DARENDELİLER

September 2007, 140 pages

Forging temperature is one of the basic considerations in forging processes. In warm forging, the metals are forged at temperatures about the recrystallization temperature and below the traditional hot forging temperature. Warm forging has many advantages when compared to hot and cold forging. Accuracy and surface finish of the parts is improved compared to hot forging while ductility is increased and forming loads are reduced when compared to cold forging.

In this study, forging process of a part which is currently produced at the hot forging temperature range and which needs some improvements in accuracy, material usage and energy concepts, is analyzed. The forging process sequence design with a new preform design for the particular part is proposed in warm forging temperature range and the proposed process is simulated using Finite Element Method. In the simulations, coupled thermal mechanical analyses are performed and the dies are modeled as deformable bodies to execute die stress analysis. Experimental study is also carried out in METU-BILTIR Center Forging Research and Application Laboratory and it has been observed that numerical and experimental results are in good agreement. In the study, material wastage is reduced by proposing using of a square cross section billet instead of a circular one, energy saving and better accuracy in part dimensions is achieved by reducing the forging temperature from the hot forging to the warm forging temperature range.

Keywords: Warm Forging, Finite Element Analysis, Die Stress Analysis, Metal Forming, Closed-die Forging

ÖZ

ILIK DÖVME PROSESİ VE KALIPLARI İÇİN TASARIM VE

TERMO-MEKANİK ANALİZ

SARAÇ, Sevgi

Yüksek Lisans, Makina Mühendisliği Bölümü

Tez Yöneticisi: Prof. Dr. Mustafa İlhan GÖKLER

Ortak Tez Yöneticisi: Prof. Dr. Haluk DARENDELİLER

Eylül 2007, 140 Sayfa

Dövme sıcaklığı, dövme uygulamalarındaki temel etkenlerden birisidir. Ilık dövme uygulamalarında, metalller yeniden kristallenme sıcaklığı civarında ve geleneksel sıcak dövme sıcaklığının altında dövülürler. Ilık dövme sıcak ve soğuk dövme ile karşılaştırıldığında bir çok avantaja sahiptir. Sıcak dövmeye göre daha hassas ve yüzey kalitesi daha yüksek parçalar elde edilirken, soğuk dövmeye göre de daha yüksek süneklik ve daha düşük şekillendirme kuvvetleri elde etmek mümkündür.

Bu çalışmada, sıcak dövme sıcaklığında üretilmekte olan ve hassasiyet, malzeme kullanımı ve enerji konularında iyileştirmeye ihtiyacı olan bir parçanın dövme uygulaması analiz edilmiştir. Sözedilen parça için, yeni önşekillendirme kalıpları tasarımı ile birlikte ılık dövme sıcaklığında bir dövme uygulaması önerilmiş ve önerilen uygulamanın Sonlu Elemanlar Metodu kullanılarak benzetimi yapılmıştır. Benzetimlerde, termo-mekanik analizler yapılmış ve kalıp gerilimlerini hesaplayabilmek için kalıplar şekillenebilir olarak modellenmiştir. ODTÜ-BİLTİR Merkezi Dövme Araştırma ve Uygulamaları Laboratuvarında deneysel çalışma da yapılmış ve sayısal sonuçlarla deneysel sonuçların birbiriyle tutarlı olduğu gözlenmiştir. Çalışmada, yuvarlak kesitli malzeme yerine kare kesitli malzeme kullanılması önerilerek malzeme kaybı azaltılmıştır. Dövme sıcaklığı sıcak dövme aralığından ılık dövme aralığına düşürülerek enerji tasarrufu ve parça ölçülerinde yüksek hassasiyet elde edilmiştir.

Anahtar Kelimeler: Ilık Dövme, Sonlu Elemanlar Analizi, Kalıp Gerilim Analizi, Metal Şekillendirme, Kapalı Kalıp Dövme

To My Family & Mete,

ACKNOWLEDGEMENTS

I would like to express my deepest gratitude to my supervisor Prof. Dr. Mustafa İlhan Gökler and my co-supervisor Prof. Dr. Haluk Darendeliler for their great guidance, advice, criticism, patience and insight throughout the research.

I wish to thank Mr.Cevat Kömürcü, Mrs.Tülay Kömürcü, Mrs.Tülin Özkan, Mr.Yakup Erişkin, and Mr.Yalçın Şahin from AKSAN Steel Forging Company, Mr.Aydın Kuntay and Mr.Çağrı Doğan from BIAS, Mr.Ahmet Özortakçı.from Assab Korkmaz. The technical assistance of them is gratefully acknowledged. I also would like to thank to METU-BILTIR Research & Application Center for the facilities provided for my work.

My special thanks go to my colleagues, Arda Özgen, Hüseyin Öztürk, İlker Durukan, Mehmet Maşat, Özgür Cavbozar, Kazım Arda Çelik, Ulaş Göçmen, Cihat Özcan, Derya Akkuş, Ali Murat Kayıran and Yusufu Jande for their valuable support and aid; to my senior colleagues Pelin Genç, Gülgün Aktakka, Ömer Köktürk, Evren Anık, Atayıl Koyuncu, Özkan İlkgün and Ender Cengiz and for their support and guidance.

Further, thanks go to Halit Şahin, Ali Demir, Hüseyin Ali Atmaca, Tarık Öden, Filiz Güngör Sutekin, Arzu Öztürk, Halime Küçük and Mehmet Ali Sarıhan for their supports and encouragement.

I am grateful to the late Meltem Yıldız, Osman Kılıç, Özgün Yılmazok, Pınar Karpuz and Caner Şimşir for the care with which they helped me prepare this thesis. Their friendship and professional collaboration meant a great deal to me.

And - last but by no means least! - I am deeply indebt to my parents Nilüfer and Mehmet Fehmi Saraç and my brother Ali Emre Saraç for their never-ending love and spiritual support at critical and opportune times. As always it was Mete who provided the shelter conditions under which the work could take place: thanks to him for this and many other things.

TABLE OF CONTENTS

LIST OF FIGURES

LIST OF TABLES

CHAPTER 1

INTRODUCTION

1.1 What is Forging

Forging is a manufacturing technique in which metal is plastically deformed from a simple shape like billet, bar, ingot into the desired shape in one or more stages. Deformation takes place by means of applying compressive forces between the dies in machine tools like hammers, presses, horizontal forging machines, etc. Forging process has many advantages when compared to other manufacturing techniques, which are tabulated in Table 1.1 [1].

Virtually all metals have alloys that are forgeable, giving the designer the full spectrum of mechanical and physical properties of ferrous and non-ferrous alloys. The most common forging alloys include:

- Carbon, micro alloy and alloy steel forgings account for the greatest volume of forgings for a very wide range of applications.
- Stainless steels are widely used where resistance to heat and corrosion are required.
- Aluminum forgings are used in applications where weight of the component is an issue.
- Copper, brass and bronze forgings offer excellent corrosion resistance with high thermal and electrical conductivity.
- Iron, nickel and cobalt high temperature alloy forgings are preeminent for applications of cyclical and sustained loads at high temperatures.

Table 1.1 Forging Advantages Compared to Other Manufacturing Technologies [1]

Forging versus	Forging Advantages When Using a Similar Alloy
Casting	Stronger Preworking refines defects More reliable, lower cost over component life Better response to heat treatment
Welding / Fabricating	Material savings, production economies Stronger Cost effective design / inspection More consistent and better metallurgical properties Simplified production
Machining	Broader size range of desired material grades Grain flow provides higher strength More economical use of material Yields lower scrap Requires fewer secondary operations
Powder Metal	Stronger Higher integrity Requires fewer secondary operations Greater design flexibility Less costly materials
Composites / Plastics	Less costly materials Greater productivity Established documentation Broader service-temperature range More reliable service performance

- Titanium forgings are used where high strength, low weight and excellent corrosion resistance, combined with moderate heat resistance, are required.
- Magnesium forgings offer the lowest density of any commercial structural metal, at operating temperatures similar to aluminum.

The wide range of alloys and sizes, combined with excellent mechanical and physical properties has made forgings the design choice for nearly all product areas. The most common application areas are; Automotive, Aerospace, Bearings, Construction, Mining Equipment, Pipeline Fittings, Valves, Pumps and Compressors.

1.2 Forging Process

There are various classifications applied for the forging process. In general, forging processes can be classified according to:

- Temperature: Hot Forging, Cold Forging, Warm Forging
- Type of Machine Used: Hammer, Mechanical Press, Hydraulic Press, etc.
- Type of die set: Open die forging, Closed die forging

1.2.1 Classification According to Temperature

In hot forging, metal is plastically deformed at a temperature above recrystallization temperature, for steels 1100-1250 ^{o}C, strain hardening is avoided. A greater degree of deformation can be achieved in a single operation compared to cold or warm forging. Main disadvantages are extensive scale formation, low dimensional accuracy, necessity of larger tolerances for further machining and requirement of heating equipment.

In cold forging, plastic deformation takes place at or near room temperature. The primary advantage is the material savings achieved through precision shapes that require little finishing. The tool stresses are quite high in cold forging and limited geometry and volume can be forged. Consequently, the prediction of the forming load and stresses is quite important for die design and machine selection.

In warm forging, the billet is heated to temperatures about the recrystallization temperature, for example, for steels the range of 800-1000 ^{o}C, which is lower than the conventional hot forging range, is considered as warm forging temperature range. In warm forging, flow stress and the forging pressures are reduced compared to cold forging.

The process has the advantages listed below, compared to hot and cold forging.

- Reduced forming loads compared with those for cold forging
- Greater ductility compared with that for cold forging
- Improved accuracy compared with that for hot forging
- Better surface finish compared with that for hot forging
- Enhanced product properties through grain refinement and controlled phase transformations in heat treatable steels
- A potential for the reduction of production costs

In subsequent chapters, warm forging process will be discussed in detail since the study is conducted on warm forging.

1.2.2 Classification According to Type of Machine Used

Forging hammers have a weighted ram which exerts a striking force by moving vertically in a downward stroke. When forging dies are fastened to the weighted ram and the anvil assembly, and a workpiece is placed between them, the striking force is imposed on the workpiece, causing it to deform plastically with each successive blow. The hammer is an energy-restricted machine. During a working stroke, the deformation proceeds until the total kinetic energy is dissipated by plastic deformation of the forging stock, heat loss and by elastic deformation of the ram and anvil when the die faces contact with each other. Forging hammers have types of power drop hammers, gravity drop hammers and counterblow hammers.

Mechanical presses are most widely used equipment for closed die forgings. They develop far less noise and vibration than forging hammers. The drive of the most mechanical presses is based on a slider-crank mechanism that translates rotary motion into reciprocating linear motion. The eccentric shaft is connected through a clutch and brake system directly to the flywheel. The drive shaft imparts a constant stroke to a vertically operating ram. The ram carries the top, moving die; the bottom or stationary die is fixed to the die seat of the main frame. Mechanical presses are displacement-restricted machines. The ram stroke is generally shorter than a forging hammer or a hydraulic press. The ram velocity and the available ram load vary in accordance with the position of the slide before the bottom dead center.

In hydraulic presses, the ram is driven by hydraulic cylinders and pistons that are part of a high-pressure hydraulic or hydropneumatic system. After a rapid approach speed, the ram with upper die attached, moves at a low speed while exerting a squeezing action on the workpiece which is retained in the lower die. Hydraulic presses are essentially load restricted machines. Pressing speed can be controlled, permitting the control of metal flow velocity. Since most of the load is available during the entire stroke, relatively large energies are available for deformation.

Hot upset forging (also called hot heading or machine forging) is essentially a process for enlarging and reshaping some of the cross-sectional area of a bar, tube or other product form of uniform, usually round section. Upset forging employs split dies that separate enough for the heated bar to advance between them and move into the position. They are then forced together and a heading tool or ram moves longitudinally against the bar, upsetting it into the die cavity. By starting a new piece with each die separation and having all cavities perform their operations simultaneously, a finished product can be made with each cycle of the machine. Upset forging is performed on horizontal forging machines.

In roll forging, the metal stock usually round or flat in cross-section is reduced in thickness and increased in length to produce the desired shape. The stock material is passed between two semi-cylindrical rolls that are slightly eccentric to the axis of rotation. The rolls contain a series of shaped grooves. Main aim of use is to save material and number of hits in subsequent forging in closed dies or in an upsetter.

1.2.3 Classification According to Type of Die Set

In open die forging, workpiece surfaces deform freely, therefore parts produced by open die forging have less accuracy and dimensional tolerance than impression die or closed die forging. However, the tooling is simple, relatively inexpensive and can be designed and manufactured with ease.

In closed die forging (also called as impression die forging), shape is obtained by filling the die cavity formed by upper and lower dies. Excess material is allowed to escape into the clearance between the dies and form the flash. Usually some preforming steps are necessary in order to fill the die cavity without defects.

Flash is the metal, which is forced outward from the workpiece while it is being forged to the configuration of the closed-die impression. In other means, it is the metal in excess of that required to fill the impression. In terms of its contribution to the closed-die mechanical press forging processes, flash serves two basic functions [2]. First, by providing a convenient means for disposing of excess metal, it makes possible the use of slightly oversized billets and renders other billet dimensional variations, such as deviations in cutting to length or metal losses caused by oxidation during forging or heating of billet, much less critical. Availability of excess metal also increases possibility of the die filling. Second, flash provides useful constraint of metal flow during forging, which helps in filling the die impressions. Before complete closure of dies, the presence of some flash metal at the periphery of the workpiece promotes containment of the workpiece metal within the impressions.

While flash can promote complete fill of the cavity, it causes extremely high die pressures in the flash area. High pressures are undesirable because they reduce die life and require additional power. A flash gutter is often formed in the dies to receive the flash and allow the dies to reach the predetermined position at lower pressures.

1.3 Forging Design Considerations

Input for the design process of a forging operation is the geometry of the workpiece to be forged. Before a forging is put into production, there are three main stages that must be completed:

1- The design of the forging from the required machined part

2- The method and sequence of operations to produce the forging must be decided upon, including estimates of material amount required,

3- The appropriate dies, including those for all preforming operations are to be designed and manufactured.

The following sequence is a common design procedure for forging:

- Machining allowance is added to surfaces that will be machined
- Parting line is located
- Webs are constructed for large holes, if necessary
- Draft angles are given to cylindrical portions of the part
- Fillets and corner radii should be used to blend sharp corners.
- Flash and gutter geometry must be determined.
- Volume of the forging including f1ash is calculated.
- Scale allowance is considered and added to volume of forging.
- Billet geometry is selected.

- Required preform cavities are designed
- Forging load is estimated.
- Dimensional tolerances for forging and die block are determined.

Careful attention has to be paid to those decisions on critical features such as drafts, edge radii, fillet radii, ribs, machining allowances, as well as size and mass of the forging. Recommended values on these features are given in the related standard [3]. It is noted that design of the dies requires past experience and skilled personnel.

1.4 Forging Defects

A defect is a flaw in a component that is typical of a process, but not inevitable. Good forging practice can eliminate most of them. Defects most commonly found in metals in forging may be classified as follows [1]:

1- Ingot defects, such as pipes i.e. openings in the center of the ingot, cracks, scabs, or bad surface and segregation. Segregation is a condition produced by uneven concentration of elements contained in the metal.

2- Defects resulting from improper forging, such as seams, cracks, laps, etc. Excess material in the web of a forging may buckle during forging and develop laps, as shown in Figure 1.1 [5]. The solution to this problem is to increase the initial web thickness to avoid buckling.
If the web is too thick, the excess material flows past the already forged portions and develops internal cracks. In this case, the die cavities are filled prematurely and the material at the center of the part flows past the filled regions as deformation continues.

These examples indicate the importance of properly distributing material and controlling the flow in the die cavity.

The various radii in the die cavity can significantly affect formation of defects. In Figure 1.2 [5], the material follows a large corner radius better than a small radius. With small radii, the material can fold over itself and produce a lap, called cold shut.

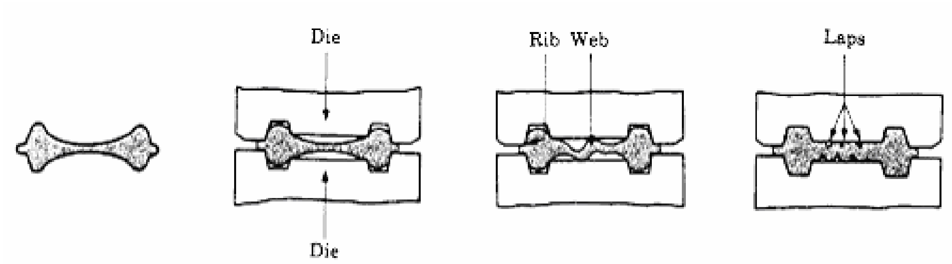

Blocked Forging   Begin Finishing   Web buckles   Laps in finished forging

Figure 1.1 Laps Formed by Buckling of the Web during Forging [5]

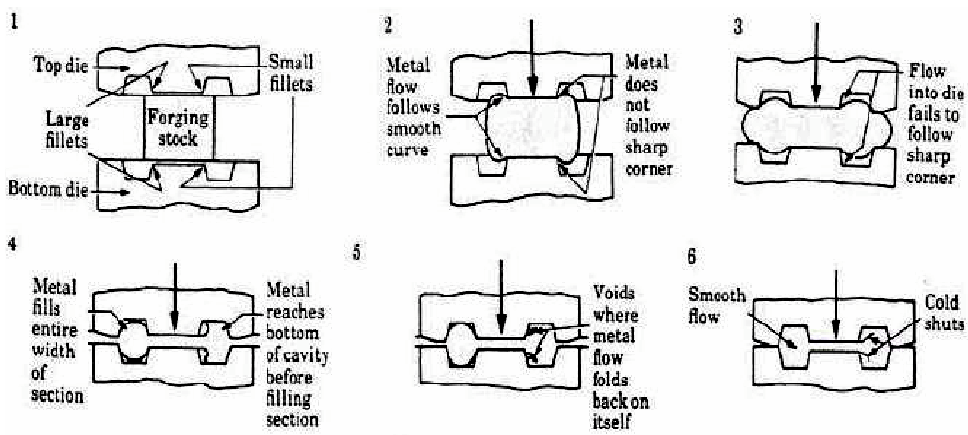

Figure 1.2 Effect of Fillet Radius on Defect Formation in Forging. Small fillets (right side of drawings) cause the defects [5]

3- Defects resulting from improper heating and cooling of the forging, such as burnt metal, decarburized steel, and flakes. Decarburized steel is caused by contact of the heated steel with the atmosphere. The carbon is removed from the surface of the solid steel by this oxidizing action.

It is often difficult to detect the defects in forgings unless they are on the surface and of such size as to be readily seen with the naked eye. Defects beneath a layer of scale or deep within the forging are much more difficult to detect.

Various testing methods have been devised to aid in the inspection and checking of metal parts, for the purpose of insuring against serious defects.

1.5 Causes of Die Failure

In forging process, the service life of dies is very important due to economical reasons and also finishing quality of productions. Die costs range from 10 to 15% of the cost of a forging. One of the biggest components of cost is tooling cost and indirect costs of bad tooling including cost of additional setups, rework, scrap and loss of productivity [4].

Failure of dies in manufacturing operations generally results from one or more of the following causes: improper design, defective material, improper heat treatment and finishing operations, overloading, misuse and improper handling.

The factors affecting die failure can be subdivided into [4]:

- Tooling Issues – Die material selection, heat treatment, surface engineering, die design and manufacture
- Billet Issues – Billet preparation, steel type
- Process Issues – Forging temperature, lubricant type and application, forging cycle times and other forging practices

The proper design of dies is as important as the proper selection of die materials. In order to withstand the forces in forging, a die must have proper cross sections and clearances. Sharp corners, radii, and fillets, as well as sudden changes in cross-section, act as stress raisers and can have detrimental effects on die life [5].

Depending on the conditions of the process and the characteristics of the material and surface conditions, one could encounter various modes of tool failure [4]. These are:

- Wear (abrasive, adhesive and oxidation)
- Thermal fatigue or heat checking
- Mechanical fatigue
- Plastic deformation

Of these, wear (abrasive and adhesive) and mechanical failures are the most common forms of failure. Abrasive wear is more common compared to adhesive wear in forging operations. The reason is presence of lubricant film and/or scales and oxide layer in forging operations prevent adhesive wear mode. Considering other failure forms, gross cracking and mechanical fatigue can be overcome by good tooling design and material selection. Thermal fatigue acts as a catalyst to accelerate abrasive wear.

1.6 Usage of CAD/CAM/CAE in Forging

The ever-increasing costs of material, energy and especially manpower require that forging processes and tooling should be designed and developed with minimum amount of trial and error with shortest possible lead times. Therefore, to remain competitive, the cost-effective application of computer aided techniques, i.e. Computer Aided Design (CAD), Computer Aided Manufacturing (CAM), Computer Aided Engineering (CAE) and especially Finite Element Analysis (FEA) and Finite Volume Analysis (FVA) based computer simulation, are an absolute necessity. [6] Since the late 1970s, the use of computer-aided techniques in the metal forming industry has increased considerably.

3-D models of the forgings, preform and finish dies can be created using CAD/CAM software, and parameters like the dimensions, shrinkage factors, etc. can easily be changed when necessary. Additionally the designer can observe the defects that may occur during forging by the help of these programs, which will reduce cost and time considerably.

Finite Volume Method (FVM) is a widely used tool for forging process simulations. The method has been used for many years in analyzing the flow of materials in liquid state. However, in recent years, some codes for computer simulation of solid state metal forming operations, like MSC. Superforge [7], have been established on the basis of this method. In FVM, the grid points are fixed in space and the elements are simply partitions of the space defined by connected grid points. The finite volume mesh is a “fixed frame of reference”. The material of a billet under analysis moves through the finite-volume mesh; the mass, momentum, and energy of the material are transported from element to element. The finite volume solver, therefore, calculates the motion of material through elements of constant volume, and therefore no remeshing is required [8].

In the Finite Element Method (FEM), the deformation zone in an elastic-plastic body is divided into a number of elements interconnected at a finite number of nodal points. The actual velocity distribution is then approximated for each element. A set of simultaneous equations is then developed representing unknown velocity vectors. From the solution of these equations, actual velocity distributions and the stresses are calculated [5]. Because of the severe element distortion common in metal forming operations, remeshing is necessary to follow the gross material deformation.

To be able to successfully apply the finite element method to the metal forming operations, the following requirements should be fulfilled [9]:

1- The physical problem should be well-defined for the application of simulation.

2- The idealization of this problem should be done correctly: Simplifications and assumptions should be reasonable. Unnecessary details should be eliminated.

3- The idealized problem should have the correct spatial discretization: Type of elements used, topology of element mesh, and the density of element mesh should be constructed according to the nature of problem.

4- Boundary conditions of the physical model should be investigated and applied in the simulation: friction, heat transfer, machines, dies etc.

5- Correct material laws and parameters should be used in the simulation: flow curve, anisotropy, failure, etc.

6- Numerical parameters used in the simulation should be chosen accordingly: penalty factors, convergence limits, increment sizes, remeshing criterion etc.

7- The simulation should be “economical”: Computation times and the time required to prepare the model should be reasonable, storage requirements of the model and the results should also be within physical limits.

8- The results should be evaluated carefully and checked whether they are reasonable or not.

Finite Element simulation of the forging process is complicated by the large displacement and the large strains that the material is subjected to. Because of the large displacements, the relationship between the strain and the displacement becomes nonlinear. There are other causes of nonlinearity in forging problems. Basically there are three types of nonlinearity:

1- Material nonlinearity (physical)

2- Geometric nonlinearity (kinematic)

3- Changing boundary conditions

Material nonlinearity is due to the nonlinear relation between stress and strain like in elastic-plastic (elastoplastic), elasto-viscoplastic materials, creep, composite and concrete structure problems etc. Geometric nonlinearity is aroused from nonlinear relationship between strains and displacements, and nonlinear relationship between stresses and forces. Changing boundary conditions also contribute to nonlinearity. If the loads on the structure vary with the displacements, nonlinearity occurs. Moreover contact and friction problems lead to nonlinear boundary conditions.

1.7 Some Previous Studies

Some previous studies have been conducted in METU-BILTIR Center [11-24]. Based on Gökler's study [10], Kazancı [11] developed a program named as Pro/UPSETTER for the sequence and die design of solid hot upset forgings having circular shanks and upset regions with non-circular cross-sections.

Moğulkoç [12] studied on upsetting and piercing on horizontal forging machines by using the finite element analysis technique.

A study on upset forging process and the design limits for tapered preforms had been conducted by Elmaskaya [13] by using the elastic-plastic finite element method.

İsbir [9] studied on the finite element simulation of shearing using the element elimination method to examine trimming operation on forged parts.

In the study of Doğan [14], the effects of the tapered preform shapes on the final product in cold upset forging had been investigated by using the elastic-plastic finite element method.

In another study, Alper [15] developed a computer program for axisymmetric press forgings, which designs the forging geometry and the die cavity for preforms and finishing operation.

Kutlu [16] studied on the design and analysis of preforms in hot forging for non-axisymmetric press forgings.

Karagözler [17] studied on the analysis and preform design for long press forgings with non-planar parting surfaces.

Gülbahar [18] focused on the analysis and design of bent forgings with planar and non-planar parting surfaces.

Civelekoğlu [19] studied forging of specific steel alloys. The forging sequence was investigated and the effects of material selection on the processes were observed. Results of the forging experiments were compared with the computer simulations.

Karacaovalı [20] analyzed the multistage roll-forging process based on the finite element analysis and experimental studies.

Aktakka [21] focused on hot and warm forging of a part which is used in automotive industry. Computer simulations and forging experiments are completed at different temperatures in the range of warm and hot forging.

Abachi [22] studied the analysis of die wear. Results from computer simulation were compared with the measurement on the worn die taken from industry and evaluation of wear coefficient from comparison of computer simulation and the measurement from worn die were done.

In the study of Ceran [23], hot forging process was simulated coupled with thermal analysis, in order to determine effects of the process on the header die for the taper perform stages in upset forging process. The effects of wall thickness and base thickness of the header die on the stress distribution in the header die were examined. For different cases, the stress distribution in the header die had been presented. The obtained stress distributions were also used for the fatigue analysis of the die.

Masat [24] has recently studied on precision forging of a spur gear.

In the following paragraphs, studies of some researchers will be summarized.

In the study of Garat, Bernhart and Hervy [25], hot forging die for a nut was investigated in order to increase its life time. In the paper, brittle failure phenomenon of tools is addressed and the influence of process parameters like billet length, billet initial temperature or tool design are studied. Service life prediction considering fatigue is made using the universal slope method proposed by Manson.

Kim, Lee, Kim, Kim [26] studied the estimation method of die service life based on wear and the plastic deformation of dies in hot forging processes. Two methods are suggested for estimating the service life of hot forging dies by plastic deformation and abrasive wear, and these are applied to predict the product quantity according to two main process variables, forming velocity and initial die temperature for a spindle component. Through the applications of the suggested methods, the thermal softening of dies due to the local temperature rise led to the reduction of the service life of hot forging dies by plastic deformation more than by abrasive wear.

Brucelle and Bernhart [27] described the methodology that has been applied to gain understanding of the thermomechanical stress field in a cemented carbide punch used for the manufacture of airbag container type parts. The stresses are the result of a combination of purely mechanical stresses due to the forging process, and thermomechanical stresses induced by the thermal cycling of the punch surface during successive hot forging and waiting periods. In the paper, the importance of a simultaneous use of numerical simulation (process simulation and thermomechanical stress calculation) and experimental testing (laboratory and industrial tests) is highlighted.

In the study of Jeong, Kim, Kim, Kim and Dean [28], experiments and numerical analyses were performed under various conditions, two kinds of surface treatment, two lubricants, different initial billet temperatures and different loads, to investigate the effects on thermal softening and the amount of heat transfer. Carbon Nitride (CN_x), ion-nitride and no surface treatment for the dies were used and oil-based and water-based graphite were used as lubricants. Experiments were also performed to take the heat- transfer coefficient into account with the combination of surface treatments and lubricants. The coefficients determined were then used in a finite element model for the analysis of the backward extrusion process, the results produced were compared with experiments.

In the study of Lee and Jou [29], the experimental techniques, wear model and numerical simulation method was combined to predict the wear of warm forging die. The non-isothermal ring compression test was adopted to estimate the friction coefficient in different temperatures and the on-line temperature recording system was setup to correct the heat transfer coefficient of the interface. The wear coefficients in different temperatures were acquired from high temperature wear experiment. Additionally, the Archard wear theory and a FEM code, were used to analyze the warm forging of automotive transmission outer-race and predict the die wear condition.

In the study of Kim, Yagi, Yamanaka [30], a history of practical use of FE simulations in forging area was briefly reviewed. Then, practical use and benefits of FE simulations in forging area were discussed with examples. Finally, key points for successful and effective use of FE simulations were explained followed by current issues for better use of the FE simulation as a must tool in the forging industry.

1.8 Scope of the Thesis

Warm forging offers better material utilization, improved surface finish, and dimensional accuracy, when compared to hot forging while it requires reduced press loads when compared to cold forging. However, die/tool stresses are more significant in warm forging than those in hot forging.

The scope of this study is to analyze the warm forging process and to analyze the die stresses during warm forging. Basic principles of warm forging will be given in Chapter 2 to provide a basis for the study.

The design of dies and selection of process conditions in forging operations are still performed by trial and error methods to a large extend in industry. In many cases, this trial and error procedure causes material wastage, unsuccessful die filling, high energy consumption and unacceptable products. In this study, forging process of a part which is currently hot forged in AKSAN Steel Forging Company, Ankara, will be taken into consideration. Some problems related to unacceptable accuracy in part dimensions, excessive wear in the tooling and excessive material wastage are encountered in the company with the particular product. Current application in the forging company and the problems of the process will be presented in detail in Chapter 3. In the same chapter, Finite Element Analysis of the current practice will also be given.

To overcome the problems, forging process sequence design with a new approach will be evaluated. By considering the advantages of warm forging as discussed above, forgeability of the particular part at the warm forging temperature range and the preform die design will also be studied. 3-D modeling and Finite Element Analysis techniques are used for the proposed design. The analyses are implemented as coupled thermal mechanical and the dies are modeled as deformable bodies to obtain the stress distribution on the dies. The modeling and simulation of the proposed forging sequence will be given in Chapter 4, in detail. Experimental study is carried out in METU-BILTIR Center Forging Research and Application Laboratory, which will be presented in Chapter 5.

Conclusion, discussion and recommendations about the future work will be given in Chapter 6.

CHAPTER 2

WARM FORGING

2.1 Introduction

Over the last few years, cold and warm forming of steel has gained greater importance. This is mainly due to one fact: there is an increasing demand for precision parts with high volumes especially in the automotive industry. Therefore, special manufacturing methods for special parts have been developed with warm and cold forging and with combinations of these processes.

The world-wide growth in the demand for forgings by the automobile industry since the 1950's resulted in the application of cold forging to serial mass production of a wide range of component types. Cold forging techniques have been developed and refined to enable near-net and in some cases net-shape components to be produced in large batch quantities. Limitations to the economic production of parts of complex geometry, and large size by cold forging, increased the potential for commercial warm forging between the market sectors of hot and cold forging.

When compared to cold forging, warm forging is applicable when high performance and less forgeable steels are used, particularly in the following situations: [31]

- When the flow stress of the workpiece material is too high for cold forging
- For shapes with great differences in cross-section when the number of process steps in a cold forging route is too large for economic production.
- To provide a highly accurate preform for a cold forming operation.

- When the component is too large for the capacity of a cold forging press.
- When the cost of annealing and relubricating in a cold forging process is too high.
- When the accuracy, surface finish, material yield or subsequent machining associated with the alternative hot forging route are unacceptable, warm forging may be considered as an alternative.

2.2 Process Characteristics of Warm Forging

A detailed comparison of the characteristics of hot, warm and cold forging technologies is given in Table 2.1 [31].

Table 2.1: Comparison of Typical Process Characteristics [31]

Characteristic	Hot forging	Warm forging	Cold forging
Shape spectrum	Arbitrary	Rotationally symmetrical if possible	mainly rotationally symmetrical
Use steel quality	Arbitrary	Arbitrary	Low alloyed steels C<0.45%
Normally achievable Accuracy	IT 12 – IT 16	IT 9 – IT 12	IT 7 – IT 11
Economic lot size	>500 parts	>10,000 parts	>30,000 parts
Initial treatment of billets and slugs	generally none	Generally none or a graphite layer	annealing/phosphating
Intermediate treatments	None	Generally none	annealing/phosphating
Tool materials	hot work tool steels	hot work tool steels, high speed steels, hard metals	Cold work tool steels, high speed steels, hard metals
Typical tool life	5,000 - 10,000 parts	10,000 - 20,000 parts	20,000 – 50,000 parts
Material utilization	60 – 80%	approximately 85%	85 - 90%
Energy required per kg gross of forging	460 - 490 J	400 – 420 J	400 - 420 J

As it can be seen from the table, the shape spectrum of cold and warm forged parts is similar but in warm forging, increased detail may be achieved. The economic batch quantities for warm forging are greater than for hot, but less than those for cold forging, mainly due to tooling costs. The shorter life of warm forging tools compared with cold forging ones and the higher costs of surface treatment of cold forging slugs results in similar overall energy costs for the two processes.

2.3 Physical Characteristics of Warm Forging Process

Physical properties of hot, warm and cold forgings are compared in Table 2.2. As it can be seen from the table, warm forging at temperatures below recrystallization temperature, provides the benefit of less distortion on cooling to room temperature and less decarburization during heating. It is apparent that cold forging leads to the highest accuracy and therefore for greatest precision warm forging is followed by cold finishing in a processing route.

Table 2.2: Typical Physical Properties of Steel Forgings [31

Comparison item	Hot forging	Warm forging		Cold forging
Temperature range	1050~1250 °C	Over recrystallization temperature	Below recrystallization temperature	Room temp
Decarbonized layer (mm)	0.3~0.4	0.10~0.25	0.1	0
Roughness (R_A)	>100μm	<50μm	<20μm	<10μm
Draft	<7°	<1°	<1°	0°
Dimension (mm)	±0.5~±1.0	±0.05~±0.20	±0.05~±0.15	±0.005~±0.1
Thickness (mm)	±0.5~±1.5	±0.20~±0.40	±0.10~±0.25	±0.10~±0.20
Eccentricity (mm)	0.5~1.5	0.10~0.70	0.10~0.40	0.05~0.25

2.4 Forgeability in Warm Forging Temperature Range

Most engineering steels may be warm forged but there are limitations to deformation, depending on chemical composition and forging temperature. Deformation limits of cold forgeable steels are increased under warm forging conditions. Provided tool temperatures do not exceed about $400^{o}C$, the limits of deformation are dictated by tool stresses.

Different classes of steel have characteristics which influence the choice of working temperature. [31]

a) Carbon Steels: These may be brittle to some degree at temperatures between $200^{0}C$ and $550^{0}C$, depending on the rate of deformation. To obtain a significant reduction in flow stress together with high ductility these steels should be forged at temperatures above $600^{0}C$.

b) Alloy Steels: Generally the flow stress decreases with increasing temperature. Any temperature in the warm forging range may be used , depending on circumstances.

c) Austenitic Stainless Steels: Flow stress reduces greatly with small increases in temperature although they may strain harden significantly. Temperatures between 200°C and 300°C are commonly used.

2.5 Tooling Equipment in Warm Forging

The choice of forging machine will depend on a number of factors such as forging load, batch quantities, required productivity and ultimately availability relative to budget.

In principle, the ideal warm forging machine should have a rapid stroking rate to reduce dwell times and avoid overheating of tools. Note however that higher stroking rates can increase the flow stress of the workpiece material and hence the forging load. Press stiffness and accuracy of ram guidance should be similar to those for cold forging. Slide geometry should be temperature compensated so that small clearances can be maintained. Ejection should be built into the press operating system and should be rapid acting to minimize workpiece die contact time.

Crank presses with their rapid stroking rates are the ideal type of machine. They can accommodate multi-stations with mechanical ejection and transfer systems, and integral lubrication/cooling facilities. Production rates of typically 40 parts a minute are achievable.

Hydraulic presses are used in some companies for relatively small batch quantities. Often they are manually fed at a rate which allows time for the extra cooling necessitated by the long dwell times. Lack of automation results in less process control (transport and dwell time in particular) and therefore a tendency for lower product consistency than for completely mechanical systems.

Tool loads for warm forming are cyclic and nearly as high as for cold forging, at the same time tools are in contact with warm workpieces causing thermal shocks. The surface expansion of the work-piece can be very great resulting in severe tribological conditions. To secure a stable process and consistent product accuracy, wear and fracture resistance must be high.

For an adequate tool design, tool material selection must be correct and process planning optimized and to achieve this, the following reliable data are needed

- Physical properties of work-piece material
- Number of components to be forged
- Forging loads and tools stresses
- Forging temperature
- Production rate
- Kinematics of forging machine
- Geometric limits to shape of tools

2.6 Tool Manufacture for Warm Forging

Tools for warm forming are mostly made from high alloyed tool steels. To specify the most appropriate machining processes additional knowledge and experiences must exist.

The following list shows common machining operations used in tool making:

- turning
- hard turning
- milling
- high speed milling (HSM or HSC) of heat treated elements
- drilling
- grinding
- electro-discharge machining (EDM)
- wire electro-discharge machining (WEDM)
- honing
- lapping
- polishing

In tool production, special care must be dedicated to the problems of surface quality, to avoid micro-cracks, white layers and other defects.

When the tool manufacturing for warm forging is considered, the whole procedure is usually limited only on two technologies, other technologies are applied only as assisting technologies. These two technologies used for tool making for warm forging are:

- Electro-discharge machining (EDM) and wire electro-discharge machining (WEDM)
- High speed cutting (HSC) or high speed milling (HSM)

It is very well known that the EDM technology is not so flexible but any tool shape can be produced. HSC technology is very flexible, but there are some geometrical limitations. The advantage of HSC is much faster material removal and greater precision.

2.7 Characteristics of Warm Forging Affecting Tooling

The tools for warm forging and predominantly the active elements of these tools such as dies and punches are exposed to a high, cyclical mechanic stress. The combination between rather high forming temperatures and the still relatively high forming forces make the selection of suitable tool material as well as the design of the entire tool construction for warm forging more difficult than for cold or hot forging [32].

In warm forging, as with any forming operation, the choice of tool material can be critical both technically and economically. Technical failures of tooling due to excessive wear, deformation, cracking or heat checking occur because either the wrong steel has been selected or because the heat treatment, coating or machining procedures have not been optimized. All technical failures lead to financial loss due to lower tool life and therefore increased tool material costs, repair costs, maintenance costs and increased stand still time leading to lower productivity. A number of steps can be taken to help prevent the premature failure of a tool.

- Correct selection of tooling material for each specific case
- Tool design to avoid stress raisers which may cause cracking under high load
- Optimization of heat treatment in consultation with the tool steel manufacturer
- Optimization of any coatings (nitride etc.) applied to tooling in consultation with a coating specialist

- Optimization of the machining procedure
- Careful maintenance
- Adequate and even pre-heating
- Optimum choice of lubrication or cooling mediums

When switching from cold or hot forging to warm forging, care should be taken of some typical characteristics of warm forging which may lead to problems with tooling.

- Peak surface temperatures of the tools can reach up to around 800°C, and bulk temperatures 400°C. [31] The higher the temperature of the tooling, the more likely it is to lose its initial hardness quickly, resulting in wear or deformation.
- The time of contact between tool and hot work-piece, the thermal conductivity of the tooling and the type of lubricant used can affect the peak temperature in the tooling and hence its lifetime [33], either due to heat checking or by softening.
- The cyclical thermal loading on the tooling can lead to heat checking [33]. This is countered by keeping the temperature difference as low as possible (lowest possible workpiece temperature, suitable pre-heating of tooling, tooling with adequate thermal conductivity). A low thermal expansion, high toughness tooling material can also help.
- If water based lubrication is used, or tool surfaces are actively cooled, thermal shock can result. [31]
- Warm forging pressures are typically twice those for hot forging and half those for cold forging. [31]. For this reason tooling tends to be more similar to cold work tooling than hot work tooling.
- Surface abrasion (wear) is not as prevalent as in hot forging, but is more important due to the higher tolerances demanded of warm forged components.

The above bullet points indicate that the working elements of warm forging tools must have: [31]

- High hot strength/hardness and wear resistance
- Good thermal shock resistance and thermal fatigue strength.

2.8 Tool Material Selection in Warm Forging

When selecting the adequate tool material for warm forging, for existing processes the most important factor to consider is the current mode of failure (cracking, deformation, wear, heat checking), and also the working hardness which must be achieved. For a new process, possible modes of failure should be considered; e.g. are problems with deformation likely to occur because of high temperatures, high loads or long cycle times? Is wear likely to be a problem because a particular grade of work-piece is being formed (highly alloyed, high strength, hard to deform), or because flash is expected?

Therefore, firstly some common failure modes for warm forging tool steels should be examined to decide on the tool material. Summary of some common failure modes in warm forging, their causes and suggested solutions are given below [31]:

a) Catastrophic Cracking

Sign: Tool "goes with a bang". Large crack results in breakage of tool or large hairline crack appears.

Cause: Local loading on tool can not be absorbed by tool material.

Solution: Stress raisers in the tool (edges, sharp radii etc.) should be examined. Alternatively, heat treatment of the tool can be examined. For example, cooling of a tool too quickly can result in formation of internal heat treatment stresses, and the tool may fail catastrophically when loaded. If stress raisers are not present and heat treatment was correct, tool material with higher toughness should be selected.

b) Heat Checking

Sign: Formation of a network of small cracks on the surface.

Cause: Cyclical thermal and mechanical loading.

Solution: Higher strength and/or higher toughness tooling material can be selected. Additionally, tool material with higher thermal conductivity or lower thermal expansion can be used alternatively.

c) Abrasive Wear

Sign: Abrasive wear is often present in flash areas or on radii of punches as grooved but polished surface.

Cause: Soft tooling material is being gouged away by hard work-piece material.

Solution: Selection of tool material with higher strength / hardness or wear resistance (greater carbide content), or addition of a wear-resistant coating to the tool like nitriding.

d) Deformation

Sign: In deformation failure mode, material is not removed from the tool as in wear, but is pushed out of place. Deformation mainly occurs at edges of tooling.

Cause: Soft tooling material is being displaced by hard workpiece material.

Solution: Selection of tool material with higher strength / hardness.

In practice, there is often a mixture of failure modes on one tool, and a compromise solution must be sought.

2.9 Lubrication and Cooling in Warm Forging

The function of a tool lubricant is essentially to:

- Maintain a barrier between tool and workpiece thereby eliminating pick-up and obviating wear.
- Reduce tool/workpiece friction thus reducing forging loads and tool stresses.
- Cool the tools to maintain their hardness and avoid plastic deformation.

Spraying is almost always used to apply tool lubrication and automatic lubricating systems synchronised to the stroking of the forging machine are essential in high productivity mass production lines.

Some lubrication systems sequentially blast air into the cavities to clear debris, blow air/water mist mixture for cooling and then spray a lubricant. Depending on the tool materials and the lubricant one or all three of these operations can be used in a sequence of forging operations.

As a result of the investigation performed to understand the factors which affect die life, it has been discovered that it is essential that an appropriate lubrication adhesion layer must exist after the lubricant has dried in order to improve die life. The conditions that are required for this to happen are thought to be die temperature and spray granularity [34].

Lubricants may be grouped into the following types:

a) Colloidal Graphite-Oil

These lubricant types have a lower latent heat of evaporation than the water based ones and are suitable for use with high-speed steel tools for which rapid cooling is detrimental. A disadvantage of this type of lubricant is the smoke and fumes which are formed on contact with a heated workpiece as well as the high cost of disposal in conformation with environmental control.

b) Colloidal Graphite-Water

These lubricants are essentially pollution free and non toxic, with the qualification that graphite forms carbon monoxide and carbon dioxide. The lubricants are corrosive however largely due to the presence of ammonia as a bactericide and fungicide, so that pipes and fittings should be of stainless steel.

Water based graphite lubricants used under the correct conditions, form a solid coating on the tools. This is an advantage in situations when an oil based lubricant would run off the tool surface or be squeezed out of the workpiece/tool interface. Current products are commonly used to coat tool surfaces at temperatures of 400°C and above and using special spraying techniques have been used to coat tools at temperatures up to 800°C. Because of their good coating and friction reducing properties, water based graphite lubricants are probably the most popular at present. However, although they are environmentally harmless, the fact that they cause plant and equipment to be covered in a black film has brought them into disfavor and attempts are underway to develop white or colorless lubricants. Another disadvantage of colloidal graphite is that unless continuously agitated, it tends to flocculate, forming sediment in the holding tanks and clogging up pipes and spray nozzles.

c) White Mineral in Water

The compositions of these lubricants are largely known only to the manufacturers. Boron nitride and aluminum silicate are minerals known to have been used and although they form robust interfacial boundaries to obviate pick-up they are not very effective at reducing friction.

d) Colorless Solutions in Water

The development of white/colorless lubricants has been underway for several years and noticeable performance improvements have been achieved. One distinct advantage of these lubricants is that being water soluble the plant and workshop environment is readily washed clean. Also as the lubricating substances remain in solution pipework does not become clogged.

CHAPTER 3

THERMO-MECHANICAL ANALYSIS OF THE CURRENT PRACTICE USING FINITE VOLUME AND FINITE ELEMENT METHODS

In this chapter, hot forging of the specified part will be simulated using Finite Volume Method (FVM) and Finite Element Method (FEM) by using the forging temperature and tooling specified by the forging company.

3.1 Sample Case and Current Process Used in the Forging Company

The part in consideration is used in automotive industry. Photographs of the part are given in Figure 3.1. The technical drawing of the part is given in Appendix A.

Figure 3.1 Photographs of the Part [35]

The part is currently forged at 1150 ^{o}C which is in hot forging temperature range, in the steel forging company. The circular billet is heated in an induction heater of 100 KVA and having coil diameter of 40 mm. A 1000 ton eccentric mechanical press having three stations for three sets of dies is used in the process. The billet material is St 52-3 according to DIN 17100 standard. The chemical composition of the material is given in Table 3.1 and the mechanical properties are given in Table 3.2.

Table 3.1 Chemical Composition of St 52-3 [36]

DIN	C %	Si %	Mn %	P %	S %
St 52-3	≤ 0.20	≤ 0.55	≤ 1.60	0.040	0.040

Table 3.2 Mechanical Properties of St 52-3 [36]

Tensile Strength, R_m	490-630 MPa
Yield Strength, $R_{p0,2}$	345 MPa
Elongation, A_5	22 %

The part is forged in three steps in current application as seen in Figure 3.2. The initial billet has a diameter of 30 mm and its length is 30 mm and the weight of the reference sample parts are measured on the scale as 175 g. First, the billet is upsetted between flat dies to a cross section of approximately 43 mm x 27 mm and a height of 22 mm. Since this stage is open die forging, these geometrical dimensions can not be hundred percent controlled. Those dimensions may change for subsequent parts that are forged. In upsetting stage, the billet is forged two times in the rolling direction. Aim of this upsetting stage is to prepare an optimum shape for the subsequent stages and additionally to get rid of scale layer that is formed on the surface of the billet in heating stage. As a second step, the upsetted billet is forged in closed preform dies, and at this stage, unfortunately there is excessive flash formation which is usually accepted unfavorable in perform stages. Finally closed finish dies are used to obtain the finish geometry.

(a) Upsetted geometry (b) Preform geometry (c) Finish geometry with flash

Figure 3.2 Photographs of Reference Sample Parts at Three Stages of Forging

There are three sets of dies used in the process. First set consists of two flat dies which are used in upsetting process. They are basically simple, flat, circular dies. Their material is DIN 1.2714, corresponding to AISI L6. Second stage which is the preform stage is closed die forging. Finally the third die set is for finishing stage. The technical drawings of the preform and finish dies are given in Appendix A. Photograph of the current preform die set is given in Figure 3.3 and photograph of the current finish die set is given in Figure 3.4.

Figure 3.3 A View of Current Preform Die Set

Figure 3.4 A View of Current Finish Die Set

The material of the preform dies and finish dies is also DIN 1.2714, corresponding to AISI L6. The chemical composition of DIN 1.2714 (AISI L6) is given in Table 3.3. [36] The mechanical properties of DIN 1.2714 are given in Table 3.4 [37]

Table 3.3 Chemical Composition of DIN 1.2714 (AISI L6) [36]

AISI	DIN	C %	S %	Mn %	P %	S %	Cr %	Mo %	Ni %	V %
L6	1.2714 56NiCrMoV7	0.50-0.60	0.10-0.40	0.65-0.95	0.030	0.030	1.00-1.20	0.45-0.55	1.50-1.80	0.07-0.12

Table 3.4 Mechanical Properties of DIN 1.2714 (AISI L6) [37]

Tensile Strength, R_m	1174 MPa
Yield Strength, $R_{p0,2}$	645 MPa
Elongation, A_5	25 %
Reduction of Area, Z	55 %
Modulus of Elasticity	200 GPa
Poisson's Ratio	0.28

After the finishing stage, the hole is punched and the flash is trimmed in the trim press which has a capacity of 250 ton. Trimming and punching stages will not be analyzed in this study.

Process sheet of the current process is given in Appendix B.

Some problems related to the current process are reported by the forging company [35]. These problems are:

- After the finish forging stage, cold ironing is required in the parts to get accurate hexagonal cavity dimensions,
- There is excessive wear in the preform and finish dies resulting from high stresses on the dies.

Additionally, when the process sequence is observed in the factory and when the reference sample part dimensions are measured, it is clear that the flash amount is quite high and the flash distribution is quite non-uniform around the periphery of the part.

As mentioned before, tolerances are better and closer dimensions can be obtained in warm forging compared to hot forging. Therefore, the problem of accuracy in dimensions can be solved by forging the part in warm forging temperature range.

It is concluded from the simulations that, the problem of excessive wear in preform and finish dies can be solved by improving and modifying the operation sequence and the die geometries, especially the preform dies. The simulations and design improvement stages will be mentioned in detail in subsequent sections.

3.2 Modeling the Part, the Billet and the Dies of the Current Process

The part is modeled in 3-D, based on the technical drawings provided by the company[35], using Pro/Engineer WF 3.0[38]. 3-D model is given in Figure 3.5.

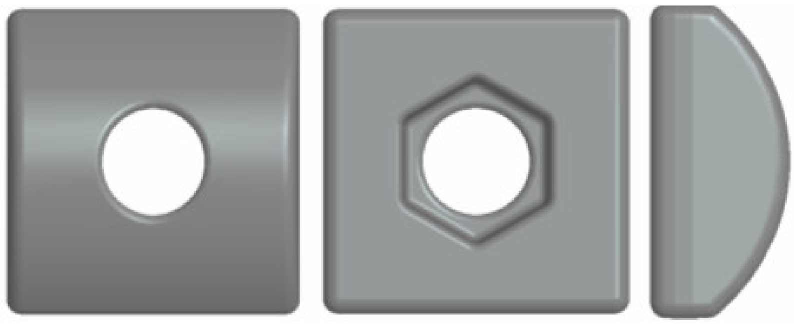

(a) Front View (b) Back View (c) Right View

Figure 3.5 Views of 3-D Model of the Part

The billet, having a radius of 15 mm and a height of 30 mm, is modeled in Pro-Engineer WF 3.0.

The dies are modeled in Pro/Engineer WF 3.0 [38] based on the technical drawings provided by the forging company. The 3-D models of the current preform die set are given in Figure 3.6 and 3-D models of the finish die set are given in Figure 3.7

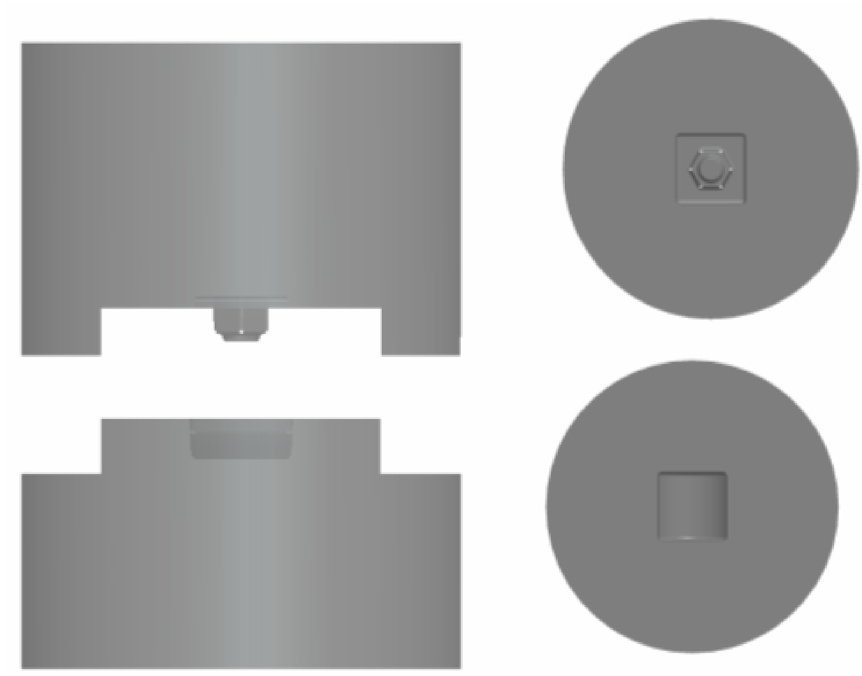

Figure 3.6 3-D Model of the Current Preform Die Set

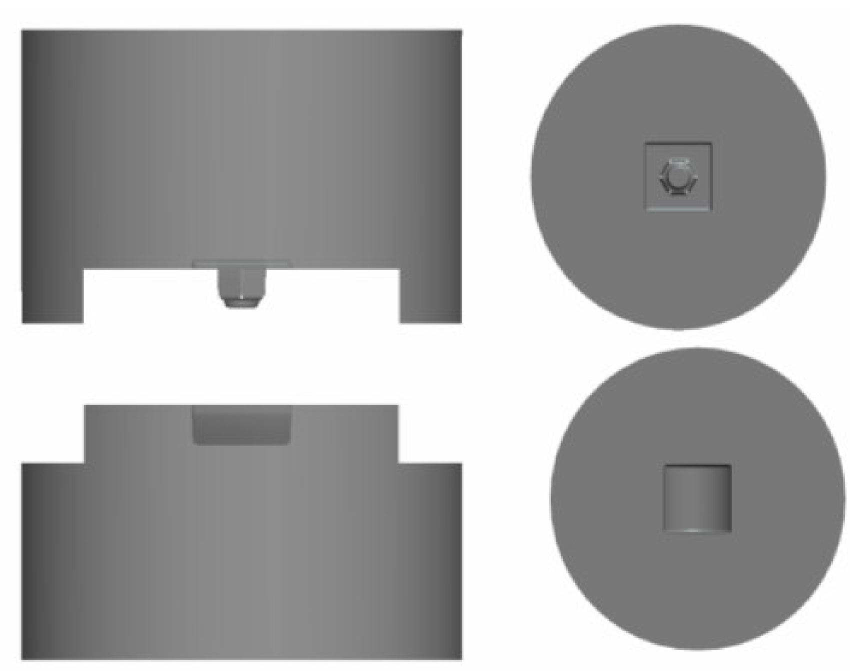

Figure 3.7 3-D Model of the Current Finish Die Set

3.3 Thermo-Mechanical Analysis of Current Process Using Finite Volume Method

In this section, MSC. Superforge 2005 [7], which is a Finite Volume Method (FVM) software, is used to simulate the process sequence. As a result of the simulations, die filling success and flash formation are obtained in the study. In MSC Superforge, the dies are assumed as rigid bodies and only allow heat conduction and heat transfer, therefore it is not possible to simulate strains and stresses on the dies in this software [39].

In MSC Superforge, the following steps are needed to be taken to obtain a complete thermo-mechanical analysis definition [39]:

1- Import models of the workpiece and the dies

2- Assign a material definition to the workpiece and the dies

3- Define the press

4- Define the heat properties, like heat conduction, heat transfer and initial temperatures

5- Define the friction model and the coefficient of friction

7- Define the simulation conditions; e.g. type of operation, stroke value, etc.

8- Visualization of the results

3.3.1 Modeling of Billet and Dies

The billet and the dies are modeled in 3-D since the geometry of the part is not suitable to reduce it to a 2-D axisymmetric model. The 3-D models are imported in “stl” format from Pro-Engineer to MSC Superforge. In “stl” format, the part is divided to triangles and the geometry is defined by these triangles.

3.3.2 Assigning Material Definition to the Workpiece and the Dies

MSC Superforge has a material database that includes physical and mechanical properties of certain metals like Aluminum, Copper, Magnesium, Steel, Tool Steel, etc., in many compositions. In the analyses, these material properties can directly be read from this database, and the related values are used in the calculations by the software.

MSC.SuperForge provides elastic-plastic material models. There are forging specific material models available for either cold-forging or hot-forging operations. In the study, the workpiece material is specified as AISI 1020, which is a Carbon steel and its physical and mechanical properties can be read from the database of MSC Superforge. The workpiece material is specified as AISI 1020, because it is decided to use a material which is readily available in the database of the simulation software. The isothermal cylinder-upset test is the most widely used method of obtaining flow-stress data at various temperatures and strain rates [39]. However, it would take so much time and effort to conduct a hot tensile test to obtain the flow curve data of St 52-3, needed for the simulation. Additionally, AISI 1020 is quite similar to St 52-3, considering its Carbon and alloy content; and mechanical properties that would affect the process. The chemical composition of AISI 1020 is tabulated in Table 3.5 [36]. The mechanical properties of AISI 1020 are tabulated in Table 3.6 [36].

Table 3.5 Chemical Composition of AISI 1020 [36]

DIN	AISI	C %	Si %	Mn %	P %	S %
1.0402 (C22)	1020	0.17-0.24	≤ 0.40	0.30-0.60	0.045	≤ 0.045

Table 3.6 Mechanical Properties of AISI 1020 (Quenched and tempered) [36]

Tensile Strength, R_m	490-640 MPa
Yield Strength, $R_{p0,2}$	295 MPa
Elongation, A_5	22 %
Reduction of Area, Z	45 %

As the dies are assumed as rigid bodies in MSC Superforge, when material is assigned to the dies, only thermal conductivity, specific heat and density are taken into account and its mechanical properties are ignored. When no material is assigned to the die, then the die is assumed to be made from H13 Die Steel, and the density and thermal properties will be assigned by default [39]. In the software, the material for the dies is assigned as DIN 1.2714 (AISI L6), the mechanical properties are given in Table 3.4, and the thermal properties that are taken from the MSC Superforge material library are given in Table 3.7 [7]

Table 3.7 Thermal properties of AISI 1.2714 (L6) [7]

Thermal Conductivity	46 (Watt / mK)
Specific Heat & Heat Capacity	420 Joule / kgK

3.3.3 Defining the Press

In MSC. Superforge, different machine tools are available which are; Crank press, Multi-blow Hammer, Screw press, Hydraulic press, Scotch Yoke press and user defined table press. The press that is used in the forging company for the process is, 1000 ton eccentric mechanical press, which corresponds to crank press in the software.

In the software, the parameters that are required to define the operation of a crank press and corresponding values in the specified press are given below. The press definition menu in MSC. Superforge is given in Figure 3.8.

- Crank radius (R) : 125 mm
- Rod length (L) : 665 mm
- Rotational Speed : 90 rpm

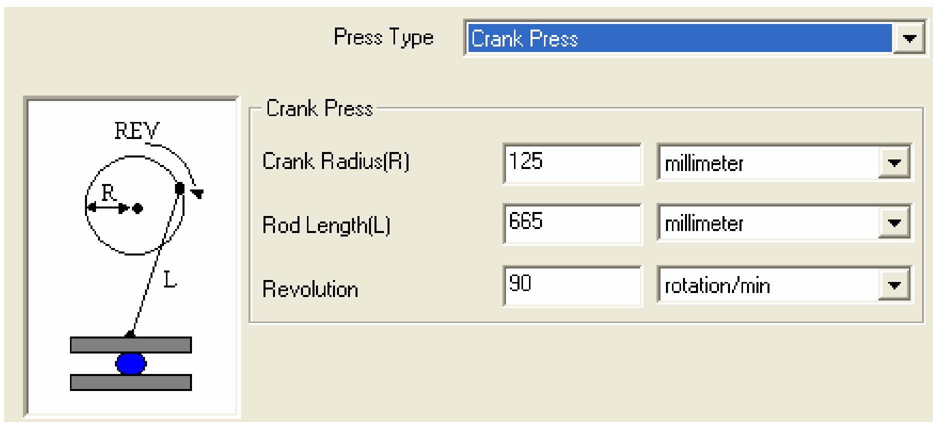

Figure 3.8 Press Definition Menu in MSC. Superforge [39]

3.3.4 Defining the Heat Properties

In the analyses, initial temperature for the dies is given as 250 ^{o}C, initial temperature for the workpiece is given as 1150 ^{o}C. Heat properties like heat transfer coefficient and emissivity for heat radiation to ambient are taken from the predefined material library automatically by the software.

3.3.5 Defining the Friction Model and the Coefficient of Friction

As the workpiece and the die have rough surfaces and are forced to move tangentially with respect to one another, frictional stresses will develop at the interface. Therefore, a friction model should be applied to both of the dies. For forging operations involving relatively low contact pressure between dry contact surfaces, the Coulomb's friction model is most appropriate [39]. If the frictional shear stress reaches a critical value, the workpiece will slip along the die. According to Coulomb's law of friction, this value is given by:

$$\tau = \mu \, \sigma_n \tag{3.1}$$

where, μ is the coefficient of friction and σ_n denotes the normal stress at the workpiece-die interface.

The alternative model to Coulomb's law of friction is Tresca's friction model, which is the law of plastic shear friction. According to this model, if the frictional shear stress, τ, exceeds a constant fraction m of the flow stress in shear, τ_{yield}, the workpiece starts to slip [39]:

$$\tau = m.\ \tau_{yield} \tag{3.2}$$

A value of zero for m represents perfect sliding, which means there is no shear or friction at the workpiece-die interface. A value of one for m represents sticking friction, which means that the friction shear stress equals the flow stress of the material in shear. For forging operations involving relatively high contact pressures, it is generally more appropriate to use the law of plastic shear friction [39].

In this study, plastic shear friction model is used as friction model for the simulations. The friction factor is assumed as 0.3. This value was also used in other similar studies [16-19,21,22].

3.3.6 Defining the Simulation Conditions

In the simulation conditions part of the software, type of the problem, whether it is open die forging, closed die forging, extrusion, etc is defined. Additionally, the stroke value is specified. Size of the finite volume elements are also specified in this part. A general rule of thumb is to include 2 finite volume elements within the smallest feature, this feature typically being the flash thickness. [39]. In the analyses, as the flash thickness is about 2 mm, the workpiece element size is taken as 1 mm and the finite volume ratio is taken as 0.2. Finite volume ratio is used to make the finite volume elements that constitute the billet, smaller compared to global elements. When the mesh is finer, simulation results get more accurate, however the computation time increases.

3.3.7 Visualization of the Results

As mentioned before, flash formation and die filling success are examined in this part using MSC Superforge. The geometry of the part at each stage of the process, namely first upsetting stage, second upsetting stage, preform stage and finish stage are given in Figure 3.9.

When the Finite Volume Analysis results are compared with the reference sample parts, the flash formation in the preform and finish stages is quite similar with the real application in the company. Like the real practice, the flash distribution is nonuniform around the periphery of the preform and finished part. Additionally, the flash amount is quite high which causes excessive material wastage. A problem related to die filling is not observed in the results, which is consistent with the real practice.

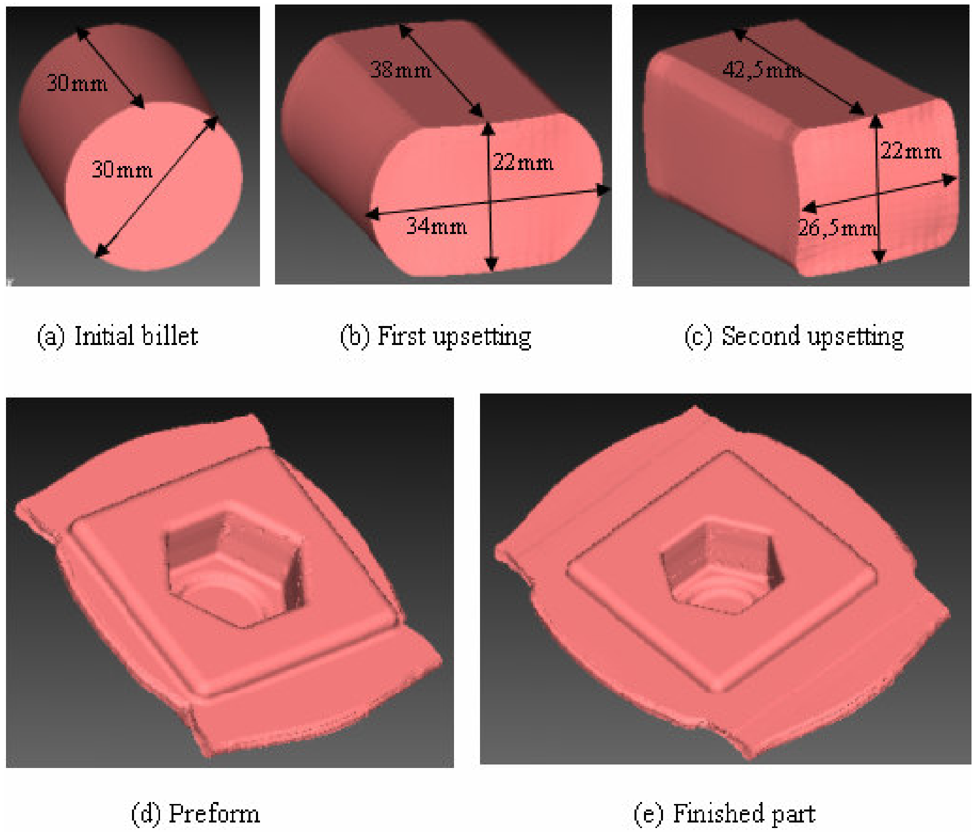

Figure 3.9 Geometry of the Part at Each Stage of the Process

3.4 Using FEM To Simulate the Process With Die Stress Analysis

In this step, analyses are made by using MSC.Superform 2005 software which uses Finite Element Analysis (FEM) method [40]. In the study, the finite element analyses are quite complex and require considerable computational time and high capacity computers. The factors that increase the complexity of the model are; modeling as coupled thermo-mechanical analysis, modeling the geometries in 3-D, modeling the dies as deformable bodies, using the pre-state option to represent the consecutive preform and finish stages. The details of these factors will be given later in detail.

The analyses are performed with following steps:

1- Modeling and mesh generation,

2- Assigning material properties,

3- Applying initial conditions,

4- Applying boundary conditions,

5- Defining contacting bodies,

6- Defining re-meshing criterion,

7- Defining load-cases,

8- Visualization of results.

After these steps, the solution process is applied for all subsequent forging stages.

The analyses are modeled as coupled thermo-mechanical analysis. The thermo-mechanical analysis is utilized in the solution of the mechanical problems, where a temperature change occurs within the material during the process and the variation of properties of the materials due to this temperature change is significant. Also, the heat generation in a mechanical problem due to plastic work or an external heat source requires a coupled analysis. The thermal and mechanical analyses are carried out in each load/time increment [41].

The thermal strains are created within the body due to change of temperature. These are calculated by the following formula:

$$\Delta \varepsilon^{th} = \int \alpha \, \Delta T \qquad (3.3)$$

where $\Delta\varepsilon^{th}$ is the strain increment, α is the coefficient of thermal expansion and ΔT is the temperature increment. The nodal forces due to thermal strains are then added to nodal force vector during solution.

In the general procedure of the coupled thermo-mechanical analysis, at a time step t, the mechanical equilibrium equations are solved using the flow curve corresponding to the temperature at the beginning of the time step. The geometry is updated at the next time step, t+Δt. A pure thermal analysis is carried out at t+Δt and a new temperature distribution is calculated. The mechanical calculations are carried out by the using the updated temperature values. The flow diagram of the coupled process is given in Figure 3.10 [42].

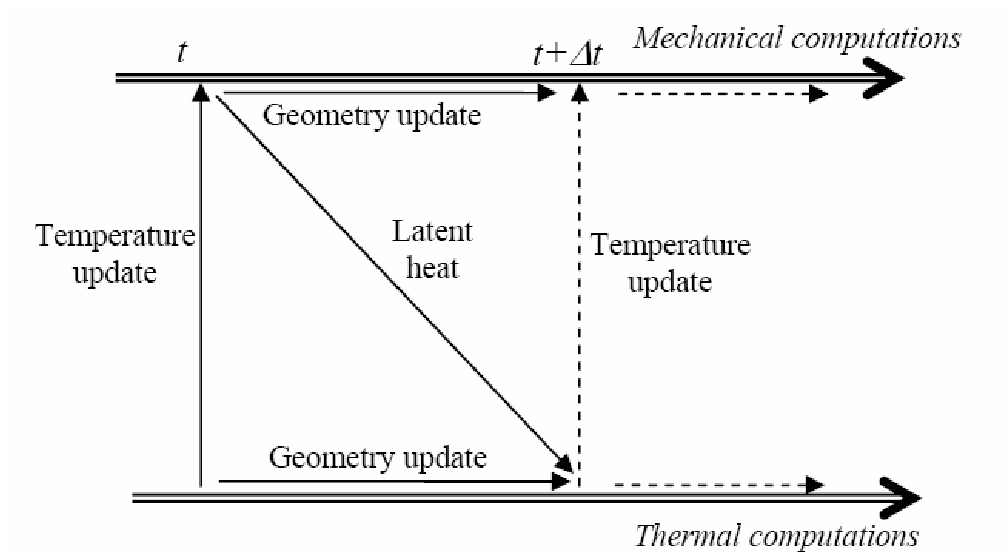

Figure 3.10 Flow chart of the coupled thermo-mechanical analysis [42]

3.4.1 Modeling and Mesh Generation

In the study, die and billet geometries are designed and modeled using Pro/Engineer WF 3.0. The models of the billet and the dies are created in 3-D space, since the geometries are not suitable to reduce it to a 2-D axisymmetric model. However, the geometry of the part at the preform and finish stages, and geometries of the dies are symmetrical with respect to the two perpendicular planes passing through the center of the workpiece. This provides the opportunity to simulate the process by using a model of one quarter of the actual specimen and reduces the computational time considerably. As the dies are modeled as deformable bodies in the study, mesh generation is required also for the dies, and as the number of elements and nodes increase in an analysis, the computational time increases in considerable amounts and stability of the analysis is hard to achieve. Therefore, it is quite important to use the symmetry case as much as possible in the finite element analyses. The upsetting stage can not be reduced to ¼ symmetrical model, therefore the billet is modeled considering the dimensions after the upsetting stage, as shown in Figure 3.11. The dimensions are obtained from the results of the Finite Volume Simulation that is explained in Section 3.3.

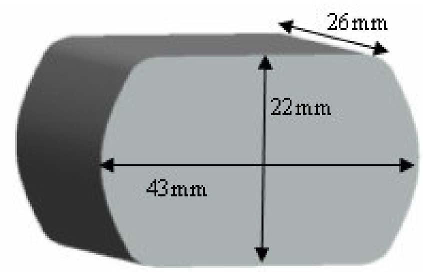

Figure 3.11 3-D Model of the Billet After the Upsetting Stage

After modeling the billet, 3-D model of the billet is exported in "iges" format from Pro/Engineer to MSC Superform, 2-D surface meshing is performed using 4 nodded quadrilateral elements, and the surface mesh is expanded to form the 3-D mesh. As a result, the billet is meshed using 8 nodded hexahedral elements. Element type 7 [43] is used in the billet. Properties related to 8 nodded hexahedral elements and element type 7 are given in Appendix C. Initial number of 3-D finite elements in the billet at preform stage is about 12000 and the initial average edge length is 0,7 mm. The elements at the end of preform stage are exported to the finish stage by using the pre-state option. Initial number of elements in the billet at finish stage is about 30000, and the initial average edge length is about 0,3 mm. These are the initial values and the number of elements and edge lengths are changing due to remeshing at the end of simulations.

After modeling the preform and the finish dies as explained in Section 3.2, the 3-D models of the dies are exported in "iges" format from Pro/Engineer to MSC Patran [44], and mesh generation using 4 nodded tetrahedral elements is performed in this software, as the geometries are quite complex and it is hard to create the mesh in MSC. Superform. MSC. Patran is an open-architecture, general software. It enables direct access to geometry from many CAD systems for creating finite element models. MSC.Patran finite element system permits the user to directly access model geometry and to quickly develop finite element meshes [45]. Properties related to 4 nodded tetrahedral elements are given in Appendix C. Number of finite elements in the preform dies is about 8000 and the smallest edge length is about 1 mm. At sections with small details, finer mesh is used and at larger sections the mesh is coarser. Number of finite elements in the finish dies is about 10000 and the smallest edge length is about 0,6 mm

3.4.2 Assigning Material Properties

After mesh generation, material properties for the elements are assigned. Material properties of the workpiece are read directly from the material library of MSC. Superform. Material of the dies is DIN 1.2714 as mentioned before.

<u>Material Properties for the Workpiece:</u>

MSC.SuperForm allows the workpiece material to be represented as either elastic-plastic or rigid-plastic material. In the elastic-plastic approach, the elastic deformations on the material are included in the solution. In the rigid-plastic approach, the effects of elasticity are not included. It is widely used in applications, in which plastic deformation occurs and the elastic strains are not considered. The computation time decreases since the formulation does not require consideration of elastic strains. Furthermore the computer implementation is simple and the numerical solution is robust and reliable. Besides the advantages, the rigid plastic formulation, have some disadvantages. Physical behaviors that depend on elasticity, such as spring back or residual stresses, cannot be observed in the solution. The exact final shape and characteristics of the specimen may not fulfill the accuracy requirements. Furthermore, the regions that deform within the elastic range are regarded as rigid and this may lead incorrect results [42]. Considering these facts, workpiece material is modeled as elastic-plastic, in the analyses.

Just like MSC Superforge, MSC Superform has its own material library. The billet material is specified as AISI 1020 and the required parameters are read from the material library. As the analyses are coupled thermal-mechanical, all material properties are taken as temperature dependent by the software.

Material Properties for the Dies:

In the investigation of the problems of forming processes, the dies are mostly regarded as rigid bodies, therefore the elastic deformation of the die is ignored. The effect of this elastic behavior on the metal flow during the forming processes is usually negligible as compared to the size of the workpiece. However, if the working conditions of the forming processes are extreme, such as high frictional constraints at the die–workpiece interface, the geometrical ratios and the flow stress of the material, involving high local pressure, the elastic deflection of the die may considerably influence the local stress and strain of the deforming body and the effect due to die elasticity will be pronounced. Thus, rigid-die analysis is mostly inadequate for forming operations if very high pressure is involved, where precision parts with close tolerances are demanded or analysis on dies is required [46].

In the study, the dies are modeled as deformable, elastic tools. Young's Modulus (E) and Poisson's ratio(ν) are used to define the elastic behavior of the dies. The value of Young's Modulus (E) is given at elevated temperatures, and it is defined as temperature dependent by entering the values at different temperatures in tabular form. Poisson's ratio(ν) is assumed as constant.

3.4.3 Applying initial conditions

In MSC Superform, it is possible to define two kinds of initial conditions which are displacement and temperature initial conditions. In the analyses, temperature initial conditions are used. The mechanical properties of the workpiece material are given as temperature dependent, so the program automatically makes interpolation and takes the values at the given initial temperature into consideration, at the first increment of the analysis. As the analyses are modeled as coupled thermo-mechanical, material properties are updated at each increment by the software as explained in Section 3.4. In the study, initial temperature for the nodes on the dies is given as 250 ^{o}C, initial temperature for the workpiece nodes is given as 1150 ^{o}C for the preform stage.

On the other hand, for the finish stage, the “pre-state” initial condition is used. In the “pre-state” initial condition, the strain values, stress values and temperature values at any increment of the solution can be directly exported to the next stage of forging. In the study, the specified values on the workpiece at the last increment of preform stage are exported and used in the finish stage.

3.4.4 Applying boundary conditions

Type of boundary conditions that can be defined in MSC Superform are; mechanical boundary conditions and thermal boundary conditions. In the study, the mechanical and thermal constraints are defined by using contacting bodies instead of using boundary conditions to get a better representation of the experimental setup. For example, the upper die and the lower die are mounted to the die holders in the press assembly in application. To define these constraints, “fixed displacement” or “hold nodes” mechanical boundary conditions could have been defined. However, two rigid contacting surfaces representing the upper and lower die holder surfaces are used instead of this. Additionally, thermal boundary conditions are represented by defining thermal properties for each contacting body.

3.4.5 Defining contacting bodies

The contacting bodies defined in MSC Superform are shown in Figure 3.12 and the list of contacting bodies is given below:

- Workpiece as deformable body
- Upper and lower dies as deformable bodies
- Symmetry planes as rigid surfaces
- Upper and lower fixing surfaces as rigid surfaces

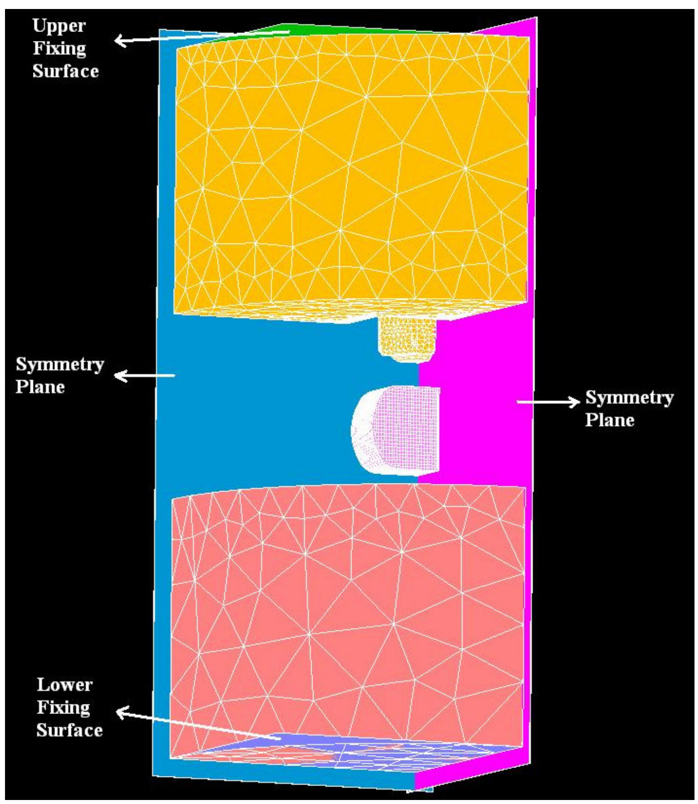

Figure 3.12 ¼ Model of the Billet, the Preform Dies and the Symmetry Planes

3.4.6 Defining re-meshing criterion

In manufacturing simulations, the objective is to deform the workpiece from some initial (simple) shape to a final, often complex shape. This deformation of the material, results in mesh distortion. For this reason, it is often required to perform a rezoning/remeshing step. In forming processes, deformation is usually very large. Moreover, the relative motion between the die surface and the deforming material is also large. Such large deformations and displacements cause the following computational problems during FEM simulation with Lagrangian mesh.

- Difficulties in incorporating the die boundary shape into the FEM mesh, with increasing relative displacement between die and workpiece.
- Difficulties in accommodating the considerable change of deformation mode with one mesh system.
- Formation of unacceptable element shapes due to large deformation

In order to overcome these difficulties, it is necessary periodically to redefine the mesh system. The rezoning consists of two procedures. One is the assignment of a new mesh system to the workpiece and the other is the transfer of information from the old to the new mesh through interpolation. Generation of the new mesh is essentially the same as the initial mesh generation. The field variables, which depend on deformation history, are effective strains and temperatures, and they must be interpolated on the new mesh. [47]

In the analyses, it is applied 3-D remeshing using "Overlay Hex Technique". In this method, when the predefined conditions are satisfied, the program automatically remeshes the workpiece using hexahedral elements. In the study, "strain change" is given the predefined condition for remeshing. Strain Change criterion records equivalent strain change of each element after remeshing. When the strain change of any element reaches the maximum allowed, the new remeshing will occur. [43]. Maximum strain change that is allowed is set to 0.6

in the analyses for adequate frequency of remeshing. In the analyses, inside coarsening level of 2 is used in remeshing to reduce computation time. The "inside coarsening levels" command reduces the number of generated elements; by allowing larger elements to be produced in the interior of the mesh. Tying equations are used to maintain compatibility of neighboring elements. A value of zero indicates that no coarsening occurs; while a value of two indicates that the elements in the interior can be up to 64 times larger than the elements on the surface [43].

In the simulations, final number of elements in the billet at preform stage is about 30000 and the final edge length is about 0,3 mm. Final number of elements in the billet at finish stage is about 20000 and the final edge length is about 0,2 mm. The reason for having less number of elements in the finish stage is using the inside coarsening option at this stage.

3.4.7 Defining load-cases

In MSC Superform, The "loadcases" option is used to group boundary conditions together and to provide additional information so that the analysis can be performed. This data includes the time period, convergence requirements, contact information, and remeshing requirements [43]. In MSC. SuperForm, motion of the tools can be defined by prescribing five substages typically used in forging equipment. These five substages are listed in Table 3.8 and representation of the substages in a forging machine (crank press) is depicted in Figure 3.13 [43]. In the study, the Crank press stage is used. For this type of machine, the stroke displacement is governed by the crank radius and the connecting rod length.

Table 3.8 Five Substages Defining Motion of Tools [43]

Substage	Behavior
1	Workpiece positioning
2	Tools moving in
3	Workpiece deformation
4	Tools moving out
5	Workpiece release

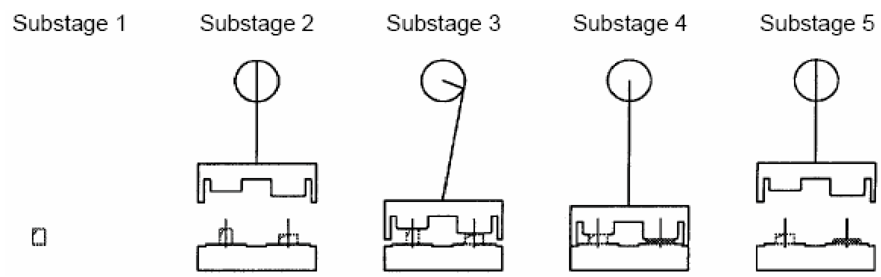

Figure 3.13 Representation of the Substages in a Crank Press [43]

The first substage is to control the positioning of the workpiece onto the fixed lower tools. The workpiece will be moved onto the machine table in the press direction. The second substage is to control the positioning of the tool such that it comes into contact with the workpiece. The third substage is to control the actual forging of the workpiece. In this substage, the stepping procedure for the computation is defined. The available stepping procedures in the software are:

1- Fixed Time Steps

2- Fixed Displacement Steps

3- Adaptive Steps (Plastic Strain)

4- Adaptive Steps (Auto Step)

In the study, “fixed time steps” is chosen as it implements faster solutions by converging fast.

The fourth substage controls the position of the tools as they are moved away from the workpiece. The fifth substage is to control the release of the workpiece from the machine table.

3.4.8 Visualization of Finite Element Analysis Results

The thermo-mechanical results that are obtained from the finite element simulations are;

- Maximum equivalent stress distribution on the preform and finish dies,
- Maximum equivalent stress distribution on the part at finish stage,
- Residual stresses on the preform and the part

The results are visualized using "contour bands" option of the software. The numerical values are tabulated in Table 3.9 and Table 3.10.

<u>Current Preform Stage:</u>

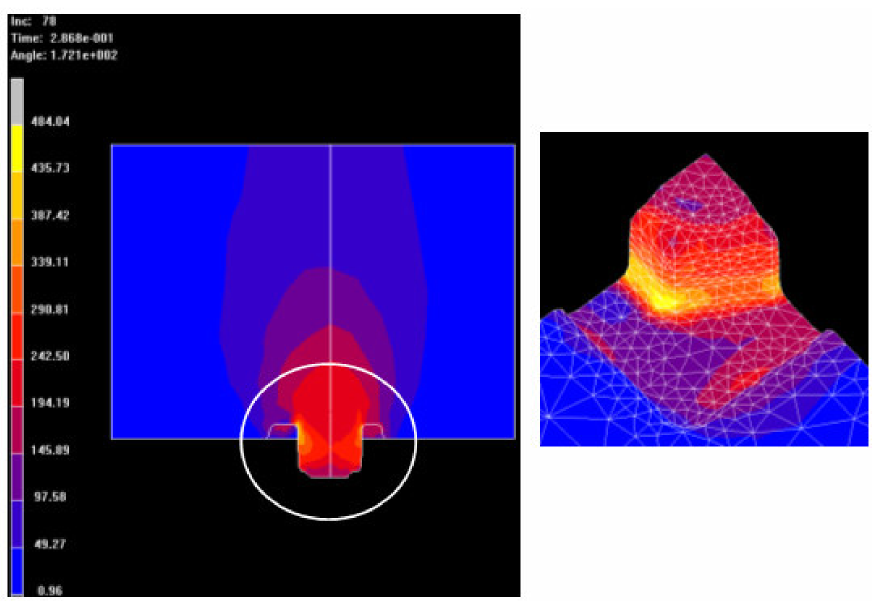

Figure 3.14 Maximum Equivalent Stress on Upper Preform Die

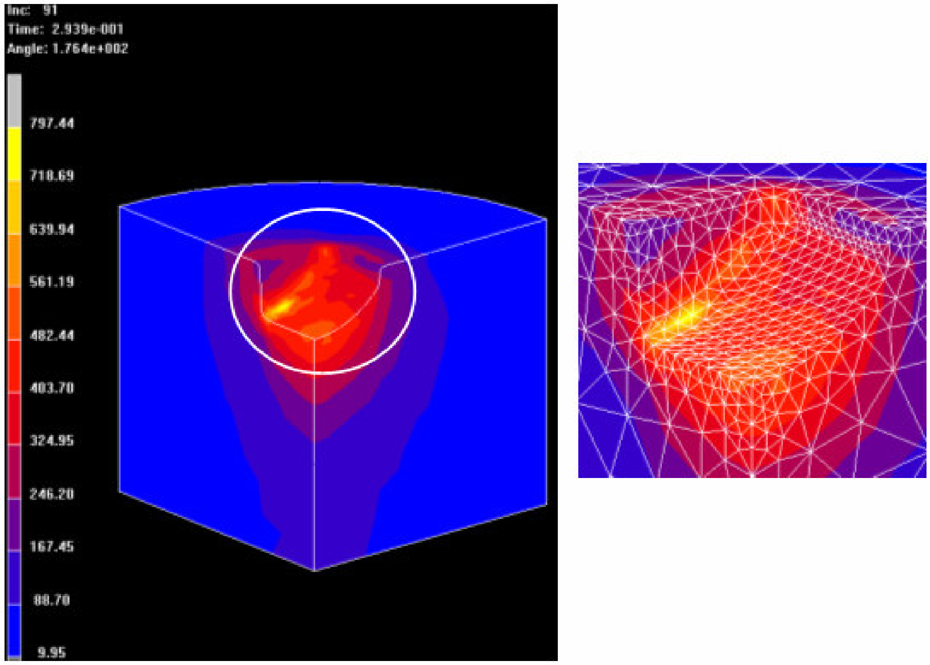

Figure 3.15 Max Equivalent Stress on Lower Preform Die

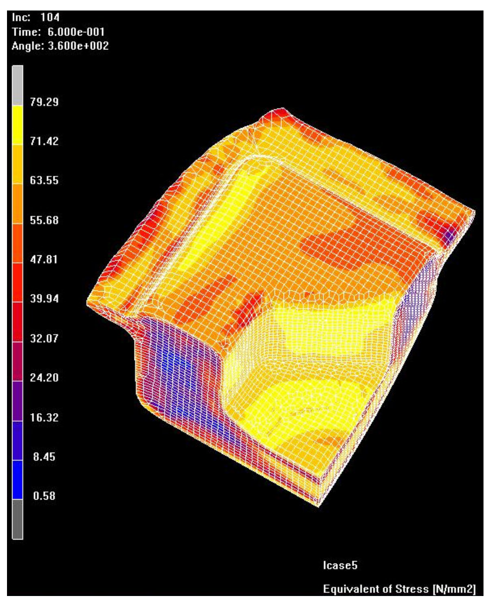

Figure 3.16 Residual Stresses on Preform

Current Finish Stage:

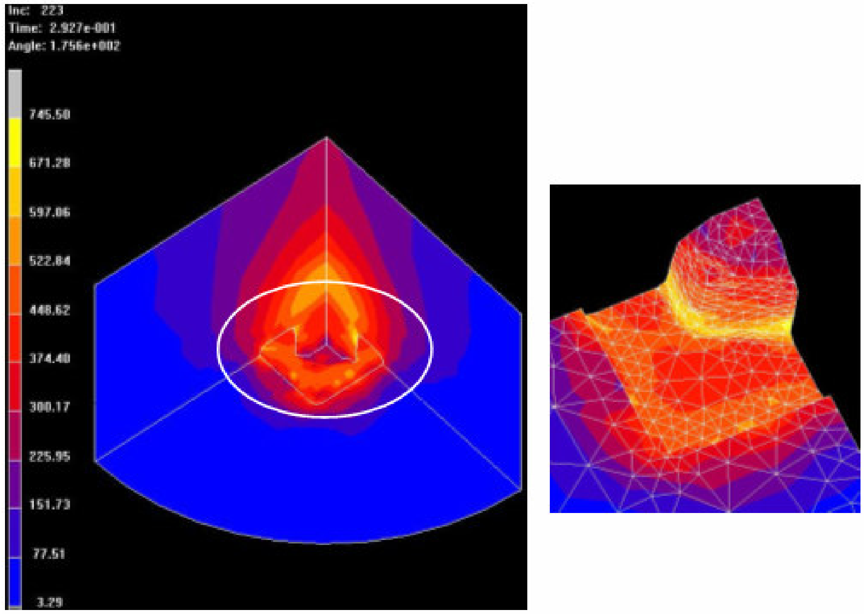

Figure 3.17 Max Equivalent Stress on Upper Finish Die

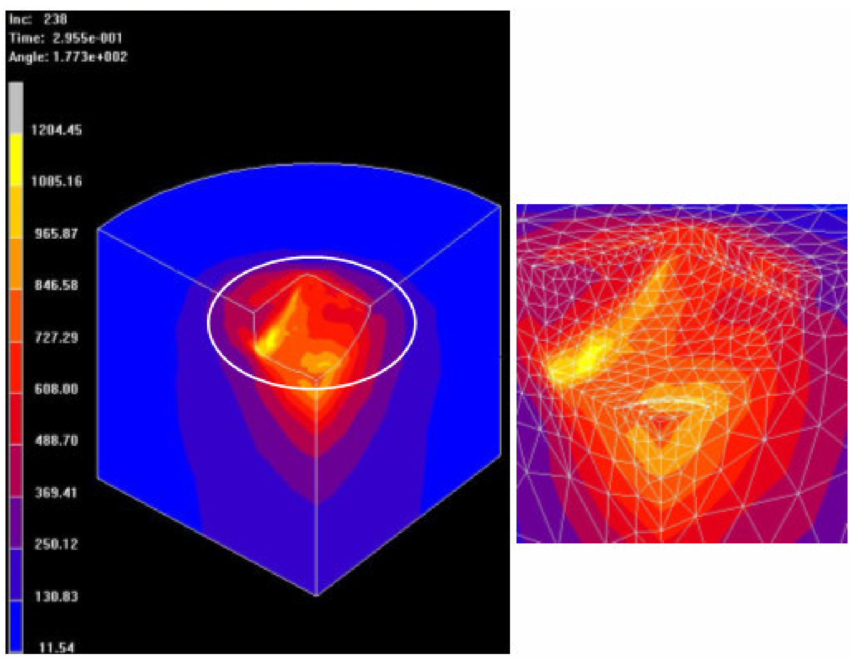

Figure 3.18 Max Equivalent Stress on Lower Finish Die

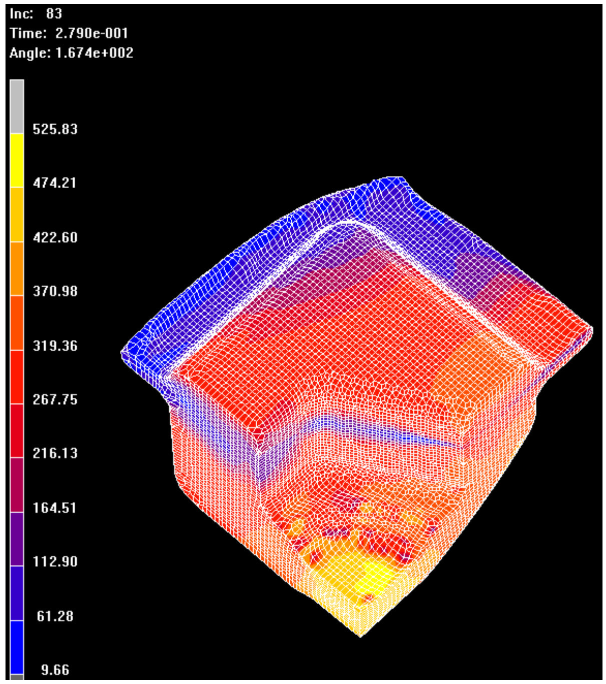

Figure 3.19 Maximum Equivalent Stress on Part at Finish Stage

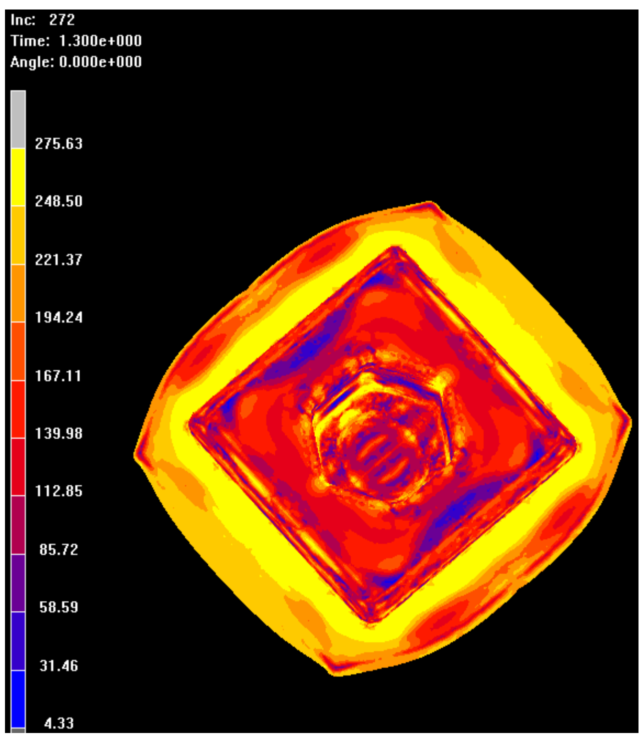

Figure 3.20 Residual Equivalent Stress on Finished Part

Table 3.9 Maximum Equivalent Stress Values

	Maximum Equivalent Stress (MPa)	Process time %
Upper Preform Die	485	47%
Lower Preform Die	800	49%
Upper Finish Die	745	22%
Lower Finish Die	1205	23%
Billet at Finish Stage	525	21%

Table 3.10 Residual Stress Values in Preform and Finished Part

	Residual Equivalent Stress (MPa)	Process time %
Billet	79	100%
Finished Part	275	100%

From the simulations results, it is observed that the flash distributions in the preform and the finished part are similar to the real case.

The maximum Equivalent Stress on the upper preform die is around the edges where the hexagonal protrusion starts, and the value is around 500 MPa. This value is lower than the yield strength of the die material. The maximum equivalent stress on the lower die is around 800 MPa, which is also below the yield strength of the die material. These results show that, plastic strains are not expected on the preform dies during the process.

The maximum Equivalent Stress on the upper finish die is again around the edges where the hexagonal protrusion starts, and its numerical value is around 745 MPa. For the lower finish die, the maximum equivalent stress is about 1205 MPa. The maximum equivalent stress on the lower die is observed to be above the yield strength of the die material, which shows that local plastic deformation is expected at the locations where maximum stress occurs.

Process time %, given in the tables, is calculated by dividing the time of the considered increment to the total process time that is calculated by the software.

Total process time is calculated as 0.6 s for the preform stage and 1.3 s for the finish stage by using the predefined press parameters, i.e. crank radius, rod length, revolution speed and the stroke.

Taking the simulation results into account, it is decided to propose a new process sequence design together with a new preform die design to reduce the equivalent stresses on the dies.

CHAPTER 4

FINITE ELEMENT ANALYSIS OF PROPOSED WARM FORGING PROCESS AND DIES

4.1 General Information About the Proposed Process

The problems that are encountered in the forging company are mentioned in Chapter 3, in this chapter solutions to these problems will be proposed by designing a new forging process sequence design together with new preform design.

In the current practice, the part dimensions after the upsetting stage are 43 mm x 27 mm x 22 mm. During the analyses, it is observed that rectangle-like geometry of the upsetted billet makes the flash distribution nonuniform in the preform and finish stages. The reason is that, the final product has dimensions of 40mm x 40mm x 17mm. Therefore, it is decided that, using a billet with square cross section would be more convenient. Cross section of the square billet is 35 mm x 35 mm, and the height is decided to be 17 mm as a result of the simulations performed in MSC. Superforge and MSC. Superform.

In the designed process sequence, the upsetting stage is eliminated. While eliminating, two aspects of the upsetting stage, which are mentioned before, are taken into account. Preparation of an optimum shape for the subsequent stages is managed by using square billet. Another aspect of the upsetting stage, which is to get rid of scale layer that is formed on the billet in heating stage, considerably, is not a problem in this case study because in the literature it is stated that, serious scaling (where substantial material may be lost and the oxidized material spalls off the surface of the material) does not begin until the material reaches about 850 ^{o}C [48]. In this study, the experiments will be carried at temperatures at which scale formation is not generally serious. Detailed information about experiments will be given in experimentation chapter.

In the design of process sequence, the preform die geometries are modified in order to reduce stress values on the dies, basically on the critical sections that are specified by the forging company and to implement a solution to the wear problem that has been reported by the company. Additionally, the material of the preform dies is improved by convenient material selection, which will be explained later in detail.

The finish die geometries are not changed. It is clear that to obtain the part dimensions specified by the forging company, the finish die dimensions should be identical with the finish dies that are used in the current application. However, the material of the finish dies is improved by convenient material selection, which will be explained later in detail.

4.2 Finite Element Simulations of the Proposed Process

In this section, the details of the Finite Element Simulations will be given. Analyses are made by using MSC.Superform 2005 software which uses Finite Element Analysis (FEM) method. The analyses are performed with the following steps as in the other available software:

1- Modeling and mesh generation,

2- Assigning material properties,

3- Applying initial conditions,

4- Applying boundary conditions,

5- Defining contacting bodies,

6- Defining re-meshing criterion,

7- Defining load-cases.

8- Visualization of the results

After these steps, the solution process is applied for all subsequent forging stages.

4.2.1 Modeling and Mesh Generation

The billet is designed to be square billet with dimensions 35 mm x 35 mm x 17 mm. The billet is modeled in Pro/Engineer WF 3.0 according to the geometrical dimensions specified. The billet and the dies are modeled in 3-D since the boundary conditions in the simulations are not suitable to reduce it to a 2D axisymmetric model. 3-D model of the square billet together with the preform dies is given in Figure 4.1.

Dies are modeled in Pro/Engineer WF 3.0. 3-D model of the designed preform dies is given in Figure 4.2 and 3-D model of the finish dies is given in Figure 4.3 and technical drawings of the preform and finish dies are given in Appendix D. While designing and modeling the dies, the dimensional requirements of the press and the die holders that will be used in the experimentation, are taken into account, and these requirements will be given in detail in experimentation chapter. As can be seen from the 3-D models and the technical drawings, the upper and lower dies have a larger diameter along a height of 50 mm and then the diameter gets smaller. In the preform die set, the outer diameter of the upper and lower dies is 197 mm along a height of 50 mm, then the diameter reduces to 175 mm. In the finish die set, the outer diameter of the upper and lower dies is 222 mm along a height of 50 mm, then the diameter reduces to 200 mm. This stair like geometry is used for clamping the dies to the die holder. Surface of the

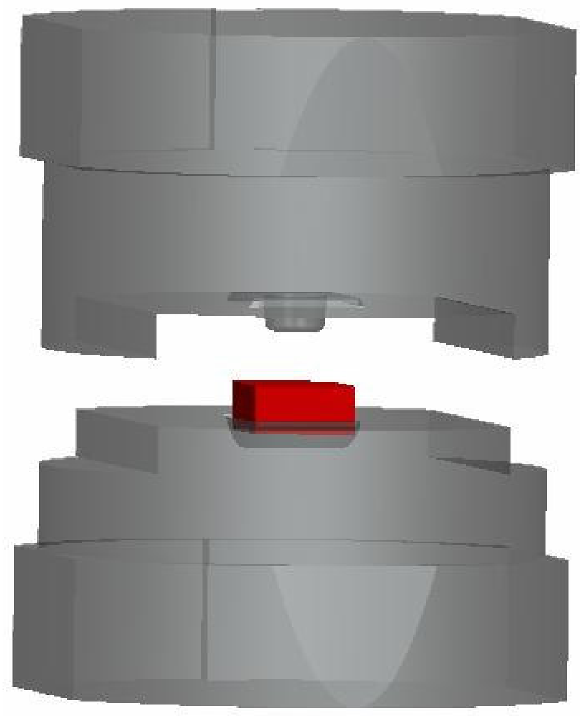

Figure 4.1 3-D model of the square billet

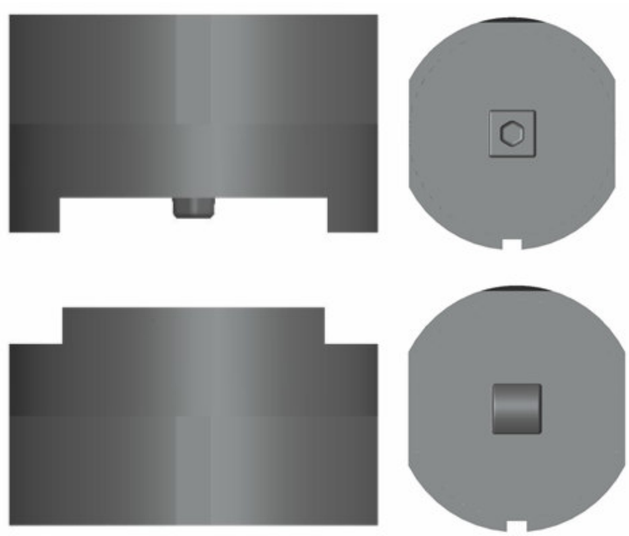

Figure 4.2 3-D model of the preform dies

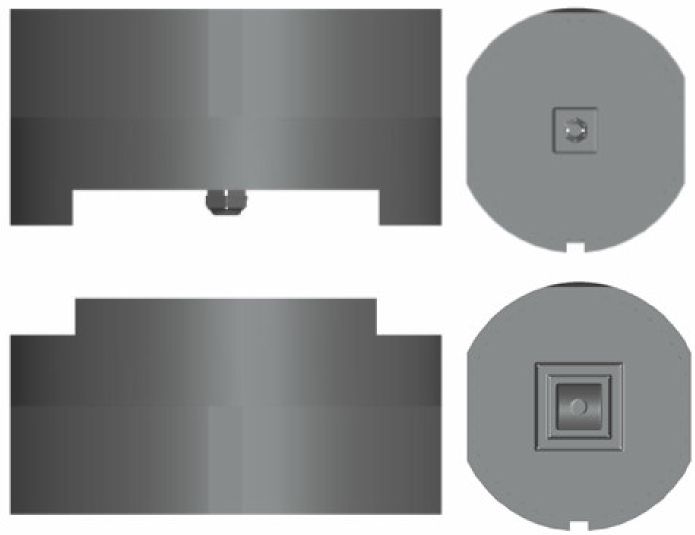

Figure 4.3 3-D model of the finish dies

die clamping elements mate with this larger diameter and when the clamping elements are fastened by bolts, the dies are fixed in the die holder. The die surfaces which are mating with the clamping elements are tapered at an angle of 5 degrees, the clamping elements also have the same angle. Additionally, the key seats having width of 16 mm with the tolerance of H8 [49]; and depth of 9 mm, are designed and modeled in the dies to prevent the rotational motion of the dies relative to the die holder.

After modeling the billet, 3-D model of the billet is exported in "iges" format from Pro/ Engineer to MSC Superform, 2-D surface meshing is performed using 4 nodded quadrilateral elements, and the surface mesh is expanded to form 3-D mesh. Billet is meshed using 8 nodded hexahedral elements.

After modeling the dies, the 3-D models of the dies are exported in iges format from Pro/Engineer to MSC Patran and mesh generation is performed in this software

4.2.2 Assigning Material Properties

After mesh generation, the material properties for the elements are assigned. Material properties of the workpiece are read directly from the material library of MSC. Superform. The material properties of the dies are obtained from the manufacturer's website [50] and entered manually to the program.

<u>Material Properties for the Workpiece:</u>

Just like MSC Superforge, MSC Superform has its own material library. The billet material is specified as AISI 1020 and the required parameters are read from the library.

<u>Material Properties for the Dies:</u>

As mentioned in the previous chapter, the dies are modeled as elastic bodies in the analyses. The material used for the dies is Dievar, which is a patented product, and the properties are obtained from the manufacturer's website [50]. Dievar is a high performance chromium-molybdenum-vanadium alloyed hot work tool steel which offers a very good resistance to heat checking, gross cracking, hot wear and plastic deformation. Dievar is characterized by:

- Excellent toughness and ductility in all directions
- Good temper resistance
- Good high-temperature strength
- Excellent hardenability
- Good dimensional stability throughout heat treatment and coating operations [50].

The chemical composition of Dievar is given in Table 4.1 [50]. The physical properties are given in Table 4.2 [50]. The mechanical properties (Tensile properties at room temperature) are given in Table 4.3 [50]. The tensile properties at elevated temperatures are given in Figure 4.4 [50]. The elastic behavior of the die material is defined by using Young's modulus at different temperatures and Poisson's ratio which is taken as a constant, having a value of 0,3.

Table 4.1 Chemical Composition of Dievar [50]

ISO/DIN	AISI	C	Si	Mn	Cr	Mo	V
PATENT	PATENT	0.35	0.20	0.50	5.00	2.30	0.60

Table 4.2 Physical Properties of Dievar [50]

Temperature	20 ^{o}C	400 ^{o}C	600 ^{o}C
Density [g/cm^3]	7.8	7.7	7.6
Modulus of Elasticity [MPa]	210 500	180 000	145 000
Coefficient of Thermal Expansion		$12.7*10^{-6}$	$13.3*10^{-6}$
Thermal Conductivity [W/m ^{o}C]		31	32

Table 4.3 Mechanical Properties of Dievar(Tensile properties at room temperature) [50]

Hardness	44 HRC	48 HRC	52 HRC
Tensile Strength, R_m	1480 MPa	1640 MPa	1900 MPa
Yield Strength, $R_{p0,2}$	1210 MPa	1380 MPa	1560 MPa
Elongation, A_5	13 %	13 %	12,5 %
Reduction of Area, Z	55 %	55 %	52 %

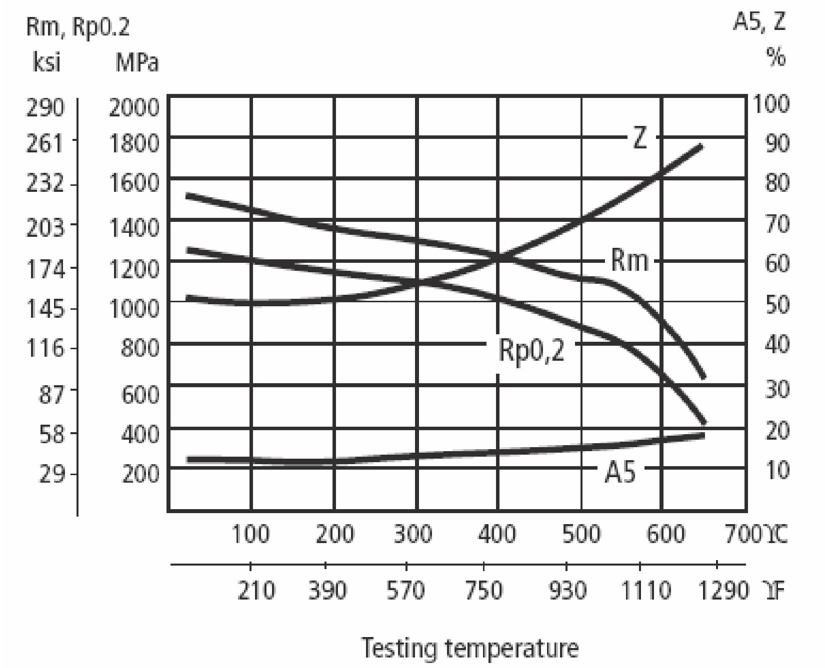

Figure 4.4 Tensile properties of Dievar at elevated temperatures [50]

4.2.3Applying initial conditions

In the study, initial temperature for the dies is given as 200 ^oC, initial temperature for the workpiece is given the values in the range 850 ^oC - 1000 ^oC, at increments of 50 ^oC and also 1150 ^oC, which is the current forging temperature in the company.

4.2.4 Applying boundary conditions

The same approach as in Chapter 4 is used regarding the boundary conditions. Therefore, in the analyses, the mechanical and thermal constraints are defined by using contacting bodies instead of using boundary conditions to get a better representation of the experimental setup.

4.2.5 Defining contacting bodies

The list of contacting bodies is given below and the contacting bodies defined in MSC Superform are shown in Figure 3.12.

- Workpiece as deformable body
- Upper and lower dies as deformable bodies
- Symmetry planes as rigid surfaces
- Upper and lower fixing surfaces as rigid surfaces

4.2.6 Defining re-meshing criterion

In the analyses, it is applied 3-D remeshing using Overlay Hex Technique. Similar to the analyses that are explained in Chapter 3, “strain change” is given the predefined condition for remeshing. Maximum strain change that is allowed is set to 0.6 in the analyses for adequate frequency of remeshing. In the analyses, inside coarsening level of 2 is used in remeshing to reduce computation time.

4.2.7 Defining load-cases

In the study, the Crank press definition is used. For this type of machine, the stroke displacement is governed by the crank radius and the connecting rod length.

In the study, the experiments will be done using the 1000 ton SMERAL mechanical press available in METU-BILTIR Center Forging Research and Application Laboratory. Technical data of the press are given in Appendix E.

- Crank radius (R) : 110 mm
- Rod length (L) : 750 mm
- Angular Speed : 100 rpm

4.2.8 Visualization of Results

The simulations are performed at temperatures 1150 ^{o}C, 1000 ^{o}C, 950 ^{o}C, 900 ^{o}C and 850 ^{o}C. The results that are obtained from the FEM simulations are;

- Maximum Equivalent stress distributions on the preform and finish dies
- Temperature distributions on the preform and finish dies at the increment of maximum Equivalent stress
- Equivalent stress distribution on the part at last stage of preform and finish
- Temperature distribution on the part at last stage of preform and finish

4.2.8.1 Results for Initial Billet Temperature of 1150 ^{o}C

The maximum Equivalent stress distribution on the preform dies and finish dies for the initial billet temperature of 1150 ^{o}C, are given in Figures 4.5 – 4.12. The maximum values are tabulated in Table 4.4 and Table 4.5.

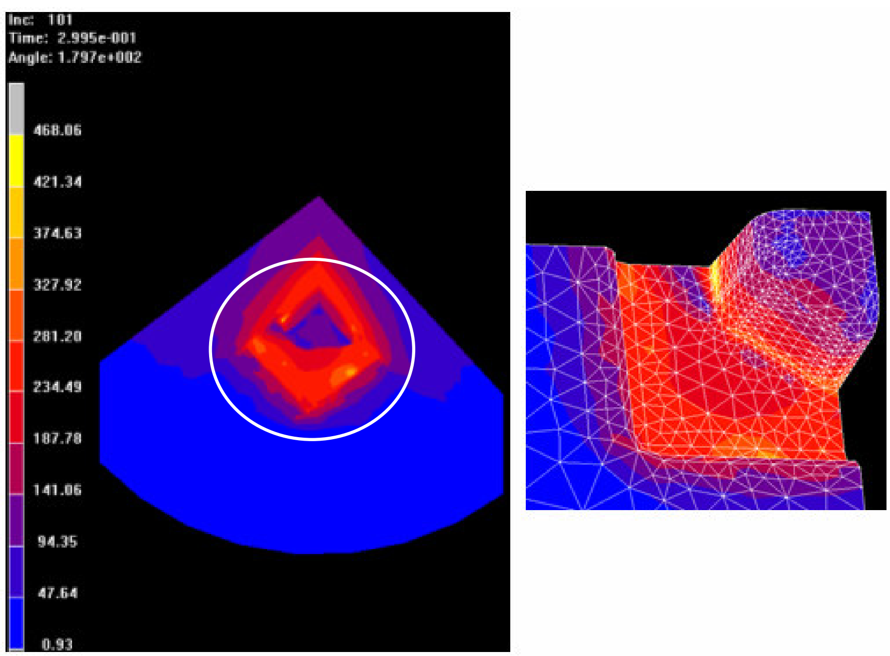

Figure 4.5 Max. Equiv. Stress on Upper Preform Die for Initial Billet Temp. of 1150 ^{o}C

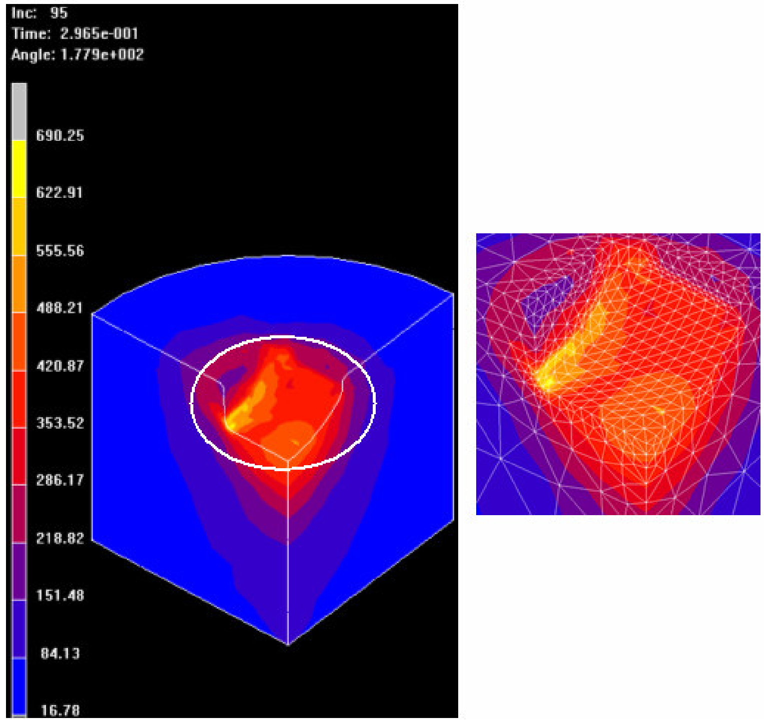

Figure 4.6 Max. Equiv. Stress on Lower Preform Die for Initial Billet Temp. of 1150 ^{o}C

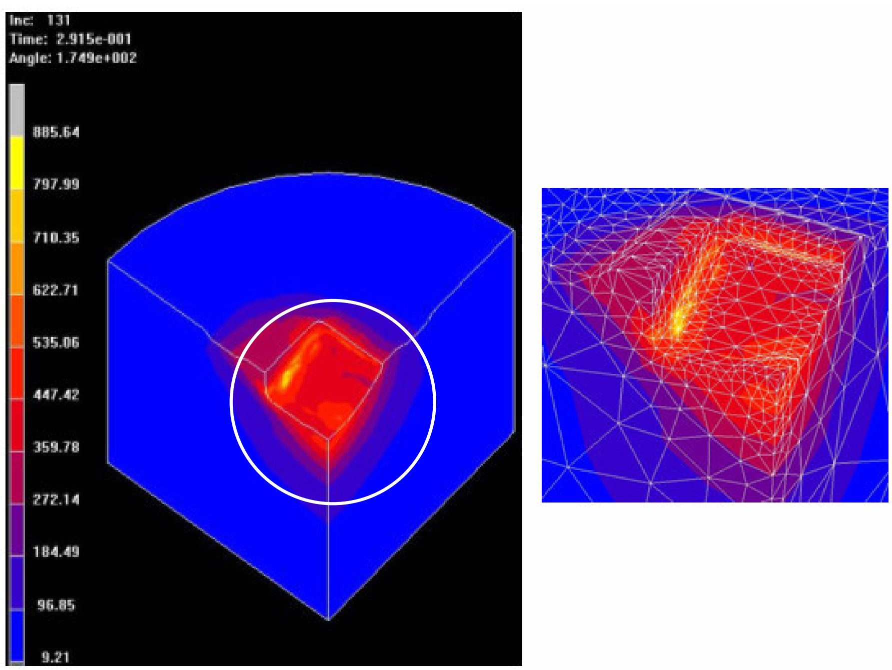

Figure 4.7 Max. Equiv. Stress on Lower Finish Die for Initial Billet Temp. of 1150 ^{o}C

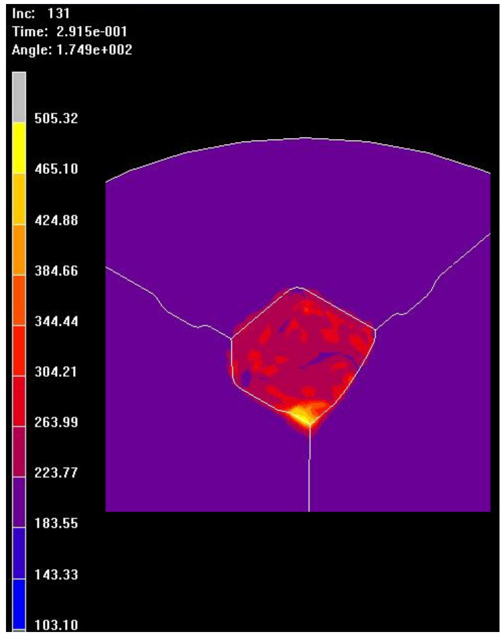

Figure 4.8 Temperature Distribution on Lower Die at Increment of Max. Equiv. Stress

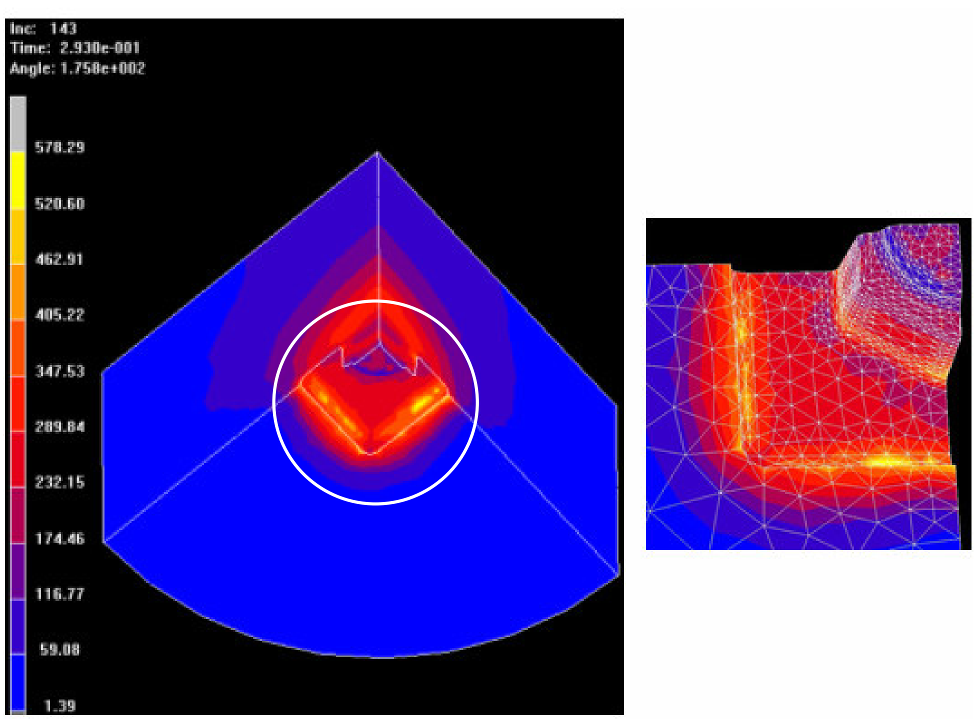

Figure 4.9 Max. Equiv. Stress on Upper Finish Die for Initial Billet Temp. of 1150 ^{o}C

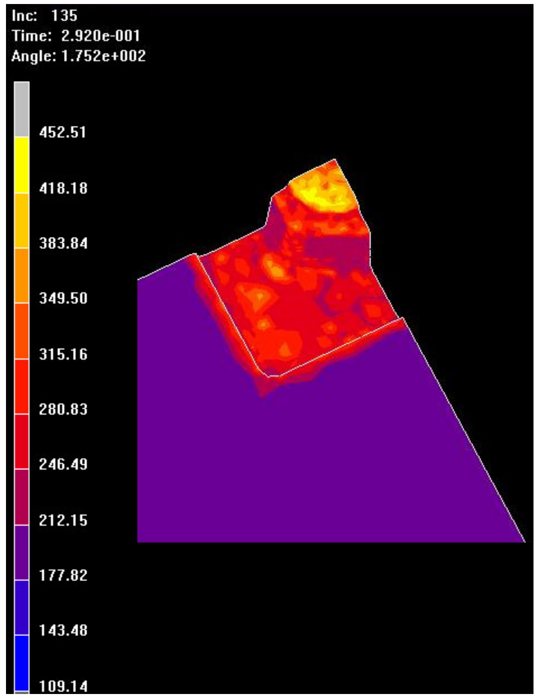

Figure 4.10 Temperature Distribution on Upper Die at Increment of Max. Equiv. Stress

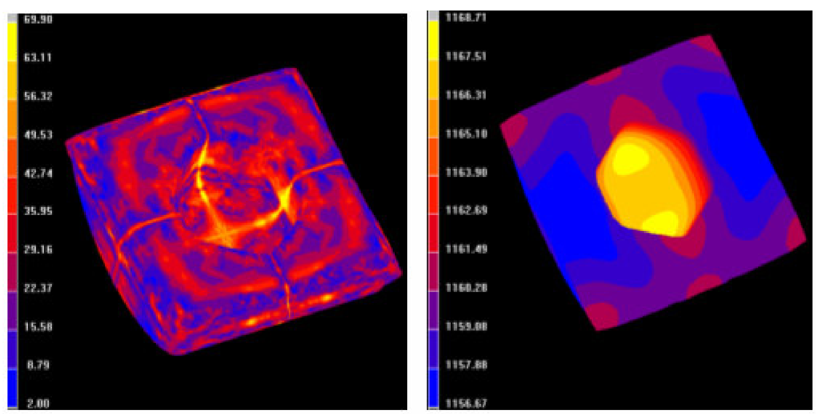

(a) (b)

Figure 4.11 Preform (a) Residual Stresses (b) Temperature Distribution

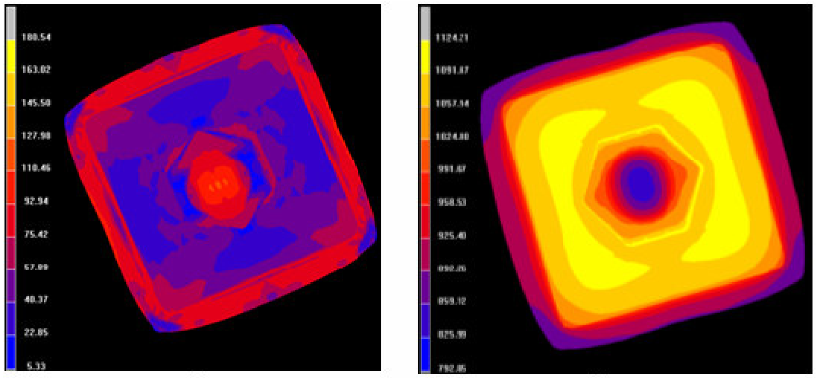

(a) (b)

Figure 4.12 Finished Part (a) Residual Stresses (b) Temperature Distribution

Table 4.4 Max. Equiv. Stress on the Dies for Initial Billet Temp. of 1150 °C

	Maximum. Equivalent Stress (MPa)	Process % (time / total simulation time)
Lower Preform Die	690	49
Upper Preform Die	465	48
Lower Finish Die	885	25
Upper Finish Die	580	24

Table 4.5 Residual Stresses and Temperatures on Preform and Finished Part

	Residual Stresses (MPa)	Temperature at Last Increment (°C)
Preform	100	1168
Finished Part	180	1124

The maximum equivalent stresses on the preform dies are around 466 MPa for the upper die and 690 MPa, for the lower die. These results are lower than the ones on the preform set that is currently used, which are 484 MPa and 797 MPa, respectively.

The maximum Equivalent Stress on the upper finish die is around 580 MPa, and the temperature at the region of maximum stress is around 200 °C. On the lower finish die, the maximum equivalent stress is around 880 MPa, at a region having peak temperatures of 200 ^oC. These values are much lower than the die stresses in the current practice in the forging company, which are 745 MPa and 1205 MPa respectively.

These results indicate that the problem of plastic deformation and excessive wear on the dies is controlled at the specified temperature with the proposed process sequence and die design. These results encouraged to reduce the forging temperature to warm forging temperature range. In the following sections, the simulations with lower initial billet temperatures will be explained.

4.2.8.2 Results for Initial Billet Temperature of 1000 ^oC

The Maximum Equivalent stress distribution on the preform dies and finish dies for the initial billet temperature of 1150 ^oC, are given in Figures 4.13 – 4.18. The maximum values are tabulated in Table 4.6 and Table 4.7.

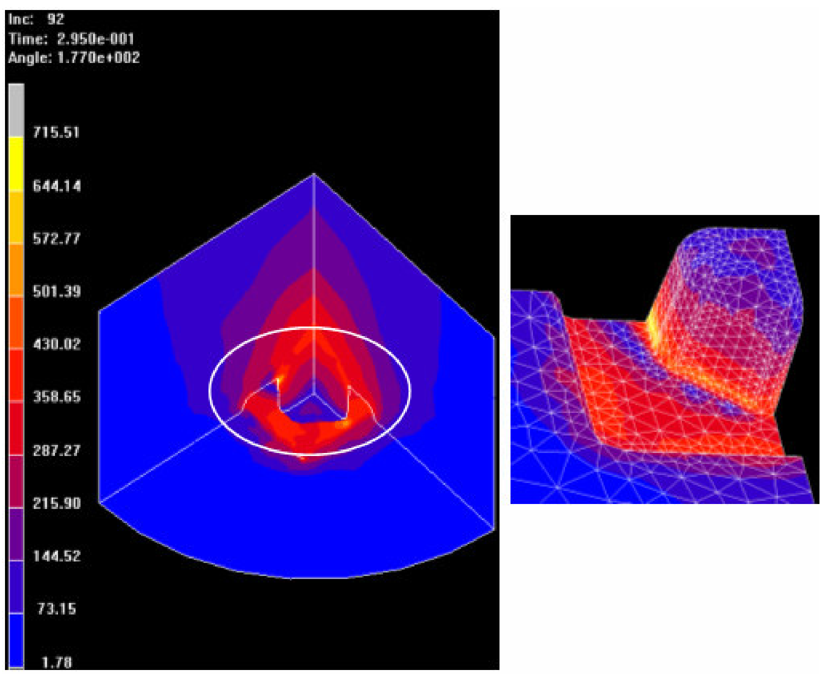

Figure 4.13 Max. Equiv. Stress on Upper Preform Die for Initial Billet Temp. of 1000 ^oC

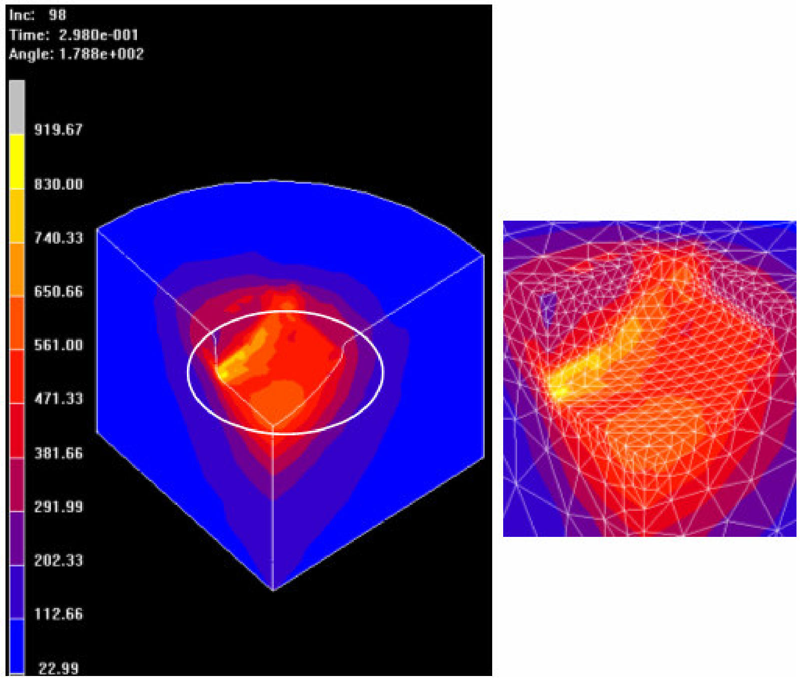

Figure 4.14 Max. Equiv. Stress on Lower Preform Die for Initial Billet Temp. of 1000 ^{o}C

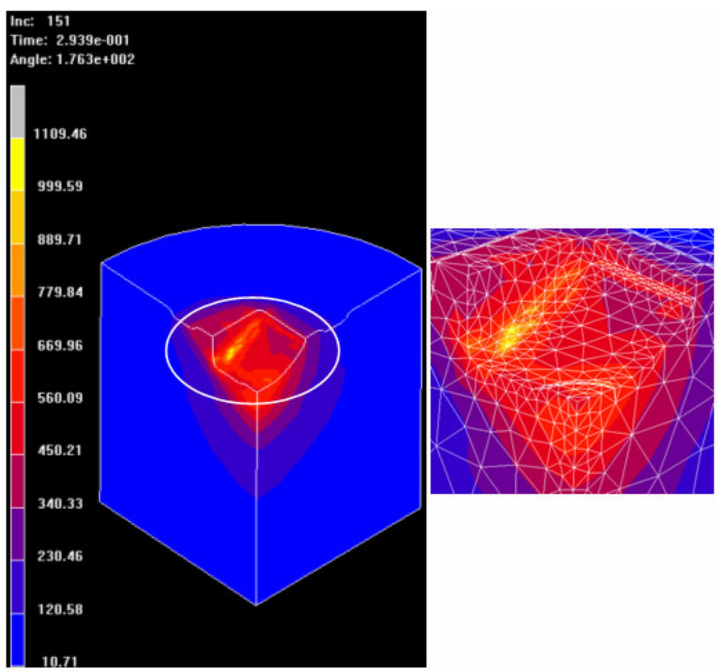

Figure 4.15 Max. Equiv. Stress on Lower Finish Die for Initial Billet Temp. of 1000 ^{o}C

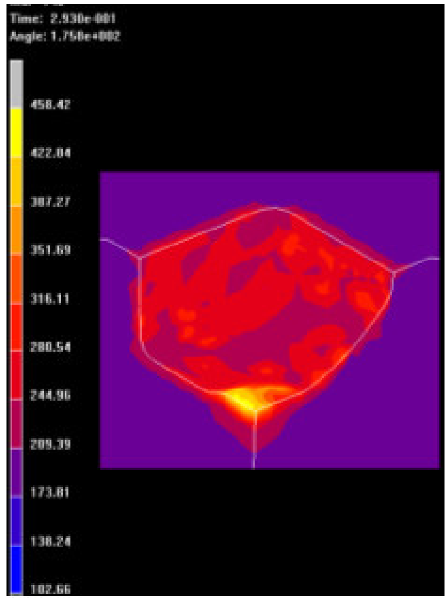

Figure 4.16 Temperature Distribution on Lower Die at Increment of Max. Equiv. Stress

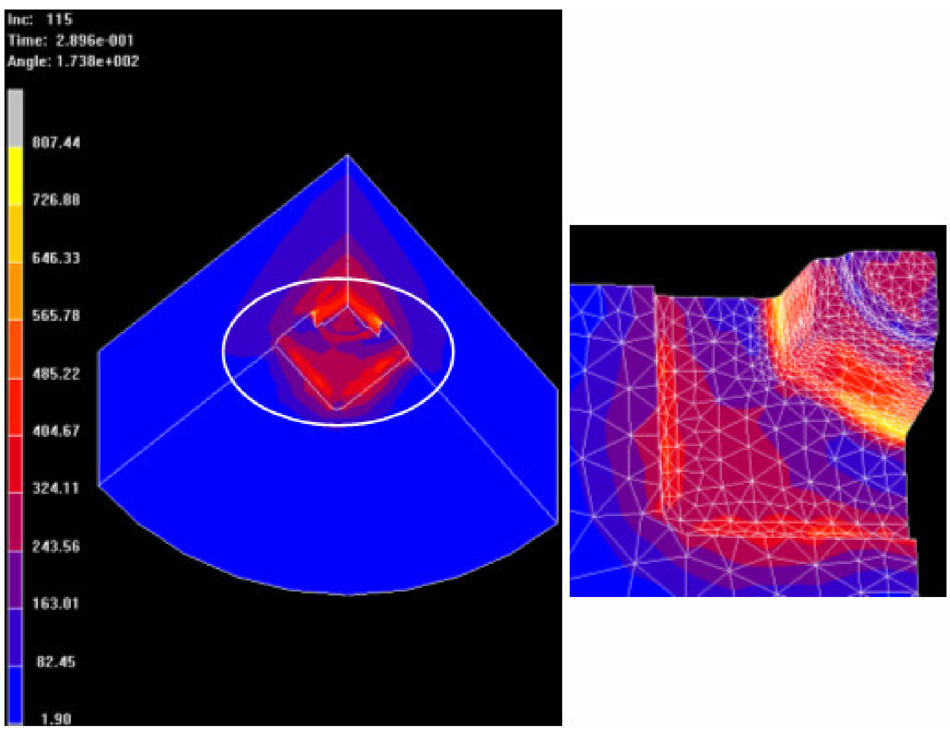

Figure 4.17 Max. Equiv. Stress on Upper Finish Die for Initial Billet Temp. of 1000 ^{o}C

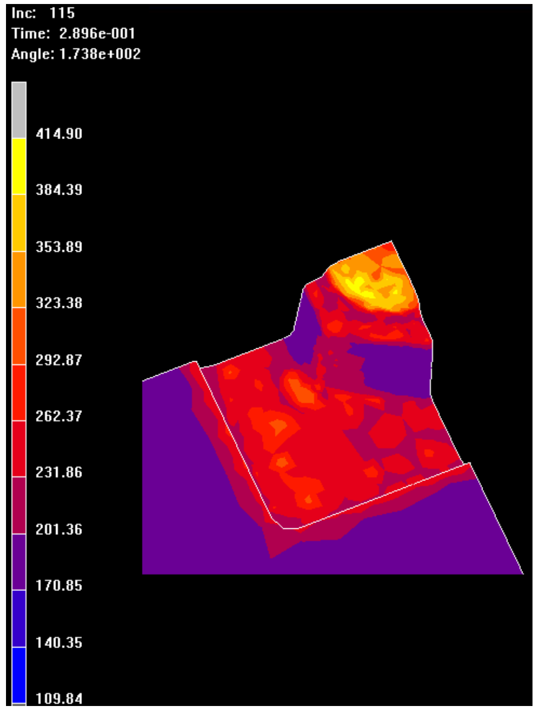

Figure 4.18 Temperature Distribution on Upper Die at Increment of Max. Equiv. Stress

Table 4.6 Max. Equiv. Stress on the Dies for Initial Billet Temp. of 1000 ^{o}C

	Maximum. Equivalent Stress (MPa)	Process % (time / total simulation time)
Lower Preform Die	920	49
Upper Preform Die	715	48
Lower Finish Die	1110	25
Upper Finish Die	805	24

The maximum equivalent stresses on the preform dies are around 795 MPa for the upper die and 940 MPa, for the lower die.

Residual stresses and temperature distribution on the preform and the finished part are very similar to the ones in 1150 ^{o}C, except the values. The values are given in Table 4.7.

Table 4.7 Residual Stresses and Temperatures on Preform and Finished Part

	Residual Stresses (MPa)	Temperature at Last Increment (^oC)
Preform	78	1024
Finished Part	224	995

The maximum Equivalent Stress on the upper finish die is around 805 MPa and the temperature at the region of maximum stress is around 200 ^oC, the maximum equivalent stress on the lower finish die is around 1110 MPa, and the temperature at that region is around 250 ^oC.. The maximum equivalent stresses on the upper and lower dies are lower than the yield strength of the die material at that temperature. Therefore, when the initial billet temperature is reduced to 1000 ^oC, no plastic deformation is expected on the finish dies.

4.2.8.3 Results for Initial Billet Temperature of 950 ^oC

The maximum Equivalent stress distribution on the preform dies and finish dies for the initial billet temperature of 950 ^oC, are given in Figure 4.19- Figure 4.24. The maximum values are tabulated in Table 4.8 and Table 4.9.

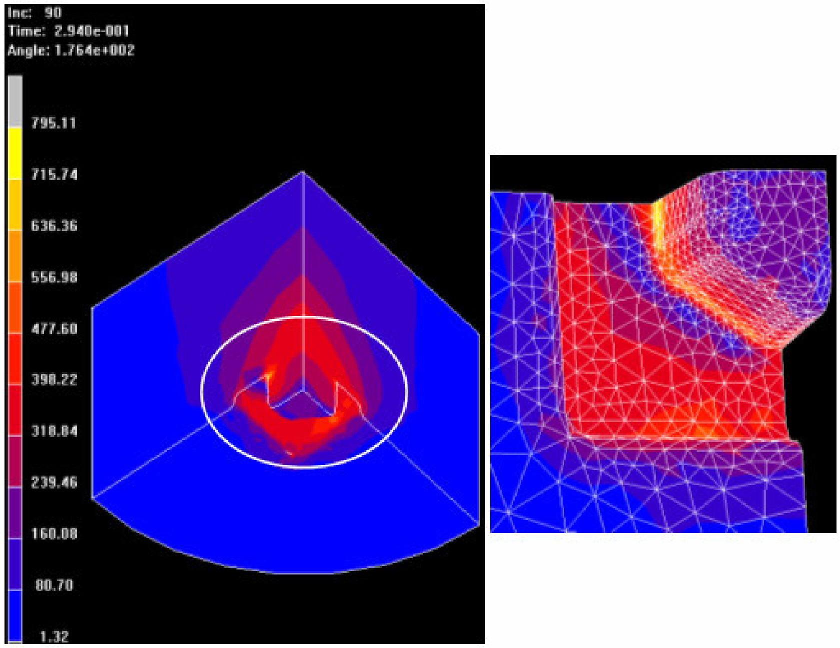

Figure 4.19 Max. Equiv. Stress on Upper Preform Die for Initial Billet Temp. of 950 ^{o}C

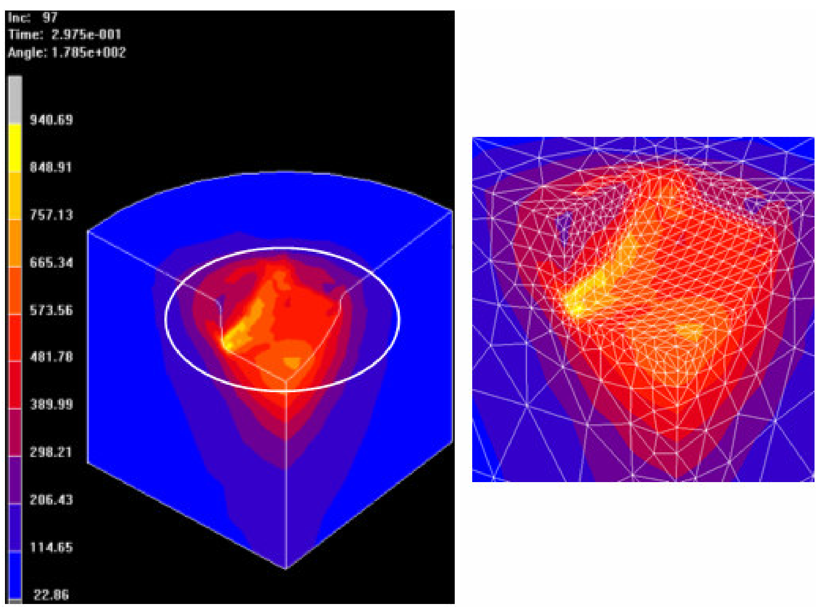

Figure 4.20 Max. Equiv. Stress on Lower Preform Die for Initial Billet Temp. of 950 ^{o}C

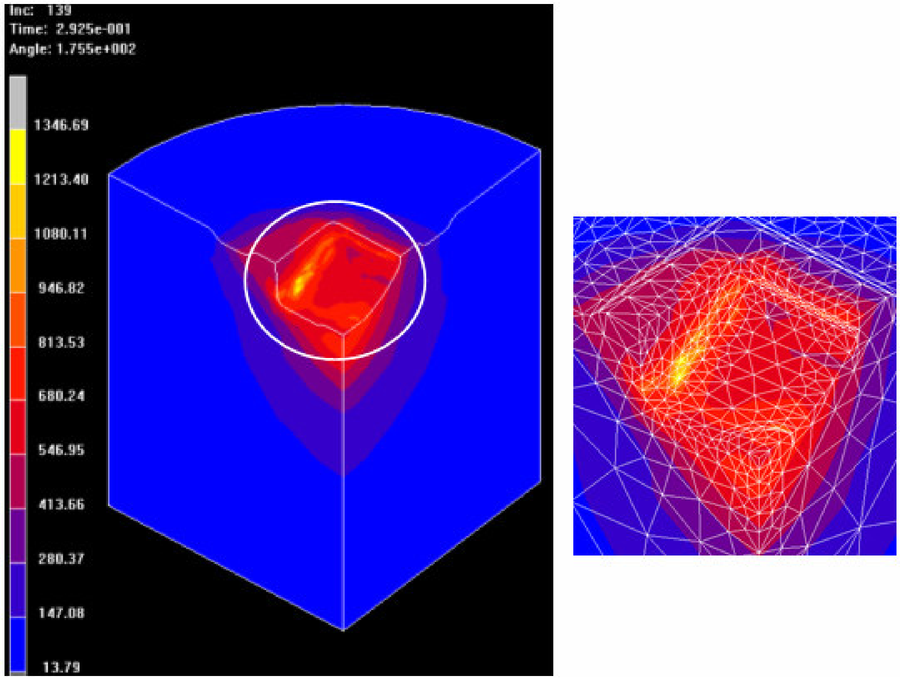

Figure 4.21 Max. Equiv. Stress on Lower Finish Die for Initial Billet Temp. of 950 ^{o}C

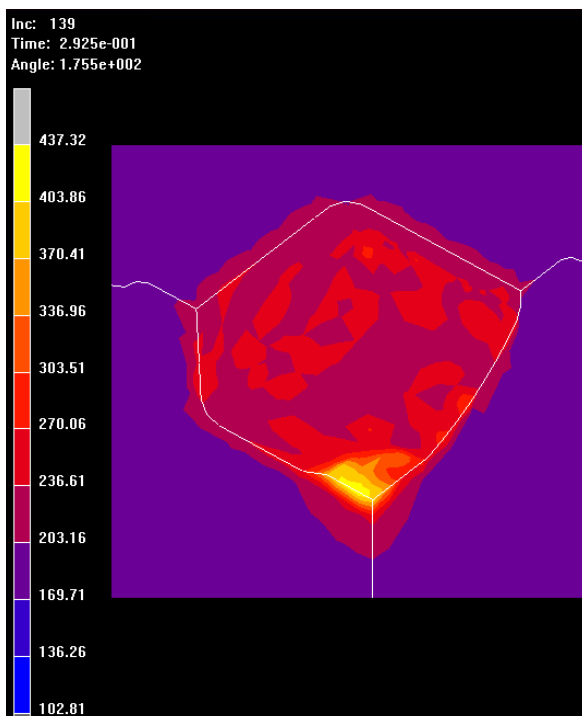

Figure 4.22 Temperature Distribution on Lower Die at Increment of Max. Equiv. Stress

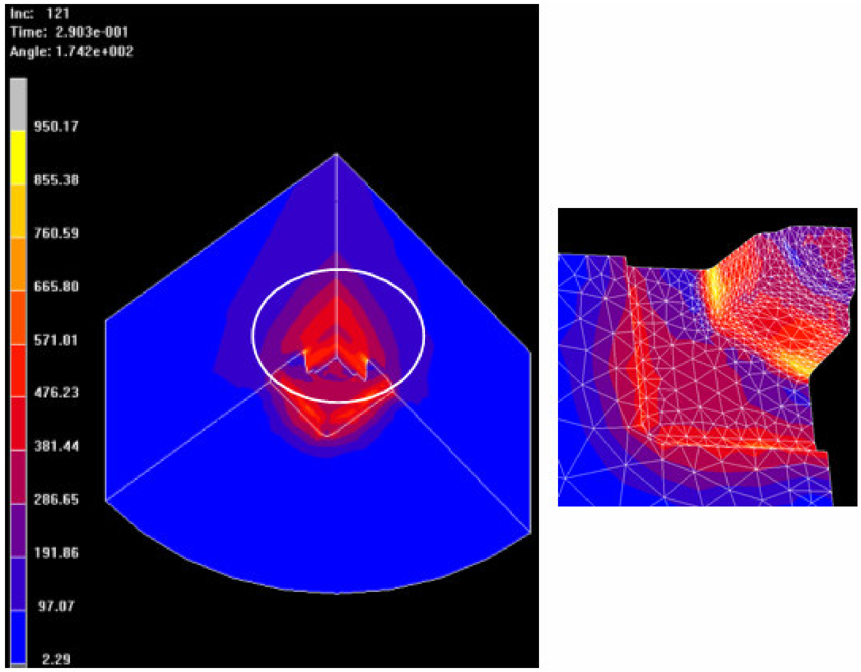

Figure 4.23 Max. Equiv. Stress on Upper Finish Die for Initial Billet Temp. of 950 ^{o}C

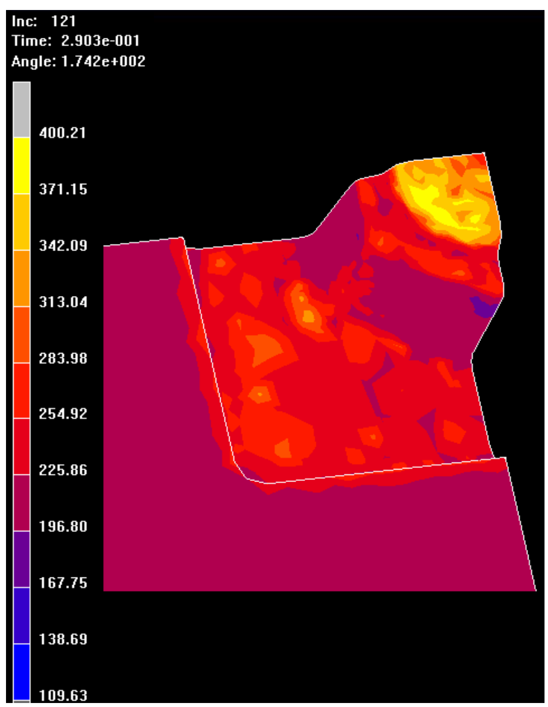

Figure 4.24 Temperature Distribution on Upper Die at Increment of Max. Equiv. Stress

Table 4.8 Max. Equivalent Stress and Temperature on Preform and Finish Dies at 950 ^{o}C

	Maximum. Equivalent Stress (MPa)	Process % (time / total simulation time)
Lower Preform Die	940	49
Upper Preform Die	795	48
Lower Finish Die	***	25
Upper Finish Die	950	24

*** Yield Strength is exceeded

Residual stresses and temperature distribution on the preform and the finished part are very similar to the ones in 1150 ^{o}C, except the values. The values are given in Table 4.9.

Table 4.9 Residual Stresses and Temperatures on Preform and Finished Part

	Residual Stresses (MPa)	Temperature at Last Increment (^{o}C)
Preform	83	978
Finished Part	235	982

The maximum equivalent stresses on the preform dies are around 795 MPa for the upper die and 940 MPa, for the lower die.

The maximum Equivalent Stress on the upper finish die is around 950 MPa and the temperature at the region of maximum stress is around 200 ^{o}C. The maximum equivalent stress on the upper die is lower than the yield strength of the die material at that temperature. Therefore, when the initial billet temperature is reduced to 950 ^{o}C, no plastic deformation is expected on the upper finish die. On the other hand, the maximum equivalent stress on the lower finish die is greater than the yield strength of the die material at that temperature, which means some local plastic strains are expected at the region of maximum stress.

4.2.8.4 Results for Initial Billet Temperature of 900 ^{o}C

The maximum Equivalent stress distribution on the preform dies and finish dies for the initial billet temperature of 900 ^{o}C, are given in Figure 4.25- Figure 4.28. The maximum values are tabulated in Table 4.10 and Table 4.11.

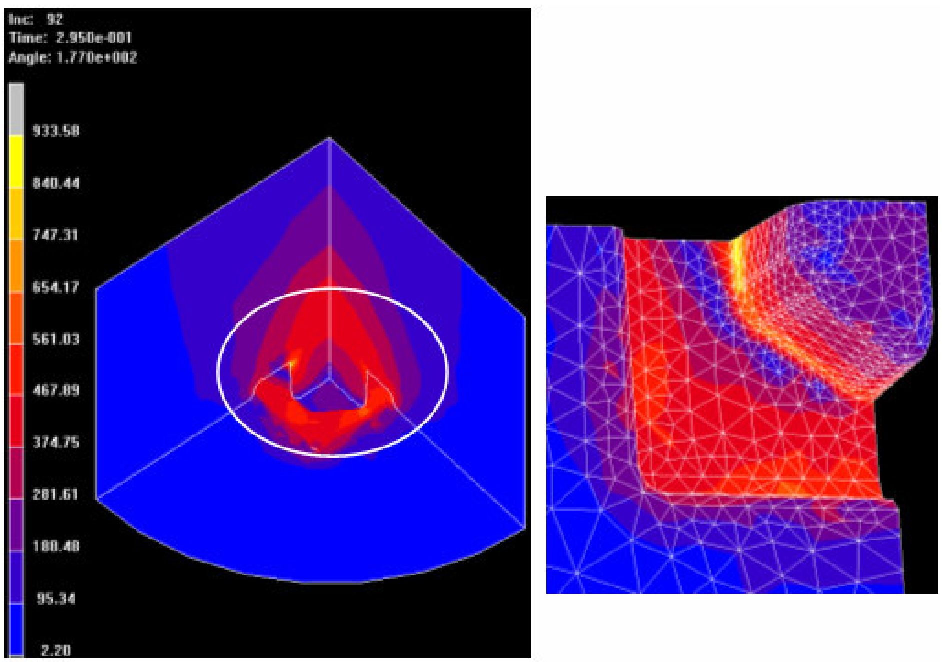

Figure 4.25 Max. Equiv. Stress on Upper Preform Die for Initial Billet Temp. of 900 ^{o}C

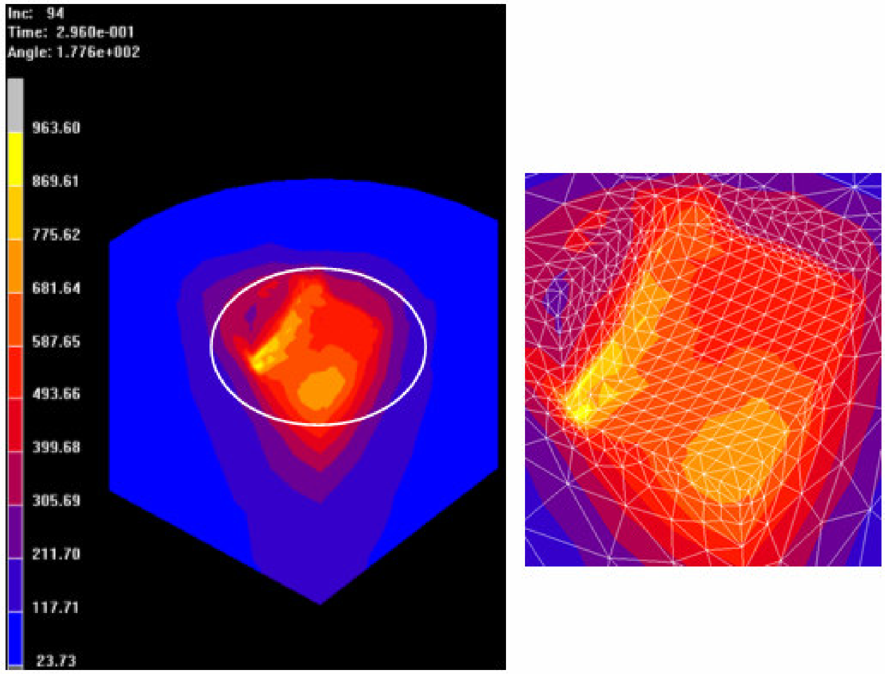

Figure 4.26 Max. Equiv. Stress on Lower Preform Die for Initial Billet Temp. of 900 ^{o}C

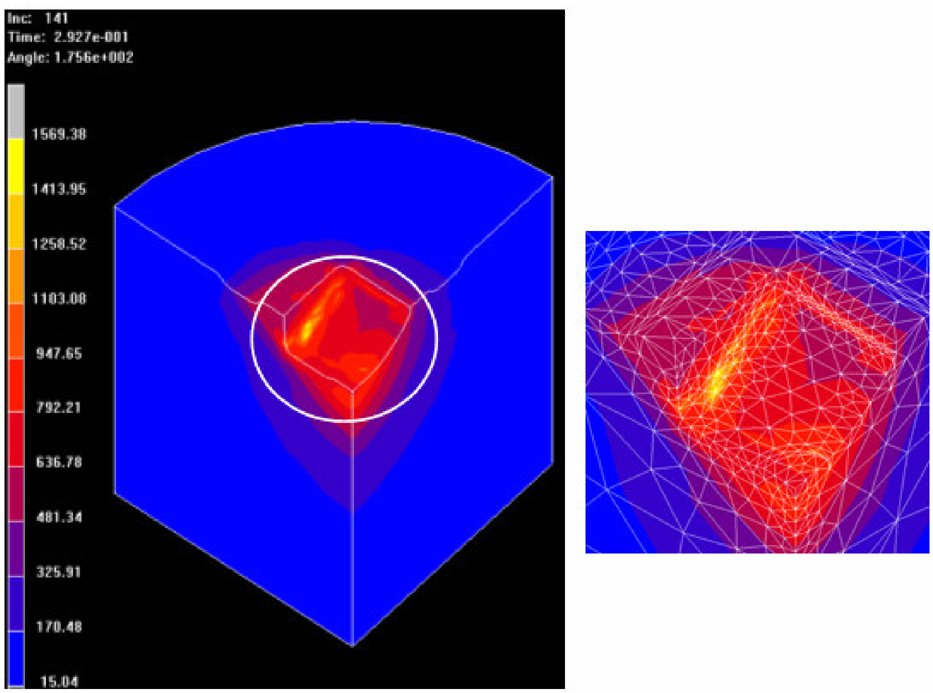

Figure 4.27 Max. Equiv. Stress on Lower Finish Die for Initial Billet Temp. of 900 ^{o}C

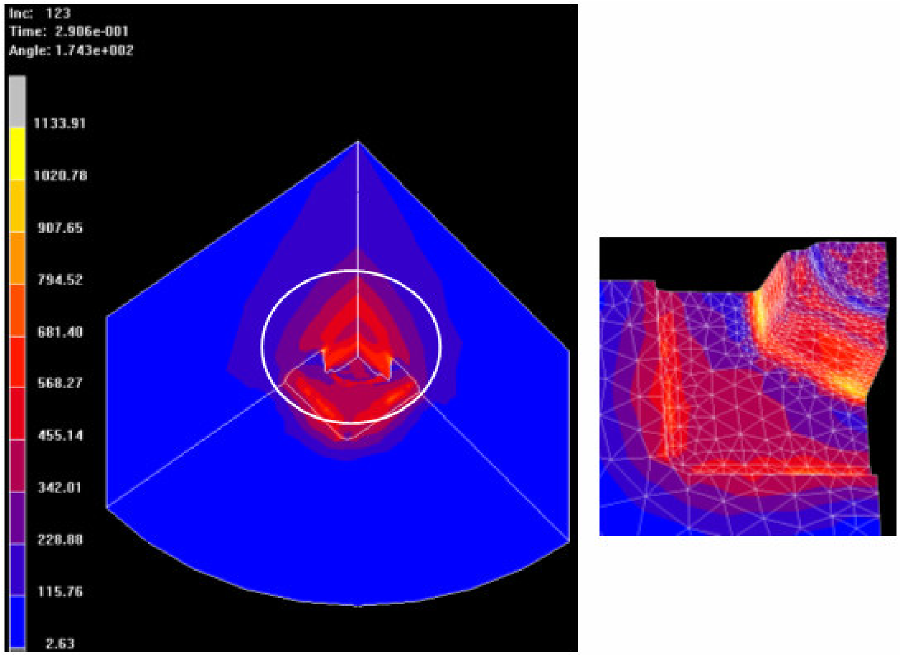

Figure 4.28 Max. Equiv. Stress on Upper Finish Die for Initial Billet Temp. of 900 ^{o}C

The temperature distributions on the upper and lower dies at the increment of maximum equivalent stress are similar to the ones that are given above for higher billet temperatures. However, the numerical values, which are 424 ^{o}C for the lower die and 392 ^{o}C for the upper die, are smaller, as expected.

The residual stresses and temperature distribution on the preform and the finished part are very similar to the ones in 1150 ^{o}C, except the values. The values are given in Table 4.11.

Table 4.10 Max. Equivalent Stress and Temperature on Preform and Finish Dies at 900 ^{o}C

	Maximum. Equivalent Stress (MPa)	Process % (time / total simulation time)
Lower Preform Die	963	49
Upper Preform Die	933	48
Lower Finish Die	***	25
Upper Finish Die	1133	24

Table 4.11 Residual Stresses and Temperatures on Preform and Finished Part

	Residual Stresses (MPa)	Temperature at Last Increment (^{o}C)
Preform	90	932
Finished Part	236	935

The maximum equivalent stresses on the preform dies are around 933 MPa for the upper die and 963 MPa, for the lower die. The maximum Equivalent Stress on the upper finish die is around 1130 MPa, and the temperature at the region of maximum stress is around 200 ^{o}C. The maximum equivalent stress on the upper die is lower than the yield strength of the die material at that temperature. Therefore, when the initial billet temperature is reduced to 900 ^{o}C, no plastic deformation is expected on the upper finish die. On the other hand, the maximum equivalent stress on the lower finish die is greater than the yield strength of the die material at that temperature, which means some local plastic strains are expected at the region of maximum stress on the lower die.

4.2.8.5 Results for Initial Billet Temperature of 850 ^{o}C

The maximum Equivalent Stress distribution on the preform dies and finish dies for the initial billet temperature of 850 ^{o}C, are given in Figure 4.29-Figure 4.32. The maximum values are tabulated in Table 4.12 and Table 4.13.

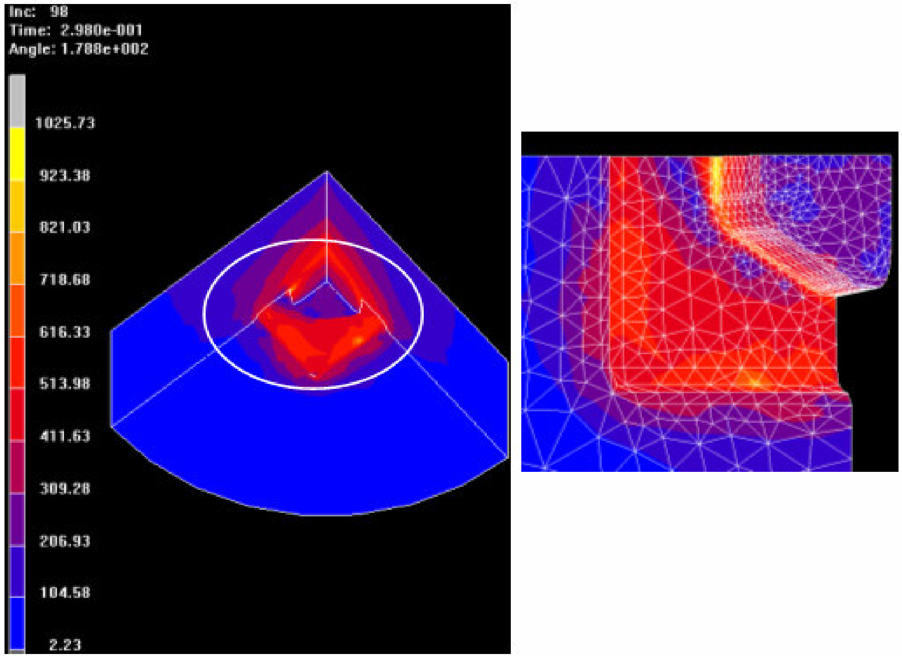

Figure 4.29 Max. Equiv. Stress on Upper Preform Die for Initial Billet Temp. of 850 °C

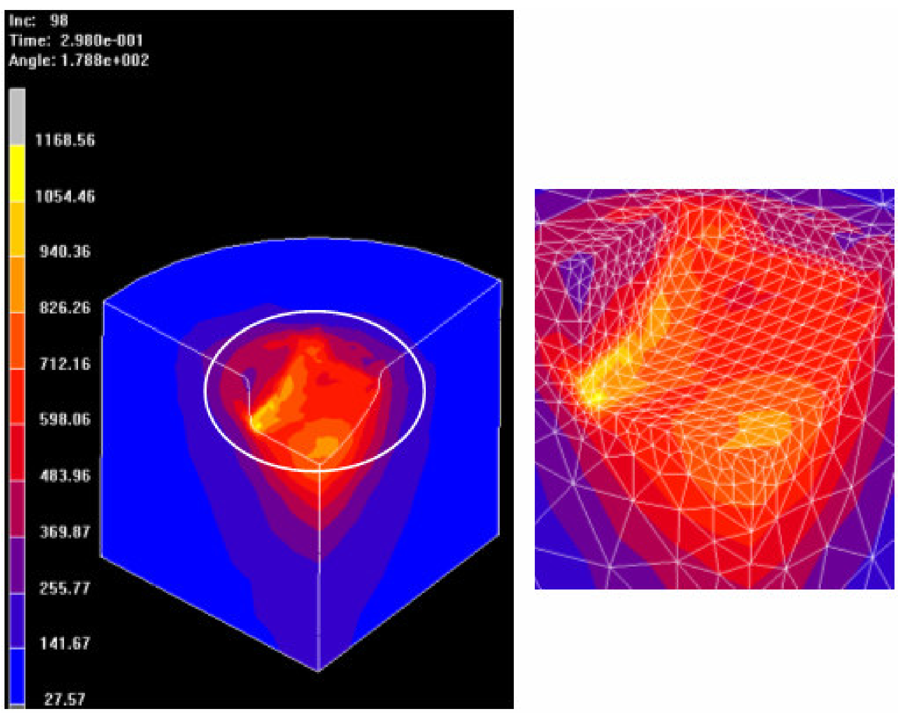

Figure 4.30 Max. Equiv. Stress on Lower Preform Die for Initial Billet Temp. of 850 °C

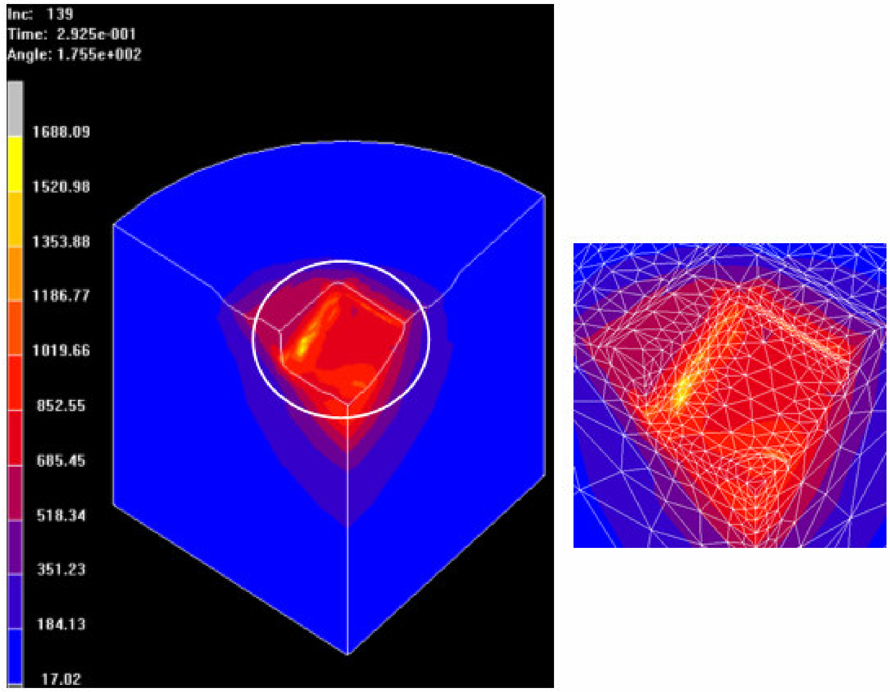

Figure 4.31 Max. Equiv. Stress on Lower Finish Die for Initial Billet Temp. of 850 ^{o}C

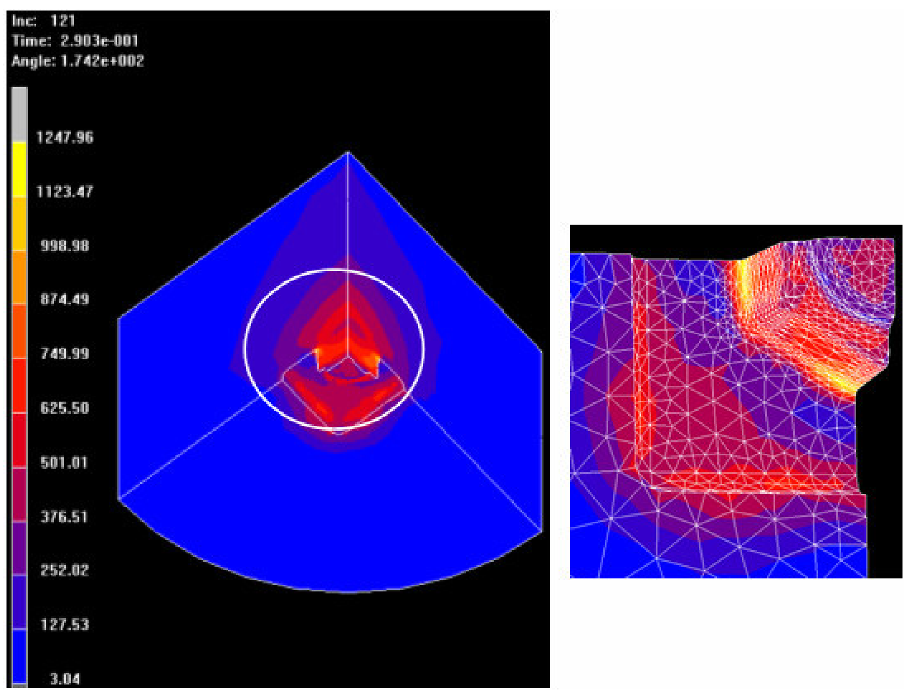

Figure 4.32 Max. Equiv. Stress on Upper Finish Die for Initial Billet Temp. of 850 ^{o}C

The temperature distributions on the upper and lower dies at the increment of maximum equivalent stress are similar to the ones that are given above for higher billet temperatures. However, the numerical values, which are 410 ^{o}C for the lower die and 382 ^{o}C for the upper die, are smaller, as expected.

The residual stresses and temperature distribution on the preform and the finished part are very similar to the ones in 1150 ^{o}C, except the values. The values are given in Table 4.13.

Table 4.12 Max. Equivalent Stress and Temperature on Preform and Finish Dies at 850 ^{o}C

	Maximum. Equivalent Stress (MPa)	Process % (time / total simulation time)
Lower Preform Die	1168	49
Upper Preform Die	1025	48
Lower Finish Die	***	25
Upper Finish Die	***	24

Table 4.13 Residual Stresses and Temperatures on Preform and Finished Part

	Residual Stresses (MPa)	Temperature at Last Increment (^{o}C)
Preform	115	886
Finished Part	262	846

The maximum equivalent stresses on the preform dies are around 1025 MPa for the upper die and 1168 MPa, for the lower die.

The maximum equivalent stresses on the upper and lower dies are greater than the yield strength of the die material at that temperature, which means some local plastic strains are expected at the regions of maximum stress.

4.3 Discussion of the Finite Element Simulations

In the simulation results, it is observed that the maximum equivalent stress values on the dies increase as the initial billet temperature is reduced. However, the locations on the upper and lower dies where the maximum equivalent stresses occur are the same for all the simulations.

In the simulations, for the initial billet temperatures of 950 ^{o}C and below, maximum equivalent stresses exceeding the yield strength of the die material are observed on the lower finish dies. The maximum equivalent stress values on the dies are given in Table 4.14.

Table 4.14 Maximum Equivalent Stress Values on the Dies

	Maximum Equivalent Stress (MPa)				
Initial Billet Temp.	1150 ^{o}C	1000 ^{o}C	950 ^{o}C	900 ^{o}C	850 ^{o}C
Lower Preform Die	690	920	940	963	1168
Upper Preform Die	465	715	795	933	1025
Lower Finish Die	885	1110	***	***	***
Upper Finish Die	580	805	950	1133	***

*** Yield Strength is exceeded

The stresses on the upper die are below the yield strength for temperatures of 1150 ^{o}C, 1000 ^{o}C, 950 ^{o}C and 900 ^{o}C, which means that no plastic deformation is expected on the upper die at these temperatures. On the other hand, the stresses on the lower die are below the yield strength for temperatures of 1150 ^{o}C and 1000 ^{o}C. For lower temperatures, local plastic strains are expected on the lower die.

The values that are exceeding the yield strength of the die material are not given in Table 4.14. The reason is, the dies are modeled as elastic bodies and the material behavior and the stress-strain values after the elastic region can not be predicted by using this assumption. In practice, for the stress values that are exceeding the yield strength of the material, plastic strains occur in the material, and the material behaves according to the plastic part of the flow curve between the yield and the fracture. "Elastic-plastic" material definition, together with flow curve specification, would give magnitudes of the plastic strains and equivalent stresses. The reason for using the "elastic dies" assumption is to reduce the complexity of the model and to be able to accomplish the simulations with the available hardware, which is suggested by the MSC Superform software developers [51]. The factors that increase the complexity of the model have been mentioned in Section 3.4.

The characteristics of temperature distribution considering locations on the dies at the increment of the maximum equivalent stress are similar for all simulations, but the numerical values are different. The locations where the temperature reaches to its peak values are the ones which are in contact with the workpiece for a longer time than other locations on the dies. The peak values of the temperature on the dies decreases as the initial billet temperature is reduced and the values are given in Table 4.15.

Table 4.15 Peak values of the Temperature on the Finish Dies

	Peak Values of the Temperature on the Finish Dies (^oC)				
Initial Billet Temp.	1150 ^oC	1000 ^oC	950 ^oC	900 ^oC	850 ^oC
Upper Finish Die	452	414	400	392	382
Lower Finish Die	505	458	437	424	410

CHAPTER 5

MANUFACTURING OF THE DIES AND EXPERIMENTATION

Designing and 3-D modeling of the dies and the process are explained in detail in Chapter 4. In this chapter, manufacturing of the dies and verification of the previously mentioned simulations by experiments will be explained.

5.1 Dimensional Requirements of the Press and the Die Holders

In the modeling stage of the dies, dimensional requirements of the press that will be used in the experiments are taken into account, and the dies are manufactured in accordance to these dimensions.

In the experiments, 1000 ton SMERAL mechanical press available in METU-BILTIR Center Forging Research and Application Laboratory is used. The technical data of the press are given in Appendix E. The press has a ram stroke of 220 mm. The press has a shut height of 620 mm, which is the distance between the ram and the anvil when the ram is at its bottom dead center as can be seen from Figure 5.1. When the die holders are mounted and the ram is at its bottom dead center position, the distance between the die locating surfaces of the upper and lower die holders is 200 mm. That distance gives the total allowable height of the upper and lower dies when there is no flash formation. That means, when the dies are manufactured in a way that the sum of the upper and lower die heights is 200 mm, the die surfaces come into contact when the ram is at its bottom dead center position. Therefore, when there is flash formation, there should be a facial clearance equal to the flash thickness at bottom dead center position, and this facial clearance is obtained by ensuring the total height of the upper and lower dies is 200 mm minus flash thickness. This distance calculation should be made carefully to prevent the collision of the dies during the forging stroke. Additionally, when the process is multi stage, height of each die set should be calculated carefully to make sure there is proper flash thickness between the dies. In the study, the flash thickness of 2.2 mm in the preform and 2 mm in the finish stage are planned. Therefore, the total height of the preform dies should be 197.8 mm and total height of the finish dies should be 198 mm.

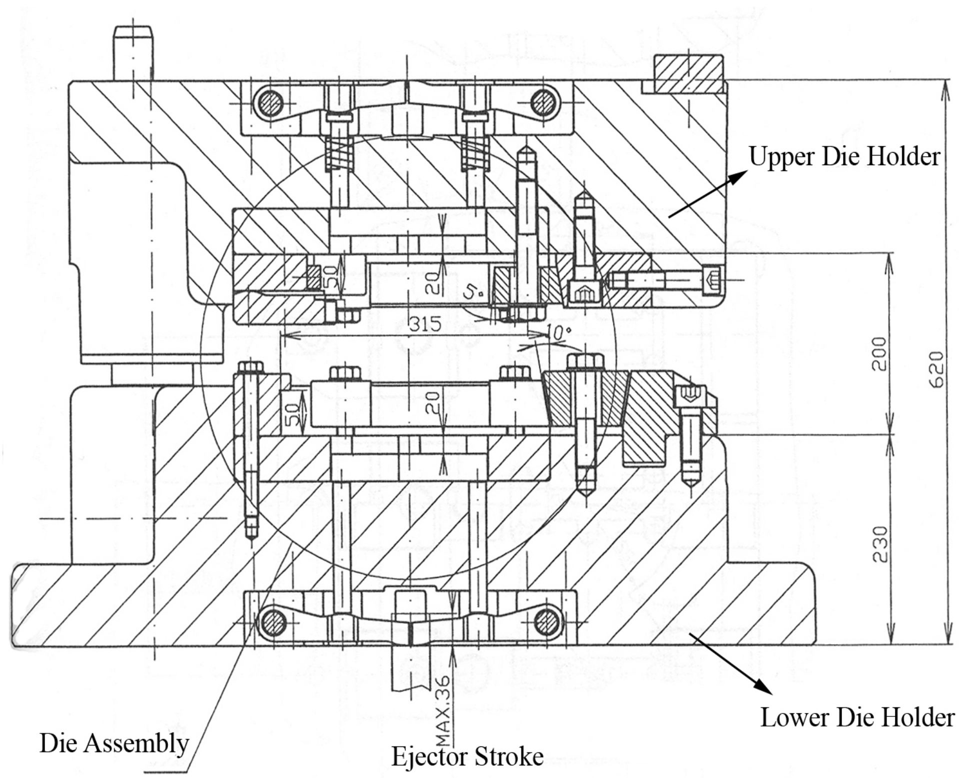

Figure 5.1 Die Holder and Shut Height of Smeral 1000 ton Mechanical Press [52]

The die holders have three stations, available for three set of dies and three stage operations. Photograph of the lower die holder is given in Figure 5.2. The upper die holder has similar elements. The stations on the left and right have equal diameter of 197 mm and the station in the middle has a diameter of 222 mm. Outer diameters of the dies should satisfy these dimensions. Technical drawings of the circular dies appropriate for the die holders are given in Figure 5.3 and Figure 5.4.

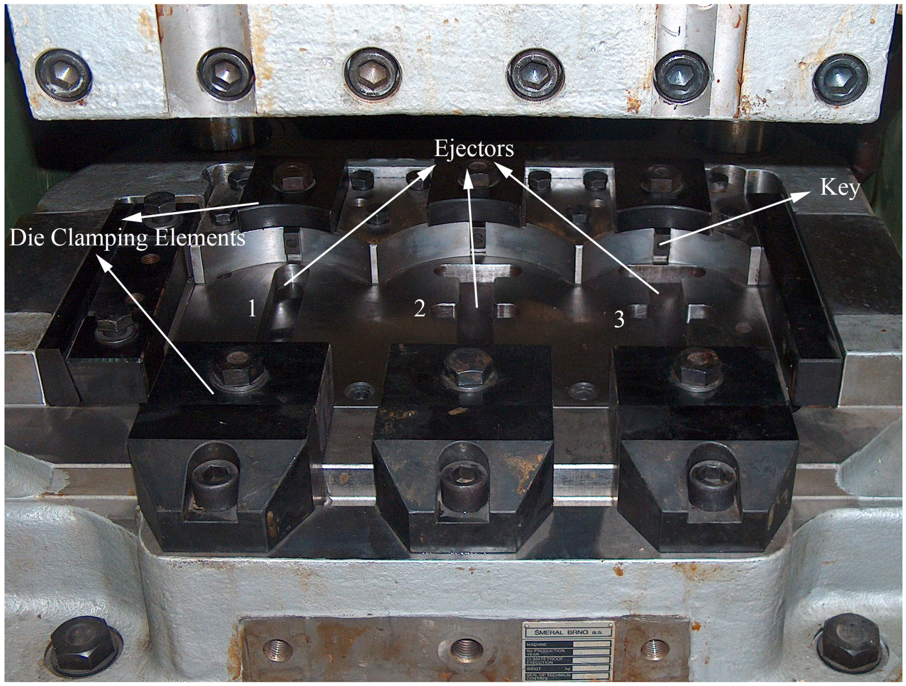

Figure 5.2 A View of Lower Die Holder

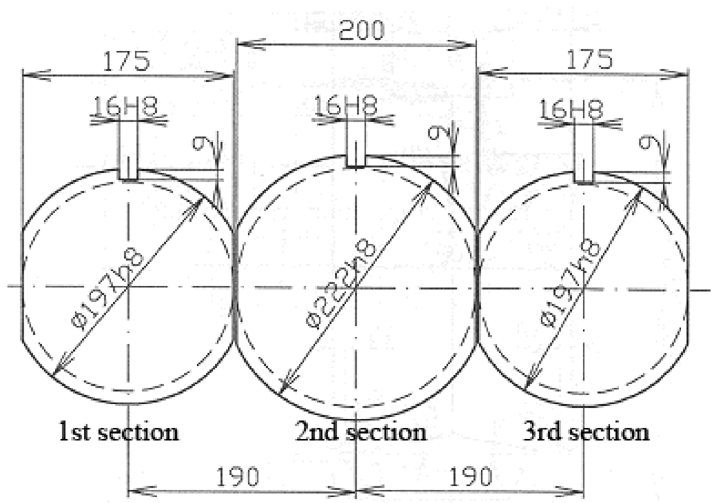

Figure 5.3 Top View of Circular Dies [52]

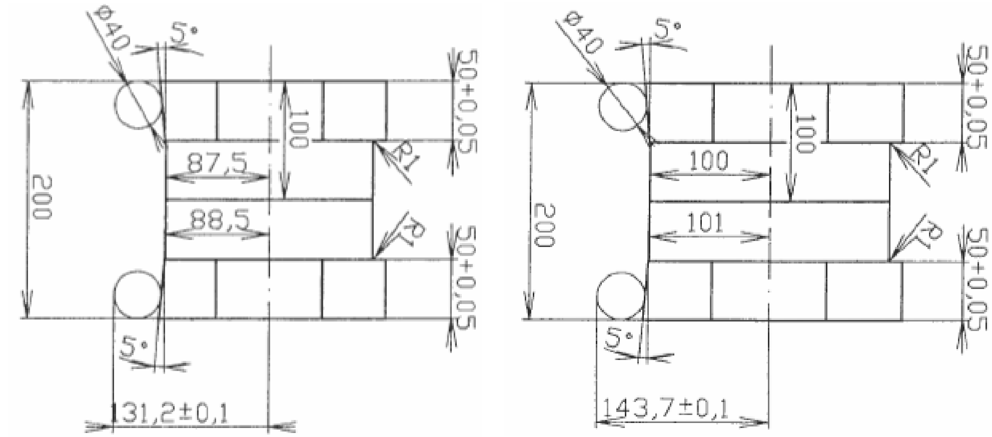

Figure 5.4 Front View of the Circular Dies [52]

5.2 Manufacturing of the Preform and Finish Dies

As mentioned before, in the study, tool design and process planning is accomplished with CAD/CAM/CAE approach. After modeling the dies in Pro/Engineer WF 3.0, manufacturing module of the software is used to obtain the NC codes for manufacturing the dies.

In general, steps in NC code development are as follows [31]:

- definition of cutter tools,
- preparation of 2D/3D model of tools (setting of coordinate system) and defining the type of modeling (depending on number of machining axes),
- creating of NC procedures (roughing, semi-finishing, finishing),
- post processing of neutral NC code and communicating with machine.

After the NC codes are developed, the dies are manufactured in MAZAK Variaxis 630-5X high-speed vertical milling machine, which is available in METU-BILTIR Center CAD/CAM Laboratory. Additionally, Wire Electro-Discharge Machine (W-EDM) available in METU-BILTIR Center CAD/CAM

Laboratory, is used to manufacture the key seats. On high-speed machines, depths of cut are small but feeds are fast so that material may be rapidly removed. Because the depths of cut are small, hardened tool steels may be machined. Another advantage of high-speed machining is that surface integrity is good and no white layer, as produced by electro-discharge machining exists. [31]

Tool steel is mostly supplied from the manufacturer in the soft annealed condition. In this state, it is soft and easier to machine. Before the tool can be used, it has to be brought up to hardness. This is usually done after the majority of the machining has been carried out Appropriate and accurate heat treatment of a tool is essential if the tool steel is to perform to its full potential. An inappropriately chosen or inaccurate heat treatment can easily destroy the essential properties of the material and cause the tool to fail. In the study, heat treatment of the die steel is made in the company which supplied the material of the dies. Details of the heat treatment process are given in Appendix F.

Photographs of the manufactured preform dies are given in Figure 5.5 and photographs of the manufactured finish dies are given in Figure 5.6.

Figure 5.5 Views of the Manufactured Lower and Upper Preform Dies

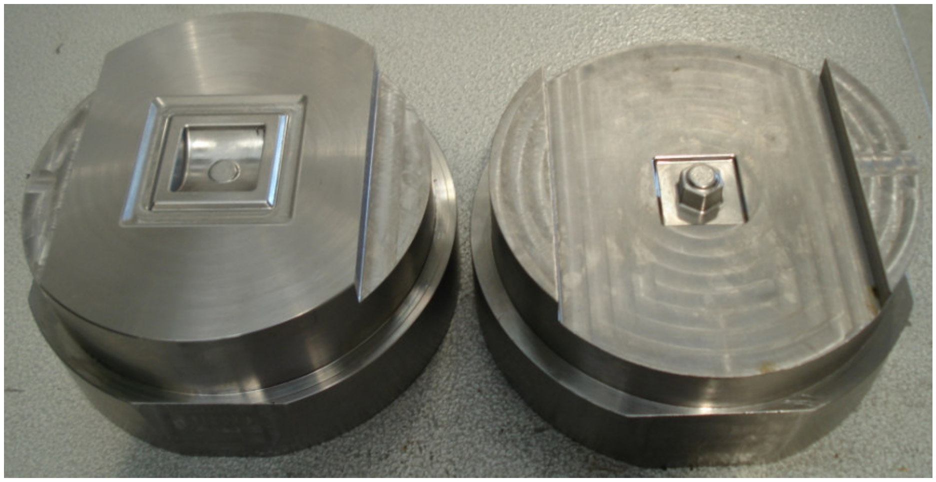

Figure 5.6 Views of the Manufactured Lower and Upper Finish Dies

5.3 Experimentation of the Proposed Process

The experiments have been realized in METU-BILTIR Center Forging Research and Application Laboratory. In the experiments, firstly the billets are cut to the specified length in KESMAK Sawing Machine, then they are heated to the specified temperatures in INDUCTOTERM 125 KVA Induction Heater, finally the forging process is applied using 1000 ton SMERAL mechanical press. Photograph of the Sawing Machine is given in Figure 5.7. Photograph of the Induction heater is given in Figure 5.8.

Figure 5.7 The KESMAK Sawing Machine in METU-BILTIR Center

Figure 5.8 A View of the INDUCTOTERM Induction Heater in METU-BILTIR Center

5.3.1 Preparation for the Experiments

The workpiece material which is AISI 1020 is supplied from a steel supplier in Ankara. The material comes in hot rolled condition and as a bar of 6m in length and with a square cross section of 35x35 mm. Then, the billets are prepared by cutting this bar into pieces of 17 mm length. Each billet is measured in length and mass, and each of them is marked and given a number. The length of the billets is measured using digital compass having an accuracy of ±0.1 mm, and their mass is measured using a digital precision scale having an accuracy of ±0.01 g. The length of each billet is measured three times in three different locations and the average value is recorded. The reason for measuring three times is the possible non uniformities in the billet lengths due to cutting conditions. Photograph of a billet on the precision scale can be seen in Figure 5.9.

Figure 5.9 Photograph of a Billet on the Precision Scale

During the die set up, firstly the upper die is lifted a certain amount by a hydraulic jack that is seated on the lower die holder as shown in Figure 5.10. Then, the clamping elements are placed and the tapered surfaces of the dies and the clamping elements are aligned and the clamping elements at the front side are fastened by using bolts. These elements prevent the dies to move in front-back direction and also in up and down direction Later, the clamping elements at the back side are fastened by bolts to ensure adequate placement of the dies in the die holder. After the upper dies, the lower dies are placed on the die holder and the keys are inserted into the key seats to lock the rotational freedom of the lower dies. Like the upper dies, the lower dies are mounted to the die holder by using the clamping elements and the bolts. After the dies are fastened, alignment of the dies is checked by visual inspection and operating the press in unloaded position.

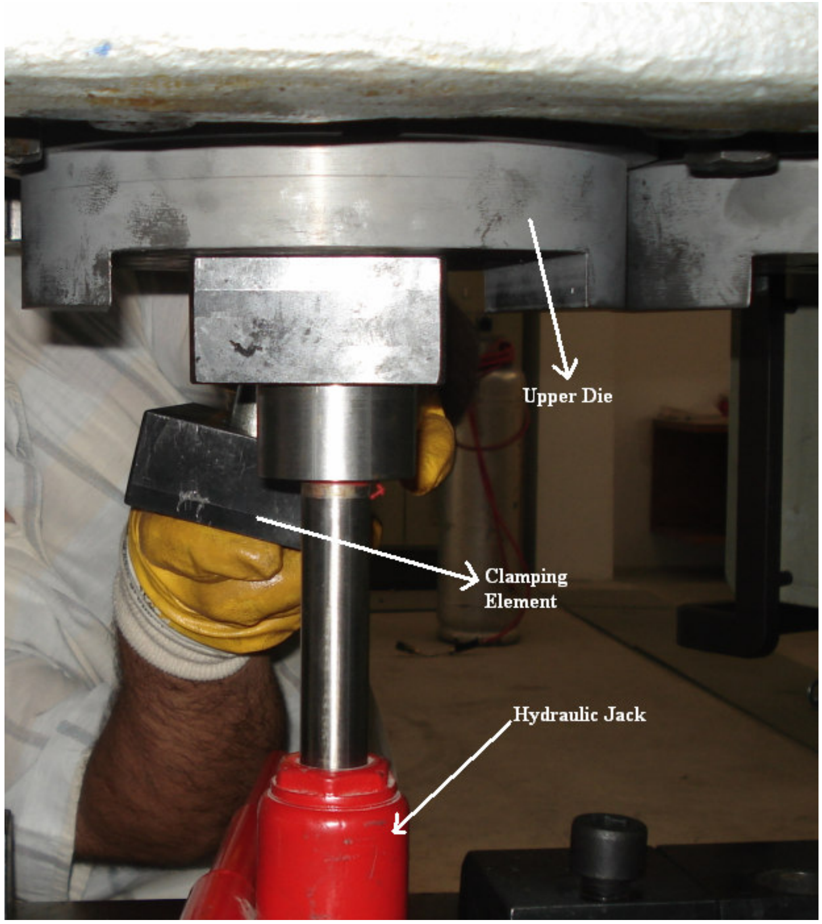

Figure 5.10 A View of Lifting of the Upper Die by Hydraulic Jack

After proper mounting of the dies, the preform and finish die sets are preheated to a temperature of approximately 200 ^{o}C. The reason for this preheating stage is to increase the toughness of the dies by decreasing the hardness in some amount. Another reason for preheating is to decrease the temperature difference between the dies and the heated billets during forging, and by this way to reduce thermal shocks on the dies. Preheating is made by positioning two LPG heater flame guns in different locations as can be seen in Figure 5.11. Preheating takes about two hours and during this period, position of the flame guns is changed in every 30 minutes to ensure homogeneous temperature in the dies. Temperature of the dies is measured in every 10 minutes using a portable optical pyrometer which has a temperature range of -32-600 ^{o}C.

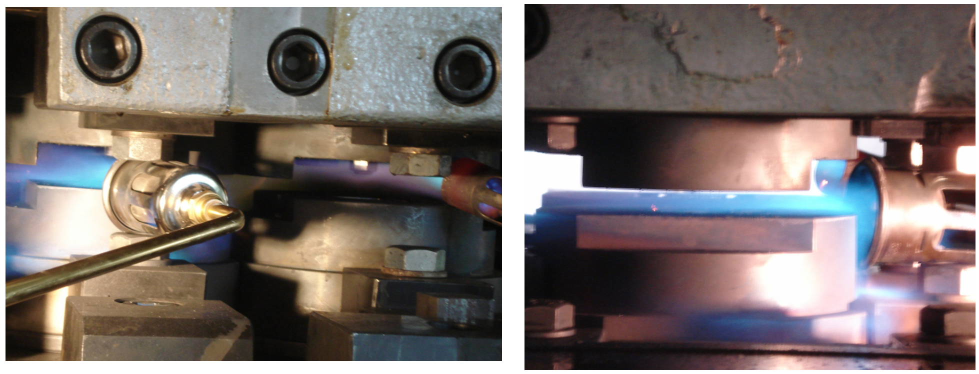

Figure 5.11 A View of Preheating of the Dies

5.3.2 Experimentation

In the experiments, one billet is forged to preform stage and put aside, and five billets are preformed and forged to finish stage for each forging temperature, according to TSE 2756 Standard.

The billets are heated in 125 KVA Induction Heater as can be seen in Figure 5.12. The experiments are made at temperatures of 750 ^{o}C, 800 ^{o}C, 850 ^{o}C, 900 ^{o}C, 950 ^{o}C, 1000 ^{o}C for warm forging. The experiments are also made for 1150 ^{o}C, which is the current hot forging temperature in the forging company. During the experiments, the temperatures of the billets are measured by using two pyrometers. First one is mounted at the induction heater exit and the other one, which has a temperature range of 600 ^{o}C – 1400 ^{o}C, is located in an appropriate position in the process line. Photographs of the pyrometers can be found in Figure 5.12 and Figure 5.13. Process line after the heating stage can be seen through Figure 5.14 to Figure 5.18.

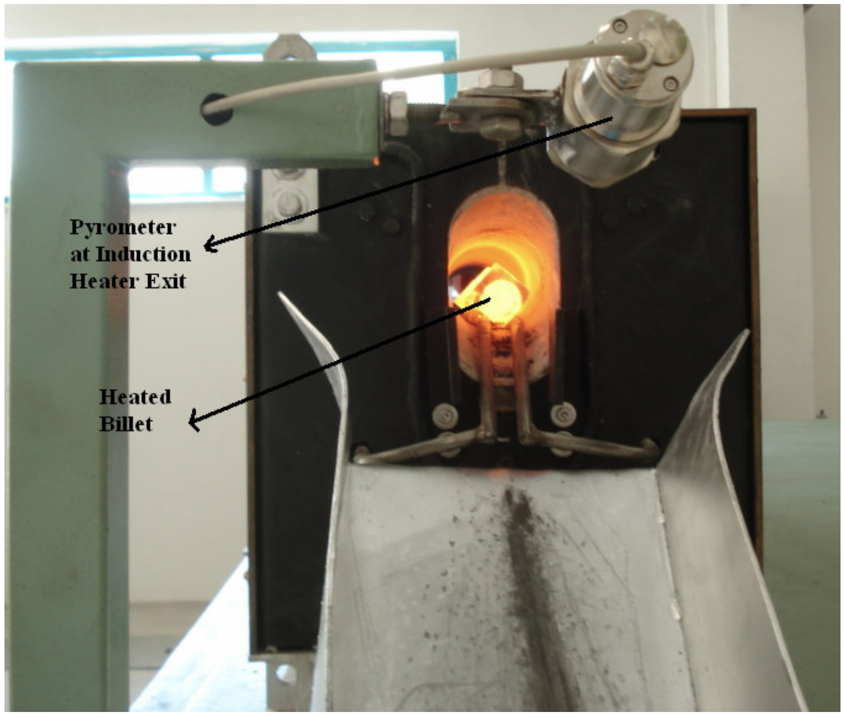

Figure 5.12 A View of Heating of Billets in Induction Heater

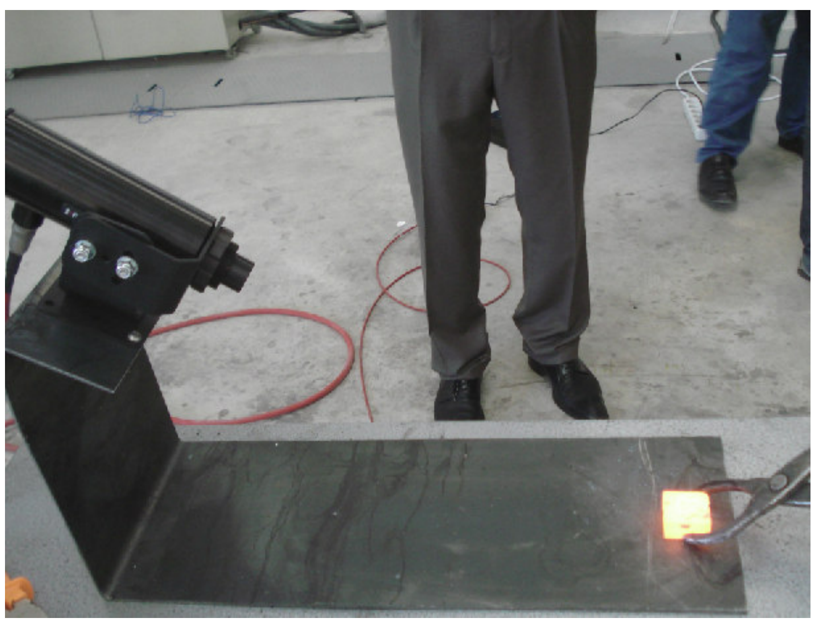

Figure 5.13 A View of Temperature Measurement in Pyrometer in the Process Line

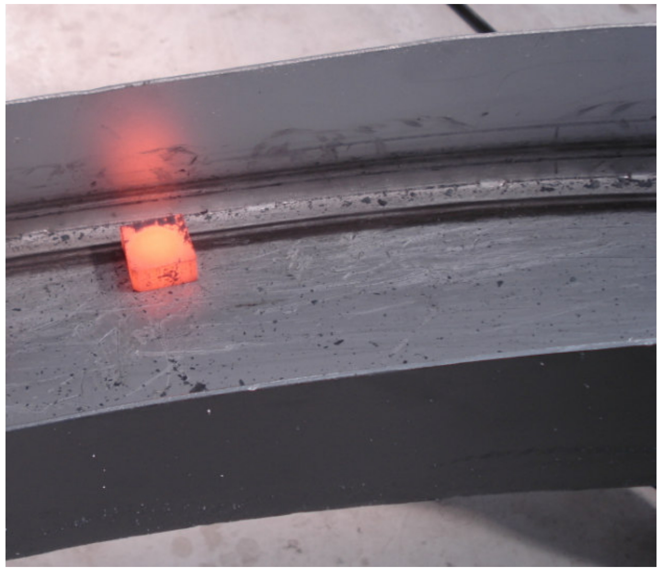

Figure 5.14 A View of Billet on the Slide Between the Induction Heater and the Press

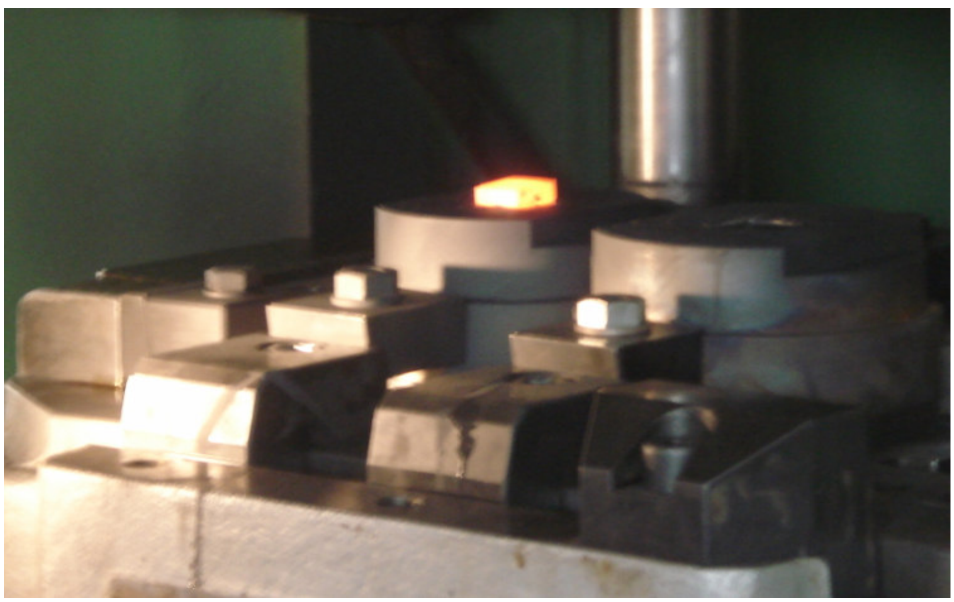

Figure 5.15 A View of Billet Before the Preform Stage

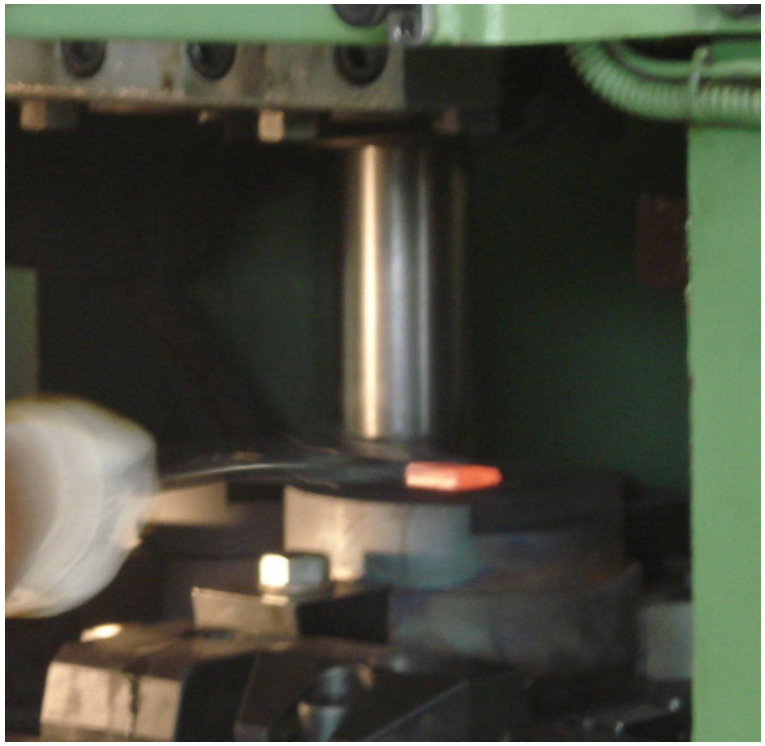

Figure 5.16 A View of Preform Before the Finish Stage

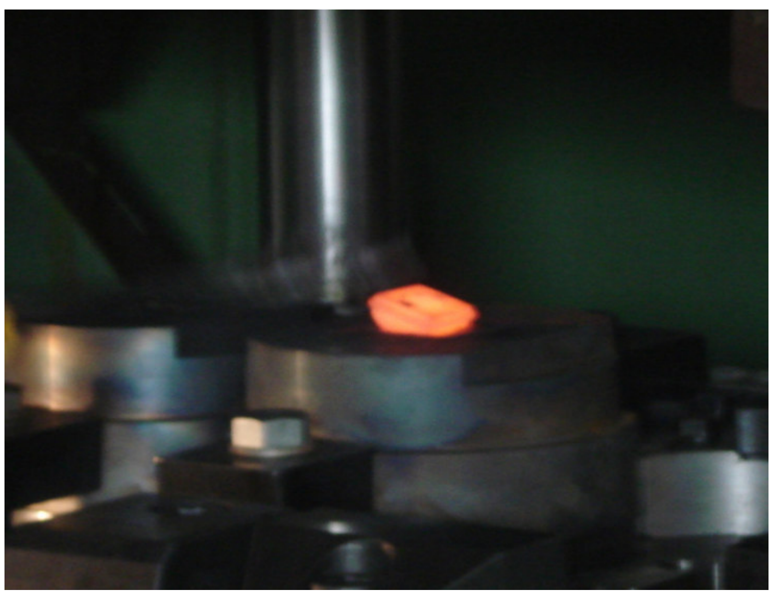

Figure 5.17 A View of Finished Part Taken by Tongs

Figure 5.18 A View of Finished Parts Cooling on the Floor

During the experiments, the parameters that are recorded on the experiment sheet are as follows:

- Billet Temperature at Induction Heater Exit
- Billet Temperature Before Preform Forging
- Preform Temperature Before Finish Forging
- Finished Part Temperature
- Lower and Upper Preform Die Temperatures Before Forging
- Lower and Upper Preform Die Temperatures After Forging
- Lower and Upper Finish Die Temperatures Before Forging
- Lower and Upper Finish Die Temperatures After Forging

As can be seen, temperatures of the workpieces are measured and recorded four times. First one is at the Induction Heater exit, second one is just before preform stage, third one is between the preform and finish stages and the last one is after the finish stage. The preform and finish die temperatures are measured and recorded before and after the operation using the portable optical pyrometer. In Table 5.1, the parameters that are recorded on the experiment sheet are tabulated. In Table 5.2, the results are rearranged according to the targeted "Billet Temperature Before Forging (^{o}C)" values.

The parameters that are measured and recorded after the experiments are as follows:

- Flash Thickness (by digital compass)
- Width, length and height of the Parts (by digital compass)
- Dimensions of the Hexagonal Cavity (by digital compass)

The results that are measured after the experiments are tabulated in Table 5.3.

Table 5.1 Experimental Data

Sample No	Av. Billet Length (mm)	Av. Billet Mass (g)	Stage No	Billet Temp. At Induction Heater Exit (°C)	Billet Temp. Before Forging (°C)	Preform Temp. (°C)	Finished Part Temp. (°C)
1	17,35	164,68	1	1214	1120	950	
2	16,85	160,71	2	1280	1185	1010	850
3	17,10	163,00	2	1090	880	795	730
4	17,05	162,44	2	1082	875	810	800
5	16,87	160,86	2	1026	970	900	780
6	17,07	162,80	2	1063	990	960	680
7	17,03	161,88	2	1185	1020	980	900
8	17,12	163,16	2	1034	950	780	680
9	17,11	163,07	2	990	950	840	760
10	17,05	162,54	2	1000	800	760	700
11	17,03	161,88	2	970	750	680	660
12	17,05	162,44	2	1203	1170	1110	880
13	17,33	164,61	2	1040	925	910	850
14	17,20	163,89	2	934	905	880	840
15	16,97	161,37	1	950	800	780	
16	16,92	161,12	1	950	750	590	
17	17,05	162,53	2	1047	1000	940	840
18	17,03	161,82	2	947	800	760	710
19	16,90	160,99	1	1100	970	920	
20	16,90	161,03	2	1016	980	930	700
21	17,16	163,50	2	1030	820	770	710
22	17,06	162,66	2	980	930	870	820
23	16,96	161,29	1	958	885	760	
24	17,03	162,06	2	1027	810	750	705
25	17,05	162,43	2	985	820	760	715
26	17,10	163,00	2	905	760	700	650
27	17,05	162,44	2	913	765	710	640
28	17,11	163,07	2	945	755	700	670
29	17,15	163,31	2	960	760	690	610
37	17,26	164,14	2	1020	900	820	750

Table 5.1 Experimental Data (Continued)

Sample No	Av. Billet Length (mm)	Av. Billet Mass (g)	Stage No	Billet Temp. At Induction Heater Exit (°C)	Billet Temp. Before Forging (°C)	Preform Temp. (°C)	Finished Part Temp. (°C)
38	17,04	162,30	2	1130	990	960	670
42	17,30	164,23	2	930	900	860	760
43	17,03	161,87	2	1200	1180	1050	980
44	17,15	163,31	2	1289	1150	980	880
46	17,16	163,50	2	1289	1160	1100	1010
47	16,80	160,43	2	1060	960	940	870
48	17,03	162,06	2	1040	880	820	780
49	17,36	164,78	2	972	850	760	700
50	17,02	161,57	2	870	840	780	660
51	17,20	163,92	1	850	800	740	
54	17,05	162,43	1	1127	1080	950	
55	17,21	164,00	2	1180	1070	1040	900

The samples 30-36, 39-41, 45, 52, 53, 56, 57 are not included in the experimental results because, while taking measurements on the dies, temperatures of these samples became out of the predefined range.

In Table 5.2, the results are rearranged according to the targeted "Billet Temperature Before Forging (^{o}C)" values, which are 1150 ^{o}C, 1000 ^{o}C, 950 ^{o}C, 900 ^{o}C, 850 ^{o}C, 800 ^{o}C and 750 ^{o}C. In forging, it is not possible to obtain the exact forging temperature for all of the billets. In induction heating, it is not possible to heat the billet to the exact targeted temperature, the obtained temperature is between certain limits. Additionally, while taking temperature measurements on the dies, the billets sometimes cool down below the targeted temperature, during the experiments. The temperature is 1185 ^{o}C-1120 ^{o}C, when the targeted temperature is 1150 ^{o}C; 1080 ^{o}C-990 ^{o}C, when the targeted temperature is 1000 ^{o}C; 980 ^{o}C-950 ^{o}C when the targeted temperature is 950 ^{o}C; 930 ^{o}C-890 ^{o}C when the targeted temperature is 900 ^{o}C; 880 ^{o}C-840 ^{o}C when the targeted temperature is 850 ^{o}C; 820 ^{o}C-800 ^{o}C when the targeted temperature is 800 ^{o}C; 765 ^{o}C-750 ^{o}C when the targeted temperature is 750 ^{o}C.

Table 5.2 Rearranged Experimental Data

		Workpiece							Preform Die				Finish Die			
Sample No	Billet No	Av. Billet Length (mm)	Av. Billet Mass (g)	Stage No	Billet Temp. At Induction Heater Exit (°C)	**Billet Temp. Before Forging (°C)**	Preform Temp. (°C)	Finished Part Temp. (°C)	Lower Preform Die Temp. Before Forging (°C)	Upper Preform Die Temp. Before Forging (°C)	Lower Preform Die Temp. After Forging (°C)	Upper Preform Die Temp. After Forging (°C)	Lower Finish Die Temp. Before Forging (°C)	Upper Finish Die Temp. Before Forging (°C)	Lower Finish Die Temp. After Forging (°C)	Upper Finish Die Temp. After Forging (°C)
1	2	16,85	160,71	2	1280	**1185**	1010	850	192	185	198	185	183	162	186	165
2	43	17,03	161,87	2	1200	**1180**	1050	980	183	240	166	239	226	294	228	350
3	12	17,05	162,44	2	1203	**1170**	1110	880	160	170	160	170	172	176	176	285
4	46	17,16	163,50	2	1289	**1160**	1100	1010	167	229	167	222	204	297	197	329
5	44	17,15	163,31	2	1289	**1150**	980	880	170	218	170	229	208	267	214	360
6	1	17,35	164,68	1	1214	**1120**	950		198	196	200	195				
7	54	17,05	162,43	1	1127	**1080**	950		142	164	158	169				
8	55	17,21	164,00	2	1180	**1070**	1040	900	129	168	126	164	141	193	139	185
9	7	17,03	161,88	2	1185	**1020**	980	900	145	196	150	175	165	215	170	206
10	17	17,05	162,53	2	1047	**1000**	940	840	119	143	130	150	120	140	130	159
11	6	17,07	162,80	2	1063	**990**	960	680	150	215	150	214	170	200	174	300
12	38	17,04	162,30	2	1130	**990**	960	670	225	210	220	286	285	295	289	345
13	20	16,90	161,03	2	1016	**980**	930	700	116	126	115	139	105	130	112	135
14	19	16,90	160,99	1	1100	**970**	920		115	127	105	142				
15	5	16,87	160,86	2	1026	**970**	900	780	160	240	165	200	185	235	175	210

Table 5.2 Rearranged Experimental Data (Continued)

		Workpiece							Preform Die				Finish Die			
Sample No	Billet No	Av. Billet Length (mm)	Av. Billet Mass (g)	Stage No	Billet Temp. At Induction Heater Exit (°C)	**Billet Temp. Before Forging (°C)**	Preform Temp. (°C)	Finished Part Temp. (°C)	Lower Preform Die Temp. Before Forging (°C)	Upper Preform Die Temp. Before Forging (°C)	Lower Preform Die Temp. After Forging (°C)	Upper Preform Die Temp. After Forging (°C)	Lower Finish Die Temp. Before Forging (°C)	Upper Finish Die Temp. Before Forging (°C)	Lower Finish Die Temp. After Forging (°C)	Upper Finish Die Temp. After Forging (°C)
16	47	16,80	160,43	2	1060	**960**	940	870	145	190	149	197	170	268	172	369
17	8	17,12	163,16	2	1034	**950**	780	680	150	160	152	170	165	180	170	210
18	9	17,11	163,07	2	990	**950**	840	760	150	155	148	165	160	173	162	200
19	22	17,06	162,66	2	980	**930**	870	820	120	110	107	135	110	183	109	250
20	13	17,33	164,61	2	1040	**925**	910	850	118	150	139	165	140	195	143	305
21	14	17,20	163,89	2	934	**905**	880	840	130	150	129	161	140	200	136	270
22	37	17,26	164,14	2	1020	**900**	820	750	230	203	213	294	291	281	292	317
23	42	17,30	164,23	2	930	**900**	860	760	173	240	166	239	226	294	218	350
24	23	16,96	161,29	1	958	**885**	760		112	120	114	129				
25	48	17,03	162,06	2	1040	**880**	820	780	146	199	150	192	168	278	165	353
26	3	17,10	163,00	2	1090	**880**	795	730	185	170	183	188	148	185	150	185
27	4	17,05	162,44	2	1082	**875**	810	800	179	160	165	166	135	175	125	186
28	15	16,97	161,37	1	950	**850**	780		120	150	138	162				
29	49	17,36	164,78	2	972	**850**	760	700	140	182	142	190	166	265	161	319
30	50	17,02	161,57	2	870	**840**	780	660	140	180	152	188	160	258	159	305

Table 5.2 Rearranged Experimental Data (Continued)

		Workpiece							Preform Die				Finish Die			
Sample No	Billet No	Av. Billet Length (mm)	Av. Billet Mass (g)	Stage No	Billet Temp. At Induction Heater Exit (°C)	**Billet Temp. Before Forging (°C)**	Preform Temp. (°C)	Finished Part Temp. (°C)	Lower Preform Die Temp. Before Forging (°C)	Upper Preform Die Temp. Before Forging (°C)	Lower Preform Die Temp. After Forging (°C)	Upper Preform Die Temp. After Forging (°C)	Lower Finish Die Temp. Before Forging (°C)	Upper Finish Die Temp. Before Forging (°C)	Lower Finish Die Temp. After Forging (°C)	Upper Finish Die Temp. After Forging (°C)
31	21	17,16	163,50	2	1030	**822**	770	710	115	108	106	138	168	200	189	300
32	25	17,05	162,43	2	985	**820**	760	715	110	118	115	136	110	175	115	280
33	24	17,03	162,06	2	1027	**810**	750	705	114	120	114	129	110	185	107	290
34	51	17,20	163,92	1	850	**800**	740		140	175	142	189				
35	10	17,05	162,54	2	1000	**800**	760	700	147	155	140	180	156	170	154	250
36	18	17,03	161,82	2	947	**800**	760	710	120	145	123	146	109	135	119	270
37	27	17,05	162,44	2	913	**765**	710	640	110	118	115	136	110	175	115	280
38	26	17,10	163,00	2	905	**760**	700	650	112	120	120	140	120	160	120	285
39	29	17,15	163,31	2	960	**760**	690	610	113	122	115	138	112	170	125	300
40	28	17,11	163,07	2	945	**755**	700	670	120	128	125	128	115	180	115	285
41	16	16,92	161,12	1	950	**750**	590		120	146	123	152				
42	11	17,03	161,88	2	970	**750**	680	660	140	170	140	170	145	199	153	270

Table 5.3 The Results That are Measured After the Experiments

Sample No	Billet No	Width	Length	Height	Hexagonal Cavity Dimensions	Flash Thickness
1	2	40,01	40,02	17,01	19,00	2,03
2	43	40,00	40,00	16,90	19,00	2,05
3	12	39,98	39,98	16,97	19,03	2,20
4	46	39,96	39,97	16,93	18,99	2,00
5	44	39,98	39,97	16,90	19,09	2,08
6	1	38,85	38,85	18,45		2,50
7	54	38,63	38,63	18,73		2,82
8	55	39,95	39,95	17,03	18,99	2,00
9	7	40,02	40,02	16,90	19,15	1,90
10	17	40,00	40,00	17,01	19,00	2,03
11	6	40,03	40,03	16,95	19,05	2,02
12	38	40,03	40,03	16,80	19,05	1,85
13	20	40,04	40,04	17,02	19,02	2,20
14	19	38,94	38,96	19,06		3,12
15	5	39,99	40,00	16,97	19,02	1,98
16	47	40,01	40,01	16,96	19,04	1,96
17	8	40,00	40,00	17,00	18,99	1,97
18	9	39,99	40,01	16,96	19,00	1,97
19	22	40,04	40,03	17,11	19,05	2,25
20	13	40,01	40,01	17,00	19,01	2,10
21	14	40,05	40,05	17,05	19,01	2,20
22	37	40,02	40,02	16,90	19,10	1,97
23	42	40,03	40,02	16,95	19,05	2,00
24	23	38,87	38,86	19,18		3,11
25	48	40,00	40,00	17,07	19,03	2,05
26	3	40,00	40,01	17,06	19,04	2,12
27	4	40,04	40,04	17,05	19,01	2,08
28	15	38,90	38,90	19,00		3,00
29	49	40,02	40,02	17,22	19,05	2,16
30	50	40,01	40,02	17,25	19,04	2,12
31	21	40,01	40,00	17,10	19,03	2,15
32	25	39,99	39,99	17,03	19,01	2,15
33	24	40,02	40,02	17,07	19,01	2,10
34	51	38,80	38,80	19,30		3,15

Table 5.3 The Results That are Measured After the Experiments (Continued)

Sample No	Billet No	Width	Length	Height	Hexagonal Cavity Dimensions	Flash Thickness
35	10	40,01	40,00	17,07	19,00	2,08
36	18	40,01	40,01	17,01	19,00	2,10
37	27	40,01	40,01	17,01	19,03	2,13
38	26	40,01	40,01	17,04	19,03	1,90
39	29	40,01	40,01	17,01	19,00	2,05
40	28	40,00	40,00	17,00	19,01	2,08
41	16	38,88	38,88	19,00		2,96
42	11	40,02	40,02	16,98	19,02	2,13

5.4 Discussion of the Experimental Results

After the parts are measured by instruments and examined by visual inspection, it is observed that, there are no forging defects like unfilled regions, folds, laps, surface cracks, etc, which is a consistent result with the simulation results.

Flash formation around the periphery of the finished parts is considerably reduced when compared to the current practice applied in the particular company. The flash thickness on the finished parts is measured in the range of 1,97-2,15 mm, which was designed to be 2mm. Besides, there is almost no flash formation in the preform stage, which shows that the proposed design is successful in improving material utilization. This result can also be verified by comparing the billet weights that are used in the current and the proposed process sequence. The current billet weight is around 175 g, on the other hand, as can be seen from Table 5.1, the average billet weight is 163 mm in the proposed process, which shows that material utilization is improved by 7 %, roughly.

The hexagonal cavity dimensions, which are critical to obtain, are mostly in the range 19-19,05 mm, which satisfy the tolerance $19^{+0,5}$ that is specified on the technical drawing of the part. There are a few exceptions like 19,10 mm and

19,15 mm, which result from using billets with which are bigger when compared to other samples.

The dimensions of the width and length of the parts are in the range of 39,96-40,04, which satisfy the tolerance $40^{\pm 0,5}$ mm. Height of the parts are in the range of 16,95-17-05 mm, which satisfy the tolerance $17^{\pm 0,5}$ mm. Some samples have lower height values, these samples are mostly forged above 1000 ^{o}C. Additionally, there are a few samples having higher height values, that results from using bigger billets when compared to other samples. The results mentioned above verify that the required accuracy and tolerances are obtained by the proposed design.

Energy saving is achieved by lowering the forging temperature from the hot forging to the warm forging temperature range. Referring to a continuing study that is currently being conducted on induction heating in METU-BILTIR Center, "Effects of Induction Heating Parameters on Forging Billet Temperature" [53], energy saving that is achieved by lowering the forging temperature from 1150 ^{o}C to 1000 ^{o}C is roughly 15%, considering the heating stage of the billet.

The temperature measurements that are taken on the billet at different stages of the process show that, the temperature of the workpiece decreases considerably between the Induction Heater exit and the press. This cooling is due to the convection and radiation between the workpiece and the ambient air -which is at about 25 ^{o}C, and also due to the conduction between the workpiece and the slide. Additionally, the temperature of the workpiece decreases continuously during the preforming and the finishing stages, again due to convection and conduction.

In the simulation part of the study, the initial die temperatures are defined as 200 ^{o}C, as the preheating temperature is around 200 ^{o}C. During the experiments, temperatures of the preform and finish dies are usually in the range of 150 ^{o}C to 200 ^{o}C. There are some higher temperatures around 250-350 ^{o}C on the dies in some parts of the experiments. These high temperatures are due to intermediate heating of the dies. During the experiments, because of taking many measurements and records in each forging stage, the production rate is low when compared to the current case in the forging company. As the production rate is high in the forging company, the workpieces heat the dies continuously and the die temperatures do usually remain in the desired range. Therefore, during the experiments, intermediate heating is applied to the dies according to the suggestions of the authorities in the forging company [35].

In some parts of the experiments, it is observed that the temperatures of the dies after forging are lower than the temperatures before forging. In reality, it is expected that there would be conduction between the hot billet and the die, which would result in an increase in the die temperature after forging. It is not possible to measure the die temperatures just after forging, and the dies cool down by convection during that period, therefore, some lower temperature measurements are taken on the dies after forging.

Additionally, during the finite element simulations, it is observed that, the temperatures of the dies reach up to 350 ^{o}C locally, during the analyses. However, as mentioned, the temperatures of the preform and finish dies are usually in the range of 150 ^{o}C to 200 ^{o}C during the experiments. There are some reasons for that difference. First of all, the software calculates the peak temperatures during forging, but in the experiments the measurements are taken just after the part is forged and taken away from the dies. During this time period, the dies cool down considerably by convection. As another reason, the temperature measurements on the dies are made by optical pyrometer at different points and it is not always possible to focus the actual local point where the temperature is at its peak value.

CHAPTER 6

DISCUSSION AND CONCLUSION

6.1 General Conclusions

In this study, initially, forging process of a part which is currently produced at the hot forging temperature range has been analyzed. The forging process sequence with a new preform design for the particular part has been proposed in warm forging temperature range. These has brought improvements in accuracy, material usage and energy saving. The proposed process has been simulated by using Finite Element Method, as explained in detail in Chapter 4. The experimental study has been carried out in METU-BILTIR Center Forging Research and Application Laboratory, as explained in detail in Chapter 5. The following conclusions have been reached due to the results of the Finite Element simulations:

- The equivalent stresses on the dies increase as the initial billet temperature is reduced, as seen in Table 4.14. However, the locations on the upper and lower dies where the maximum equivalent stresses occur are the same for all the simulations.
- The stresses on the upper die are below the yield strength for temperatures of 1150 ^{o}C, 1000 ^{o}C, 950 ^{o}C and 900 ^{o}C, which means that no plastic deformation is expected on the upper die at these temperatures. On the other hand, the stresses on the lower die are below the yield strength for temperatures of 1150 ^{o}C and 1000 ^{o}C. For lower temperatures, local plastic strains are expected on the lower die.

- The characteristics of the temperature distribution considering locations on the dies at the increment of the maximum equivalent stress are similar for all simulations, but the numerical values, which can be seen in Table 4.15, are different. The locations where the temperature reaches to its peak values are the ones which are in contact with the workpiece for a longer time than other locations on the dies.

It should be noted that, Finite Element Method is used as a tool to predict the stress and temperature distributions on the billet and the dies in this study. The results of a Finite Element Analysis cannot be considered as 100% reliable, as there are many parameters that would affect the results. Element size, number of elements, boundary conditions, convergence criteria are some of these parameters. In the study, these parameters are specified by using the technical assistance of authorities who has developed the particular Finite Element Analysis software [51]; and trial and error method to obtain the most reliable simulation results.

The following conclusions have been reached as the results of the experiments:

- It is observed that, the finite element simulation results and the experimental results are in good agreement.
- After the parts are measured by instruments and examined by visual inspection, it is observed that, there are no forging defects like unfilled regions, folds, laps, surface cracks, etc, which is a consistent result with the simulation results.
- Flash formation around the periphery of the finished parts is considerably reduced when compared to the current practice applied in the particular forging company. Besides, there is almost no flash formation in the preform stage, which shows that the proposed design is successful in improving material utilization. By comparing the billet weights that are used in the current and the proposed process sequence, it is observed that material utilization is improved by 7 %, roughly.

- The dimensions of the edges of the hexagonal cavity, which are critical to obtain, are mostly in the range 19-19,05 mm, which satisfy the tolerance $19^{+0,5}$ that is specified on the technical drawing of the part. There are a few exceptions like 19,10 mm and 19,15 mm, which result from using billets with which are bigger when compared to other samples.
- The dimensions of the width and length of the parts are in the range of 39,96-40,04, which satisfy the tolerance $40^{\pm0,5}$ mm. Height of the parts are in the range of 16,95-17-05 mm, which satisfy the tolerance $17^{\pm0,5}$ mm. Some samples have lower height values, these samples are mostly forged above 1000 ^{o}C. Additionally, there are a few samples having higher height values, that results from using bigger billets when compared to other samples. The results mentioned above verify that the required accuracy and tolerances have been obtained by the proposed design.

In the proposed design, it is aimed to avoid plastic deformations on the dies completely. Therefore, it is suggested to forge the parts at 1000 ^{o}C, with the proposed preform and finish dies to improve die life.

With the proposed process sequence and preform design, the following improvements have been achieved:

- Material utilization is improved by using of a square cross section billet instead of a circular one. The usage of square cross section billet provides more uniform flash formation around the periphery of the finished part which results in better die filling with smaller billets. Additionally, the flash formation is almost avoided in the preform stage.
- Energy saving is achieved by lowering the forging temperature from the hot forging to the warm forging temperature range.
- Production time and production cost are reduced by eliminating the upsetting stage. In the current application, there are five stages, whereas in the proposed process sequence design, there are three stages. This modification in process sequence would reduce the die costs by eliminating the upsetting and cold ironing stage, at the same time, unit

time that is required to forge a part would decrease considerably, and productivity would increase.

- Desired part dimensions are achieved by reducing the forging temperature from the hot forging to the warm forging temperature range. Especially, the hexagonal cavity dimensions which are obtained by cold ironing in the current application can be obtained accurately in the proposed process without further stage.

6.2 Recommendations for Future Work

- For the preforming stage, the lower die design can be improved to reduce the die stresses and eliminate plastic deformation below 1000 ^{o}C. For lower temperatures, more than one preform stages may be designed in the process sequence, to avoid local plastic deformations that are developed in the dies.
- The dies should be modeled as “elastic-plastic” to obtain the values of the plastic strains that are developed on the dies.
- Tool life and wear analyses can be made for the dies.
- Near-net shape forging of the particular part can be studied.

REFERENCES

[1] S.E. Rusinoff, "Forging and Forming Metals", (1952), American Technical Society, Chicago.

[2] T. Altan, H. J. Henning, "Closed-Die Forging of Round Shapes Flash Design and Material Savings", Metallurgia and Metalforming, March, p. 83, 1972.

[3] "DIN STANDARD 7523 Design of Drop and Press Forgings", September 1986, Part 2.

[4] S. Babu, D. Riberio, R. Shivpuri, "Material and Surface Engineering of Precision Forging Dies", The Ohio State University, June 1999.

[5] S. Kalpakjian, "Manufacturing Processes for Engineering Materials", (1991) Addison-Wesley.

[6] T. Altan, G. Ngaile and G. Shen, "Cold and Hot Forging-Fundamentals and Applications", March 2004.

[7] MSC Superforge 2005.

[8] V. Bhavin Mehta, Ibrahim Al-Zkeri, Jay S. Gunasekera, "Evaluation of MSC.SuperForge for 3D Simulation of Streamlined and Shear Extrusion Dies", Ohio University, Athens, Ohio, USA, 2000.

[9] İsbir, S. Ş., "Finite Element Analysis of Trimming", M.S. Thesis, 2002, p.24, Middle East Technical University, Ankara.

[10] Gökler, M.I., "Computer Aided Sequence and Die Design for Hot Upset Forgings", Ph.D. Thesis, University of Birmingham, England, 1983.

[11] Kazancı, B., “Design and Analysis of Hot Upset Forgings with Non-Circular Cross-Sections”, M. Sc. Thesis, Middle East Technical University, Ankara, Turkey, 2002

[12] Moğulkoç, T., “Finite Element Analysis of Piercing Operation on Forging Machines”, Middle East Technical University, Ankara, Turkey, 1999.

[13] Elmaskaya, D., “Finite Element Analysis of Effects of Tapered Preforms in Cold Upsetting”, Middle East Technical University, Ankara, Turkey, 1997.

[14] Doğan, Ö., “Finite Element Analysis of Effects of Tapered Preforms on Final Product in Cold Upsetting”, M. Sc. Thesis, Middle East Technical University, Ankara, Turkey, 2000.

[15] Alper, E., “Computer Aided Design of Axi-Symmetric Press Forgings”, M. Sc. Thesis, Middle East Technical University, Ankara, Turkey, 1989.

[16] Kutlu, A, E., “Analysis and Design of Preforms for Non-Axisymmetric Press”, M. Sc. Thesis, Middle East Technical University, Ankara, 2001.

[17] Karagözler, A, B., “Analysis and Preform Design for Long Press Forgings with Non-Planar Parting Surfaces”, M. Sc. Thesis, Middle East Technical University, Ankara, Turkey, 2003

[18] Gülbahar, S., “Preform Design for Forging of Heavy Vehicle Steering Joint”, M. Sc. Thesis, Middle East Technical University, Ankara, 2004.

[19] Civelekoğlu, B., “Analysis of Forging For Three Different Alloy Steels”, Middle East Technical University, Ankara, Turkey, 2003.

[20] Karacaovalı, H., “Analysis of Roll-Forging Process”, Middle East Technical University, Ankara, Turkey, 2005.

[21] Aktakka, G., “Analysis of Warm Forging Process”, Middle East Technical University, Ankara, Turkey, 2006.

[22] Abachi, S. “Wear Analysis of Hot Forging Dies”, M. Sc. Thesis, Middle East Technical University, Ankara, Turkey, 2004.

[23] Ceran M., “Finite Element Analysis of Hot Upset Forging Dies”, M.S. Thesis, Middle East Technical University, Ankara, Turkey, 2002.

[24] Masat, M. “ Design and Implementation of Hot Precision Forging Die for a Spur Gear”, Middle East Technical University, Ankara, Turkey, 2007.

[25] Garat V., Bernhart G., Hervy L., “Influence of design and process parameters on service life of nut hot forging die”, Journal of Materials Processing Technology, 147 (2004) 359-369.

[26] Kim D.H., Lee H.C., Kim B.M., Kim K.H., ”Estimation of Die Service Life Against Plastic Deformation And Wear During Hot Forging Processes” , Journal of Materials Processing Technology, 166(2005), 372-380.

[27] Brucelle O., Bernhart G., “Methodology for Service Life Increase of Hot Forging Tools”, Journal of Materials Processing Technology, 87 (1999), 237-246.

[28] Jeong D.J., Kim D.J., Kim J.H., Kim B.M., Dean T.A. ,“Effects of Surface Treatments And Lubricants For Warm Forging Die Life”, Journal of Materials Processing Technology, 113 (2001), 544-550

[29] Lee R.S., Jou J.L., “Application of Numerical Simulation For Wear Analysis Of Warm Forging Die”, Journal of Materials Processing Technology, 140 (2003), 43–48.

[30] Kim H., Yagi T., Yamanaka M., "FE simulation as a must tool in cold/warm forging process and tool design'', Journal of Materials Processing Technology, 98 (2000), 143-149.

[31] WAFAM-The Warm Forging Practical Handbook

[32] S. Sheljaskov, "Current Development of Warm Forging Technology", Journal of Materials Processing Technology 46 (1994), 3-18.

[33] D. Schmoeckel, S. Sheljaskov, P.D. Speck, "Werkzeugwerkstoffe für die Halbwarmumformung".

[34] Iwama T., Morimoto Y., "Die Life and Lubrication in Warm Forging", Journal of Materials Processing Technology, 71 (1997), 43-48.

[35] AKSAN Steel Forging Company.

[36] C. W. Wegst, " Nachschlagewerk Stahlschlüssel", 1983.

[37] Efunda – Engineering Fundamentals

http://www.efunda.com/materials/alloys/alloy_home/show_alloy_found.cfm?ID=AISI_L6&prop=all&Page_Title=%20Metal%20Alloys%20Keyword%20Search%20Results, Last Access: 27.08.2007

[38] Pro/Engineer Wildfire 3.0

[39] MSC Superforge User Manual

[40] MSC. Superform 2005

[41] Cook, R.D., "Concepts and Applications of Finite Element Analysis; a Treatment of the Finite Element Method as Used for the Analysis of Displacement, Strain, and Stress". 1974, New York,: Wiley. xvii, 402 p.

[42] Okman, O., "Free Forming of Locally Induction Heated Specimens", M. Sc. Thesis, Middle East Technical University, Ankara, Turkey, 2005

[43] MSC Superform Userguide Manual

[44] MSC PATRAN 2005

[45]MSC PATRAN User Manual

[46] Lin, S., "Upsetting of a Cylindrical Specimen Between Elastic Tools", Journal of Materials Processing Technology 86 (1999), P:73-80

[47] Kobayashi, S., Oh, S., Altan, T., "Metal Forming and the Finite Element Method", New York, Oxford, 1989

[48] Douglas, R., Kuhlmann, D. "Guidelines for Precision Hot Forging With Applications", Journal of Materials Processing Technology 98 (2000), 182-188

[49] TS 1845, February 1975

[50] ASSAB KORKMAZ

http://www.assabkorkmaz.com/sicak.html, Last access: 27.08.2007.

[51] Personal communication with MSC Superform developing authorities from Femutec company, Germany.

[52] Accompanying Technical Documentation of the Die Holder for the Press LZK 1000 P/SH

[53] Durukan, İ., "Effects of Induction Heating Parameters on Forging Billet Temperature", Middle East Technical University, Ankara, Turkey, 2007

APPENDIX A

TECHNICAL DRAWING OF THE PART AND THE CURRENT DIES

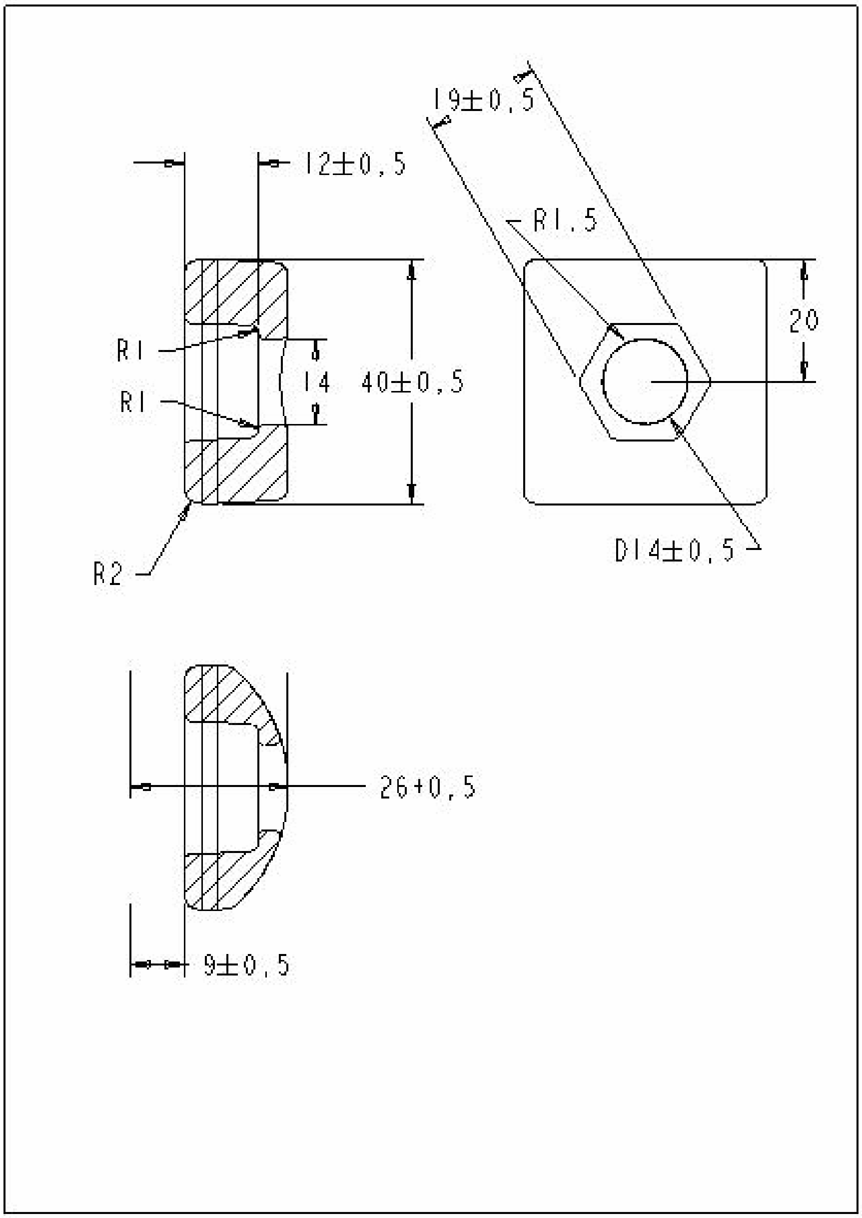

Figure A. 1 Technical Drawing of the Part

TECHNICAL DRAWINGS OF THE CURRENT PREFORM DIES

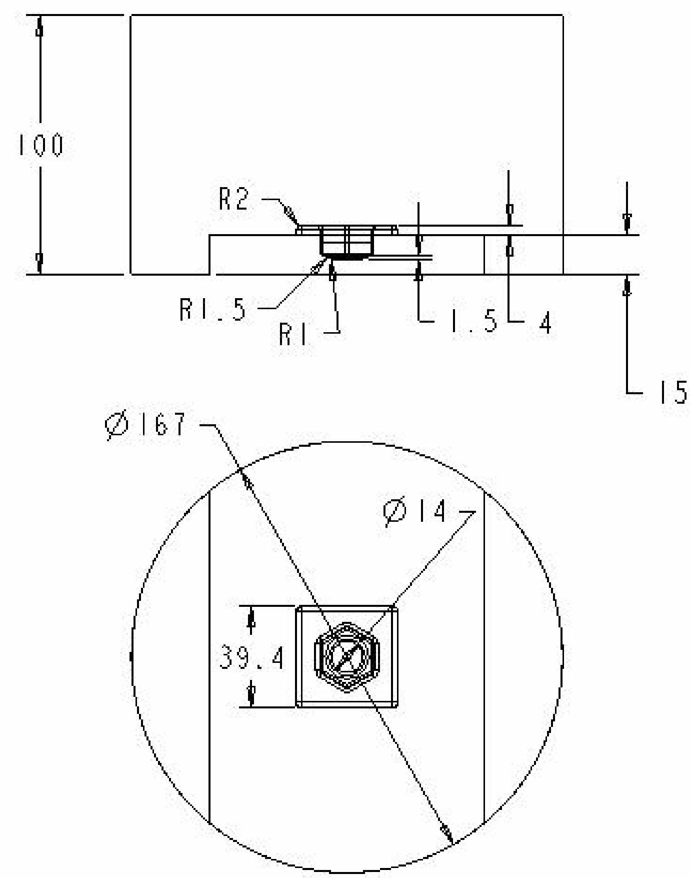

Part Name	Upper Preform Die
General Toleraces	±0,5 mm
Draft Angles	3º

Figure A. 2 Technical Drawing of the Current Upper Preform Die

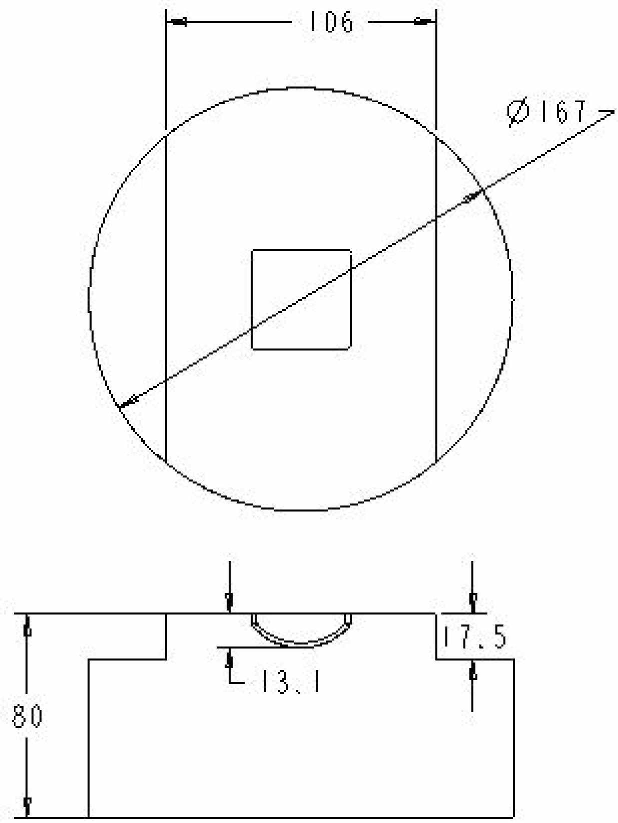

Part Name	Lower Preform Die
General Toleraces	±0,5 mm
Draft Angles	3º

Figure A. 3 Technical Drawing of the Current Lower Preform Die

TECHNICAL DRAWINGS OF THE CURRENT FINISH DIES

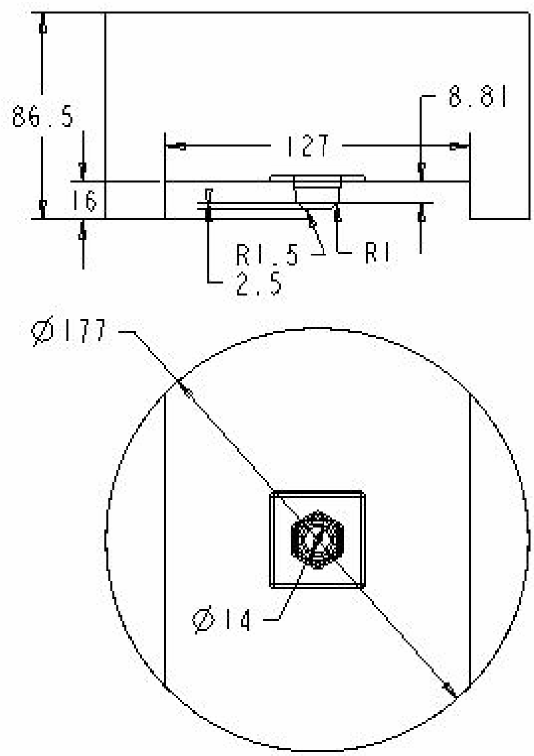

Part Name	Upper Finish Die
General Tolerances	±0,5 mm
Draft Angles	3°

Figure A. 4 Technical Drawing of the Current Upper Finish Die

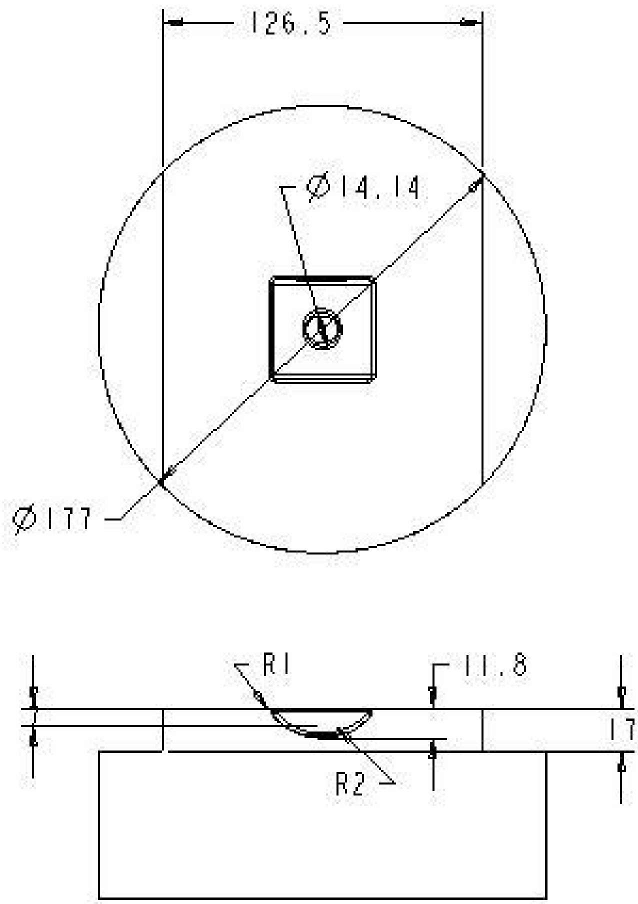

Part Name	Lower Finish Die
General Tolerances	±0,5 mm
Draft Angles	3º

Figure A. 5 Technical Drawing of the Current Lower Finish Die

APPENDIX B

PROCESS SHEET OF THE CURRENT PRACTICE

Process No	Process Definition	Capacity of Equipment
1	Upsetting (2 times in rolling direction)	1000 ton
2	Preform	1000 ton
3	Finish Forging	1000 ton
4	Trimming	250 ton
5	Punching out the hole	250 ton
6	Cold ironing	250 ton

APPENDIX C

Properties of Element Type 7

Element type 7 is a eight-node, isoparametric, arbitrary hexahedral. It is a full integration type element and stiffness of the full integration elements are formed using eight-point Gaussian integration. The element has eight nodes which are located at the corners of the cube as shown below in Figure C.1.

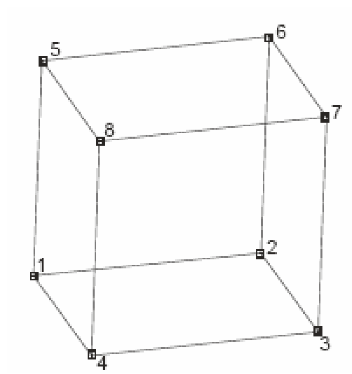

Figure C. 1 Hexahedral Element

Properties of Element Type 134

This class consists of four nodded tetrahedral elements with linear interpolation functions. The tetrahedral element with its nodes is given in Figure C.2.

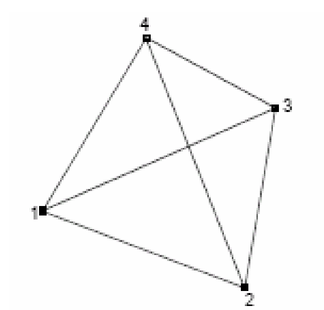

Figure C. 2 Tetrahedral Element

APPENDIX D

TECHNICAL DRAWINGS OF THE PROPOSED PREFORM AND FINISH DIES

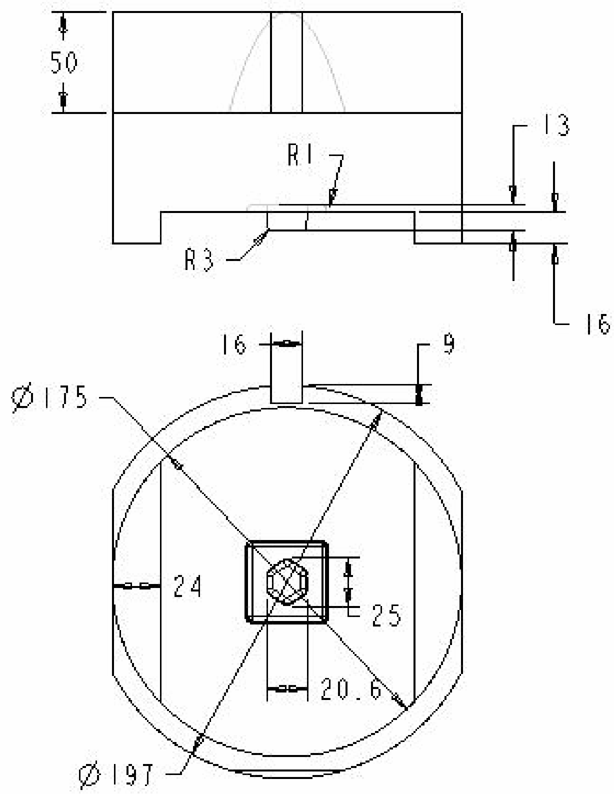

Part Name	Upper Preform Die
General Tolerances	±0,5 mm
Draft Angles	3º

Figure D. 1 Technical Drawing of the Upper Preform Die

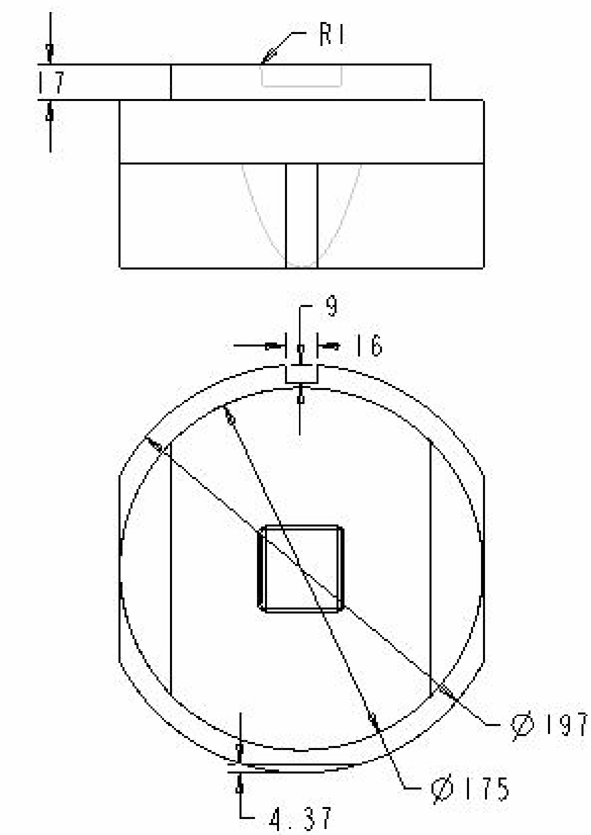

Part Name	Lower Preform Die
General Tolerances	±0,5 mm
Draft Angles	3º

Figure D. 2 Technical Drawing of the Lower Preform Die

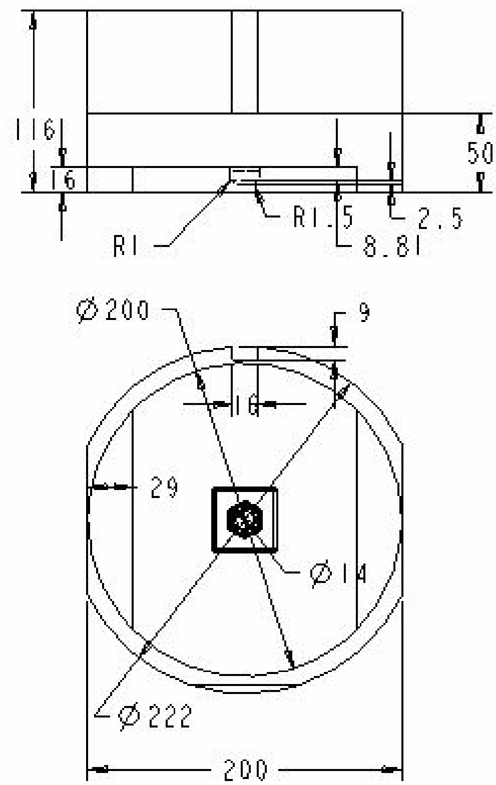

Part Name	Upper Finish Die
General Tolerances	± 0,5 mm
Draft Angles	3º

Figure D. 3 Technical Drawing of the Upper Finish Die

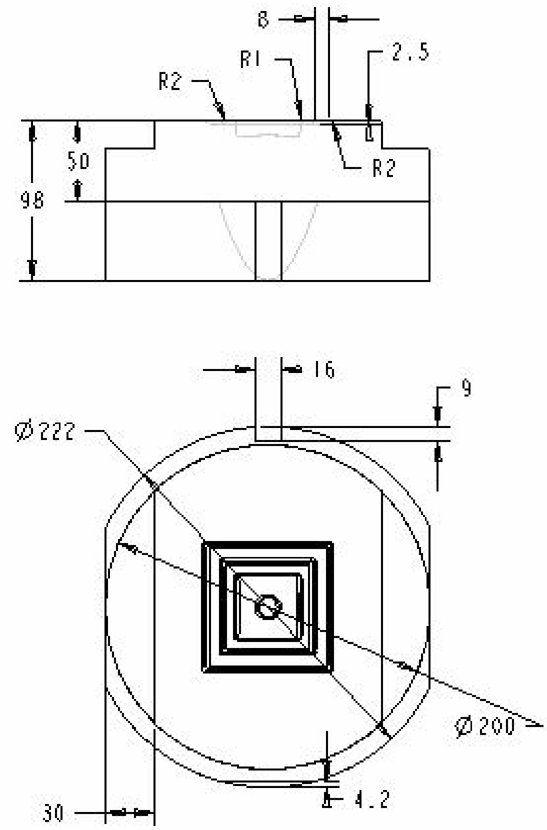

Part Name	Lower Finish Die
General Tolerances	±0,5 mm
Draft Angles	3º

Figure D. 4 Technical Drawing of the Lower Finish Die

APPENDIX E

TECHNICAL DATA OF 1000 TON SMERAL MECHANICAL PRESS IN METU-BILTIR CENTER

Figure E. 1 1000 ton Smeral Mechanical Press in METU-BILTIR Center

Nominal Forming Force	: 10 MN
Ram Stroke	: 220 mm
Shut Height	: 620 mm
Ram Resetting	: 10 mm
Rod Length	: 750 mm
Crank Radius	: 110 mm
Number of Strokes at Continuous Run	: 100 min^{-1}
Press Height	: 4840 mm
Press Height above Floor	: 4600 mm
Press Width	: 2540 mm
Press Depth	: 3240 mm
Press Weight	: 48000 kg
Die Holder Weight	: 3000 kg
Main Motor Input	: 55 kW
Max. Stroke of the Upper Ejector (without die holder)	: 40mm
Max. Stroke of the Lower Ejector (without die holder)	: 50 mm
Max. Force of the Upper Ejector	: 60 kN
Max. Force of the Lower Ejector	: 150 kN

APPENDIX F

HEAT TREATMENT PROCESS

In the study the forging die sets are heat treated in vacuum furnaces available at a private company in Izmir [53]. As it can be seen from Figure F.1, the dies are heated to austenitizing temperature of 1000°C under 5 bar Nitrogen gas. Afterwards the dies are cooled rapidly. Then the tempering process is applied. In tempering, toughness of the material is increased by reducing the hardness that is introduced by austenitizing in an optimum level. First tempering process is applied for about 4 hours at 580 °C, second tempering is applied for about 4 hours at 610 °C and the last tempering process is applied for about 3 hours at 580 °C. The hardness value is measured as 46 HRc after the heat treatment is completed.

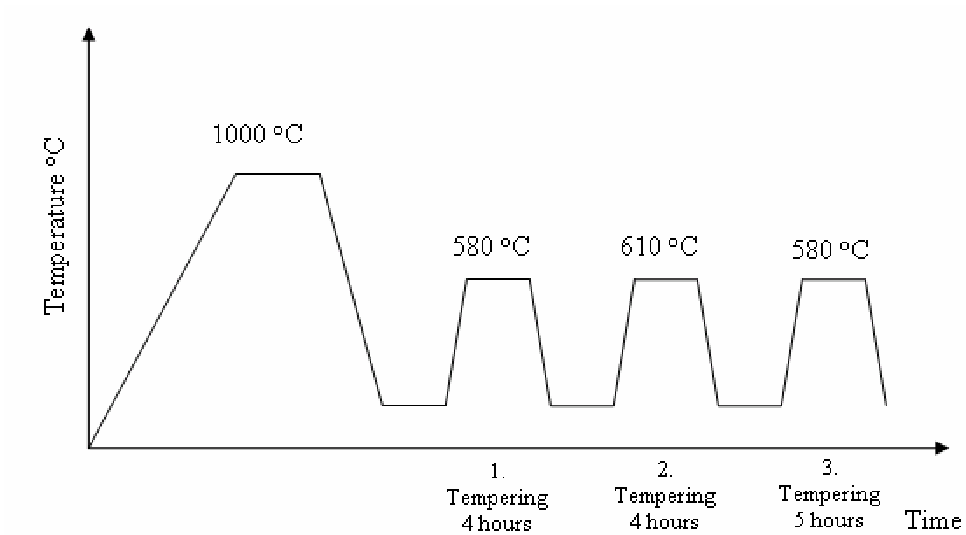

Figure F. 1 Heat Treatment Process